

MINISTERE DE L'ENSEIGNEMENT SUPERIEUR ET DE LA
RECHERCHE SCIENTIFIQUE

UNIVERSITE MOHAMED KHIDER BISKRA

FACULTE DES SCIENCES EXACTES
ET
DES SCIENCES DE LA NATURE ET DE LA VIE

Département des Sciences de la matière

THESE

Présentée par

BENBRAHIM Imane

En vue de l'obtention du diplôme de :

Doctorat en chimie

Option :

Chimie Moléculaire

Intitulée:

**Etude par des méthodes quantiques et empiriques des
relations SAR et QSAR dans des hétérocycles à intérêt
médicinale**

Soutenue le : 09/07/2017

Devant la commission d'Examen :

| | | | |
|------------------------|-------|-----------------------------------|--------------------|
| Mr. Mahmoud Omari | Prof. | Université Mohamed Khider- Biskra | Président |
| Mr. Salah Belaidi | Prof. | Université Mohamed Khider- Biskra | Directeur de thèse |
| Mr. Noureddine Tchouar | Prof. | Université USTO-Oran | Examineur |
| Mr. Youcef Boumedjane | MC/A | Université Mohamed Khider- Biskra | Examineur |

MINISTERE DE L'ENSEIGNEMENT SUPERIEUR ET DE LA
RECHERCHE SCIENTIFIQUE

UNIVERSITE MOHAMED KHIDER BISKRA

FACULTE DES SCIENCES EXACTES
ET
DES SCIENCES DE LA NATURE ET DE LA VIE

Département des Sciences de la matière

THESE

Présentée par

BENBRAHIM Imane

En vue de l'obtention du diplôme de :

Doctorat en chimie

Option :

Chimie Moléculaire

Intitulée:

**Study by Quantum and Empirical Methods of SAR and
QSAR of Heterocyclic with Medicinal Interest**

Soutenue le : 09/07/2017

Devant la commission d'Examen :

| | | | |
|------------------------|-------|-----------------------------------|--------------------|
| Mr. Mahmoud Omari | Prof. | Université Mohamed Khider- Biskra | Président |
| Mr. Salah Belaidi | Prof. | Université Mohamed Khider- Biskra | Directeur de thèse |
| Mr. Noureddine Tchouar | Prof. | Université USTO-Oran | Examineur |
| Mr. Youcef Boumedjane | MC/A | Université Mohamed Khider- Biskra | Examineur |

To my dear parents

To my husband

To my siblings

To all those who are dear to me

Acknowledgements

First of all, I pray to Allah, the almighty for providing me this opportunity and granting me the capability to proceed successfully.

At the outset, I would like to thank my supervisor Prof. BELAIDI Salah for providing me an opportunity to do my doctoral research under his supervision, continuous support, encouragement throughout my research and for his useful comments and discussion to make my thesis complete.

I wish to extend my sincere thanks to Mr. Mahmoud Omari, Professor at the University of Biskra, for accepting to chair the dissertation of my thesis.

I would also like to thank the committee members, Mr. Nouredine Tchouar, Professors at the University USTO-Oran, and Mr. Youcef Boumedjane, MC/A at the University of Biskra, for agreeing to examine and judge my work.

I would like to thank all the members of group of computational and pharmaceutical chemistry, LMCE Laboratory at Biskra University, with whom I had the opportunity to work. They provided me a useful feedback and insightful comments on my work.

I would like to express my special thanks to Prof. SOLIMAN Mahmoud and his team member from KwaZulu-Natal University for the help with a smile, the good hospitality and the good reception during my training in their Molecular Modelling and Drug Design Lab.

Last, but not least, I would like to dedicate this thesis to my beloved parents whom raised me with a love of science and supported me in all my pursuits, my husband and my siblings for their love and continuous support – both spiritually and materially.

| | |
|-----------------------|------|
| ACKNOWLEDGMENTS | i |
| TABLE OF CONTENTS | iii |
| LIST OF FIGURES | vi |
| LIST OF TABLES | vii |
| LIST OF ABBREVIATIONS | viii |

General Introduction **2**

CHAPTER I : Understanding tuberculosis

| | |
|---|----|
| 1. What is tuberculosis ? | 7 |
| 2. Your healthy lungs | 7 |
| 3. What happens if you get infected with M. tuberculosis? | 8 |
| - Latent tuberculosis | |
| - Active tuberculosis | |
| 4. Symptoms | 9 |
| 5. What puts you at risk of catching tuberculosis? | 10 |
| 6. How likely are you to get tuberculosis? | 11 |
| 7. How is tuberculosis treated? | 11 |
| - Treatment of latent tuberculosis | |
| - Treatment of active, drug-sensitive tuberculosis | |
| - Treatment of drug resistant tuberculosis | |
| 8. Intrinsic or acquired drug resistance? | 13 |
| 9. Investigation of Anti-TB Drugs structure | 13 |

CHAPTER II : Computer-Assisted Drug

| | |
|--|----|
| 1. Predictive Quantitative Structure–Activity Relationship Modeling | 16 |
| 2. Key Quantitative Structure–Activity Relationship Concepts | 17 |
| -Target properties | |
| -Chemical descriptors | |
| -Correlation methods | |
| 3. Molecular Descriptors | 19 |
| 3.1. Molecular Size and Shape | 19 |
| 3.2. Lipophilicity and Hydrophobicity | 20 |
| 3.3. Hydrogen Bonding | 22 |
| 3.4. Quantum Chemical Descriptors | 22 |
| 4. Quantitative Structure–Activity Relationship Modeling Approaches | 22 |
| 4.1. General Classification | 22 |
| 4.2. Transforming the Bioactivities | 23 |
| 4.3. Training and Test Set Creation | 24 |
| 4.4. Determination of the Best Set of Descriptors Approaches | 24 |
| 5. Building Predictive Quantitative Structure–Activity Relationship Models: The Approaches to Model Validation | 24 |

| | |
|--|----|
| 5.1. The Importance of Validation | 24 |
| 5.2. Internal Validation | 25 |
| 5.2.1. Least Squares Fit | 25 |
| 5.2.2. Fit of the Model | 26 |
| 5.3. External validation | 27 |
| 6. Applicability Domain | 28 |
| 7. Molecular Modeling Techniques | 28 |
| 8. Theoretical Background for Quantum Mechanical Calculations | 30 |
| 8.1. Ab Initio Methods | 32 |
| 8.2. Density Functional Theory Methods | 32 |
| 8.3. Semiempirical Methods | 33 |
| 8.4. Molecular Mechanics or Force Field Methods | 34 |
| 9. Application of Quantum Mechanical Calculations to Medicinal Chemistry and Drug Design | 34 |
| 10. Computational Docking | 35 |
| 11. Virtual Screening | 36 |

CHAPTER III : Results and Discussion

PART I : In Silico Modeling of Substitution-Induced Effect and Structure Property/Activity Relationship Profile of 1, 3, 4-Oxadiazole Derivatives

| | |
|--|----|
| 1. Methods validation | 40 |
| 2. Substitution effects on 1, 3, 4-oxadiazole | 41 |
| 3. Structure Activity/Property Relationships studies | 45 |
| 3.1. Drug-like properties of rule of thumb | 46 |
| 3.2. Lipophilicity profile and the ionization state | 47 |
| 3.3. Structure Activity/Affinity Relationships (PEI and GE analysis) | 52 |
| 4. Conclusion | 53 |

PART II: Quantitative Structure-Antituberculosis Activity Relationships Study in a series of oxazoline and oxazole benzyl esters derivatives

| | |
|----------------------------------|----|
| 1. Biological Data | 56 |
| 2. Descriptors Generation | 65 |
| 3. Regression Analysis | 67 |
| 4. QSAR model validation | 68 |
| 5. Interpretation of descriptors | 70 |
| 6. Conclusion | 71 |

PART III: Docking-Based Virtual Screening for Lead Optimization

| | |
|-------------------------------------|----|
| 1. Materials | 73 |
| 2. Input files | 73 |
| 3. Methods | 75 |
| 4. Docking method validation | 76 |
| 5. Free binding energy calculations | 76 |

| | |
|---------------------------|------------|
| 6. Binding Interactions | 80 |
| 7. Conclusion | 84 |
| General Conclusion | 86 |
| Appendix | 89 |
| Abstract | 100 |
| References | 104 |

| | |
|---|----|
| Figure 1 Image of healthy alveoli performing gas exchange of oxygen and carbon dioxide to blood cells | 7 |
| Figure 2 Image of healthy alveoli blocking gas exchange to and from blood cells | 9 |
| Figure 3 Image illustrating the effects of extra-pulmonary tuberculosis | 10 |
| Figure 4 Map illustrating TB prevalence around the world | 11 |
| Figure 5 General methodology of a QSAR Study | 28 |
| Figure 6 An illustration of the various terms that contribute to a typical force field | 29 |
| Figure 7 3D structure of 1, 3, 4-oxadiazole | 40 |
| Figure 8 1, 3, 4-oxadiazole systems | 45 |
| Figure 9 Changes in the energy levels of HOMO–LUMO orbital of 1, 3, 4-oxadiazole derivatives | 45 |
| Figure 10 Lipophilicity profiles for the anti-tuberculosis compounds | 50 |
| Figure 11 The multiprotic acid/base sites of anti-tuberculosis compounds | 51 |
| Figure 12 Changes of pKa values of anti-tuberculosis compounds; red atoms denote acidic groups, and blue atoms indicate basic groups | 51 |
| Figure 13 Group Efficiency analysis of the most efficient compounds of studied series | 53 |
| Figure 14 The plot of predicted pMIC values against the experimental pMIC values | 69 |
| Figure 15 The plot of standardized residuals versus leverage values | 70 |
| Figure 16 Cristal structure complexe (2W0B) interactions | 74 |
| Figure 17 CMW_pose1_-8.4 kcal/mol (pose1_blue) | 76 |
| Figure 18 Binding forces between the CMW and the protein active site residues. (A) CMW crystal structure. (B) CMW docked pose 1 | 82 |
| Figure 19 Binding forces between the 6 best binding affinity compound and the protein active site residues | 83 |

| | |
|--|----|
| Table 1 Bond lengths and valence angles of 1, 3, 4-oxadiazole | 41 |
| Table 2 Density based descriptors of 1, 3, 4-oxadiazole systems | 45 |
| Table 3 Drug-likeness parameters of anti-tuberculosis compounds | 47 |
| Table 4 Log D and Log P profile of the anti-tuberculosis compounds | 49 |
| Table 5 The chemical structures of studied molecules with their corresponding activity data | 56 |
| Table 6 Molecular descriptors used in the regression analysis | 66 |
| Table 7 Statistical results | 68 |
| Table 8 Free binding energy calculations | 77 |
| Table 9 Interaction residues of better scoring compounds | 84 |

| | |
|---|---------------------|
| Absorption, Distribution, Metabolism, and Excretion | (ADME) |
| Acquired Immune Deficiency Syndrome | (AIDS) |
| Artificial Neural Network | (ANN) |
| Assisted Model Building with Energy Refinement | (AMBER) |
| Austin Model 1 | (AM1) |
| Bacille Calmette-Guérin | (BCG) |
| Becke, three-parameter, Lee-Yang-Parr | (B3LYP) |
| Becke, Perdew 86 | (BP86) |
| Computer-Assisted Drug Design | (CADD) |
| Comparative Molecular Field Analysis | (CoMFA) |
| Cross-Validation | (CV) |
| Density Functional Theory | (DFT) |
| Descriptors | (D) |
| Electron Affinities | (EA) |
| Extensively Drug-Resistant TB | (XDR-TB) |
| Frontier Molecular Orbitals | (FMOs) |
| Group Efficiency | (GE) |
| Half maximal Inhibitory Concentration | (IC ₅₀) |
| Hard and Soft, Acids and Bases theory | (HSAB) |
| Hartree-Fock | (HF) |
| Highest Occupied Molecular Orbital | (HOMO) |
| HOMO–LUMO Gaps | (HLG's) |
| Human Immunodeficiency Virus | (HIV) |
| Ionization Potentials | (IP) |
| k Nearest Neighbor | (kNN) |
| Ligand Efficiency | (LE) |
| Linear Regression | (LR) |
| Lowest Unoccupied Molecular Orbital | (LUMO) |
| Merck Molecular Force Field | (MMFF) |
| Minimal Inhibitory Concentration | (MIC) |
| Molar Refractivity | (MR) |
| Molecular Weight | (MW) |

| | |
|--|-----------------|
| Møller-Plesset level 2 | (MP2) |
| Molecular Mechanic 2 | (MM2) |
| Multidrug-Resistant Tuberculosis | (MDR-TB) |
| Multi-Parameter Optimization | (MPO) |
| Multiple Linear Regression | (MLR) |
| Mycobacterium Tuberculosis | (MTB) |
| New Chemical Entity | (NCEs) |
| Nuclear Magnetic Resonance | (NMR) |
| Number of Hydrogen-Bond Donors and Acceptors | (NHBD and NHBA) |
| Number of Rotatable Bonds | (nrotb) |
| Oxadiazole | (ODZ) |
| P-glycoprotein | (Pgp) |
| Partial Least Squares | (PLS) |
| Parameterized Model number 3 | (PM3) |
| Per cent Efficiency Index | (PEI) |
| Polar Surface Area | (PSA) |
| Predictive Residual Sum of the Squares | (PRESS) |
| Principal Component Regression | (PCR) |
| Protein Data Bank | (PDB) |
| Protein Data Bank, Partial Charge (Q), & Atom Type (T) | (PDBQT) |
| Quantitative Structure–Activity Relationship | (QSAR) |
| Quantitative Structure–Property Relationship | (QSPR) |
| Recursive Partitioning | (RP) |
| Root-Mean Squared Error | (RMSE) |
| Self-Consistent-Field procedure | (SCF) |
| Structure–Activity Relationships | (SARs) |
| Support Vector Machines | (SVMs) |
| Target Properties | (P) |
| Tuberculosis | (TB) |
| Two-Dimensional or Three-Dimensional | (2D or 3D) QSAR |
| World Health Organization | (WHO) |

GENERALE INTRODUCTION

WHO has published a global tuberculosis (TB) report every year since 1997. As usual, the 2016 global TB report is based primarily on data gathered from 202 countries and territories all over the world. The best estimate is that there were 1.4 million TB deaths in 2015, and an additional 0.4 million deaths resulting from TB disease among HIV-positive people.¹

Tuberculosis (TB) is an illness that results from infection with *Mycobacterium tuberculosis* (MTB). This aerobic bacillus has the cell wall with a high lipid content which results in a high degree of lipophilicity and resistance to alcohol, acids, alkali and some disinfectants.

MTB is epidemiologically characterized by high rate infectivity, so the one-third of latent infection population which remains a reservoir from *mycobacterium* is the major obstacle to the total control of the disease. In normal conditions, the bacteria has the ability to live in balance with immune response but in situations such as genetic impaired, intercurrent diseases (i.e. AIDS), malnutrition and medical interventions could occur an imbalance, and the MTB multiplies rapidly developing the disease.²

Multidrug-resistant tuberculosis (MDR-TB) is another important problem to control TB worldwide. It has been reported that include patients who have never been treated with any TB drug demonstrated resistance. According to WHO, (in 2015) there were an estimated 10.4 million new (incident) TB cases worldwide (including 1.2 million (11%) among HIV-positive people), of which 5.9 million (56%) were among men, 3.5 million (34%) among women and 1.0 million (10%) among children. Recent estimates show that 10% of all new TB infections are resistant to at least one anti-TB drug.¹

Actual drug therapy for tuberculosis has involved administration of multiple drugs because it was clear that monotherapy led to the development of resistance³ and current treatment takes 6–9 months. The current TB vaccine, Bacille Calmette-Guérin (BCG), developed almost 90 years ago, reduces the risk of severe forms of TB in early childhood but is not very effective in preventing pulmonary TB in adolescents and adults — the populations with the highest rates of TB disease. TB is changing and evolving, making new vaccines more crucial for controlling the pandemic. Tuberculosis is now the leading cause of death for people living with HIV/AIDS, particularly in Africa. Multidrug-resistant TB (MDR-TB) and extensively drug-resistant TB (XDR-TB) are hampering treatment and control efforts. New

control measures, diagnostic tools and guidelines for treatment as well as development of new drugs and vaccines have been made a priority and the battle is now raging to restore the grip on the management and control of MDR/XDR TB. Winning the battle against tuberculosis will depend on the outcomes of the extensive research that is on-going to produce new, more effective and fast acting diagnostic tools, drugs and vaccines.⁴

Since the discovery of rifampicin in 60' there is no more drugs developed to treat tuberculosis. Considering the increase of resistant the discovery of new anti-tubercular drugs is urgent. A new anti-TB drug must possess some characteristics such as wide spectrum of action, adequate posology to allow the patient compliance, short duration of treatment and adequate pharmacokinetic properties (half-life, decreased drug-drug interaction among others).

Among the strategies to introduce a new drug in the market, the Computer-Assisted Drug Design (CADD) approaches has showed to be promising. Several drugs in the market was developed using this strategy. This area is known by many related names, such as computer-aided drug design, computational chemistry, and molecular modelling, together with the broader in silico term.

Although some CADD methods may appear to some people to be less prominent and relevant today, the new challenges that we face now are able to build on such methods, and use them in ways to enable powerful new approaches to impact drug design.

In silico drug design have many facets, from quantitative structure–activity relationships (QSAR), virtual screening, protein structure modelling, and pharmacophore modelling, to structure-based drug design and the modelling of absorption and metabolism. Although quantum mechanical methods often play a part in these approaches, like for example for QSAR and structure-based drug design as well as the modelling of metabolism, they are rarely referred to as an independent approach in this context.

An understanding of the many and diverse interactions of various chemicals with biological macromolecules as determined by their intermolecular forces, i.e., hydrophobic, electrostatic, polar, and steric, was critical to the formulation and development of the quantitative structure–activity relationship (QSAR) paradigm. The use of correlation analysis was useful in helping to mathematically delineate the importance of certain structural attributes of chemicals to their biological activities.

It has been 49 years since the formal beginning of QSAR and great strides have been made in that time. The types of QSAR approaches have increased and some have undergone refinement, while the number of parameters and new descriptors have grown astronomically. QSAR is far from being a finished science; it still retains the ability to predict biological activities or properties as well as the susceptibility to mechanistic interpretation. Enhancing the predictability of a model raises the spectre of appropriate validation procedures.^{5,6}

One of the fundamental problems for molecular modelling is of course the generation of accurate molecular structures and conformations. Molecular mechanics methods achieve good structural accuracy for classical molecules, whereas their reliability for species with particular combinations of atoms may be questionable, particularly for molecules containing heteroatoms, which affect the geometry and conformation via the position of their lone-pairs. This structural characteristic is only accurately reproduced by high-level ab initio and DFT methods, and perhaps surprisingly also by semi-empirical methods like AM1 and PM3.

Most molecular modelling studies can be considered to involve three basic components. First, the molecular system under study needs to be described. Many molecular descriptors are used in computational chemistry, according to the problem being addressed. The second component constitutes the algorithm or algorithms that use the molecular description to manipulate the system or to derive a mathematical model that relates the descriptors to some other (measurable) property. The third component is the computational infrastructure (hardware, operating systems, software, etc.) that enables the calculations to be performed.

Understanding tuberculosis and existing TB drugs are discussed first in **Chapter I** to cover a comprehensive picture of the anti-TB drug discovery, as these are the building blocks for the applications of all the used main CADD/in silico impact points (**Chapter II**) to select and achieve a goal of better drugs/regimen in terms of the desired properties of our anti-tuberculosis compounds (**Chapter III**).

1, 3, 4-Oxadiazole derivatives showed an interesting anti-mycobacterial activity against the reference strain of *Mycobacterium tuberculosis* H37Rv. In this context, the substitution effect study was done in order to deepen our understanding of the influence of various substituents on 1, 3, 4-oxadiazole ring. Here, we present the electronic and geometric structure calculations for 1, 3, 4-oxadiazole substituted by two functional groups of different

strengths using the conceptual DFT descriptors. After that various ‘multi-parameter optimization’ (MPO) approaches such as lipophilicity profile, rules of thumb and calculated metrics methods used to highlight the Structure Activity/Affinity and Property Relationships of our anti-tuberculosis compounds (Work published in: *REVIEWS IN THEORETICAL SCIENCE*; 2016 in press). Followed by Quantitative Structure Activity Relationship (QSAR) study of a series of oxazoline and oxazole benzyl esters as anti-tuberculosis agents and Docking-Based Virtual Screening for Lead Optimization. (Work will be published sooner) all these studies have been addressed in **Chapter III**.



CHAPTER I

Understanding Tuberculosis

1. What is tuberculosis?

Coughing, sneezing, singing, even speaking can all make the air we share hazardous at times. Tuberculosis, or “consumption” if you’ve just emerged from a novel by Charles Dickens, is an infectious disease caused by a bacterium, *Mycobacterium tuberculosis*. It mainly affects the lungs (although can also infect other parts of your body), and is usually spread to other people via the coughs and sneezes of those infected. In addition to being a potentially serious, dramatic affliction suitable for any self-respecting 19th-century character, this disease continues to be a major concern worldwide to this day. Tuberculosis is often referred to as TB.

2. Your healthy lungs

Your lungs, if everything is working as it should be, resemble large pink sponges that expand when you inhale a mouthful of air. Their main job is to transport oxygen from the air into your bloodstream and release carbon dioxide from your body into the air. To do this, small sacs located deep inside your lungs, called alveoli, fill up like balloons, which enables this gas exchange to occur. The alveoli are very thin, just one cell layer thick, which allows very efficient transport of oxygen into your blood capillaries, and carbon dioxide out.

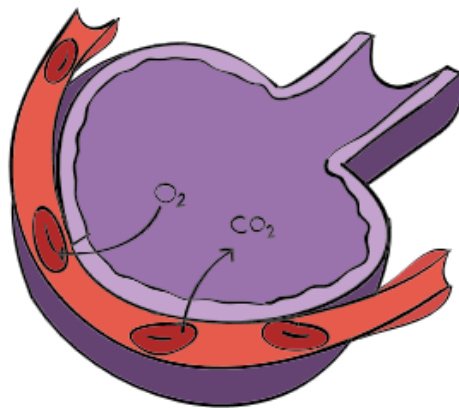


Figure 1 Image of healthy alveoli performing gas exchange of oxygen and carbon dioxide to blood cells.

3. What happens if you get infected with *M. tuberculosis*?

In most cases of tuberculosis, the bacteria spreads slowly and widely throughout the lungs. There are two distinct types, *latent* and *active*:

Latent tuberculosis - this means you are infected with tuberculosis bacteria, but you do not feel sick or have any signs or symptoms of tuberculosis disease. In this case, your immune system limits the infection by enclosing the tuberculosis bacteria within a tough calcified shell, known as a granuloma. The granulomas protect your lungs from any damage the bacteria might do. As long as the bacteria are contained, you will not have any symptoms, and are not contagious, which means you can't infect anyone else. The presence of tuberculosis granulomas can be seen on a chest X-ray.

Active tuberculosis - whether or not tuberculosis remains latent, or progresses to active tuberculosis depends on the health of your immune system. When you are healthy and everything is functioning properly, your body is able to keep the bacteria contained and under control. Sometimes, your immune system may become weaker and is no longer able to control the growth of the tuberculosis bacteria; for example, if you have a disease that attacks your immune system, like HIV/AIDS. When this happens, the calcified shell of the granuloma can deteriorate and your tuberculosis infection may transition from latent to active. This can occur anytime from weeks, to years after you were first infected. Once the tuberculosis granulomas open, the bacteria are able to emerge, inhabit your lungs, and damage the surrounding tissue. The damage causes the spongy, balloon-like tissue of the alveoli to harden and become fibrous, making them useless for gas exchange.

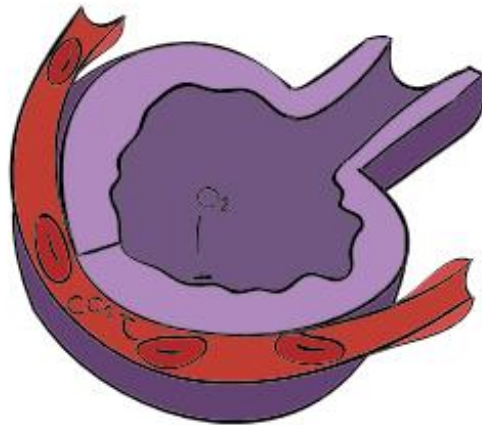


Figure 2 Image of healthy alveoli blocking gas exchange to and from blood cells.

Eventually, the lung tissue cells themselves begin to deteriorate and die. When the bacteria reach a part of your lungs which connects to an airway, they are expelled when you cough or sneeze. This releases them in an aerosol of fine droplets that may be inhaled by another person (droplet transmission). Like the flu, tuberculosis is an airborne disease, meaning that the infectious droplets can travel long distances and remain suspended in the air for a long time. Consequently, it is possible for the bacteria to circulate throughout entire buildings, and you can catch tuberculosis by entering a room that an infected person left hours ago. Masks that filter the air (e.g., N95 masks) are often used by healthcare professionals who are caring for patients with tuberculosis, and these patients are often isolated in negative pressure rooms that prevent the contaminated air from escaping from the room.

Unfortunately, because your body naturally wants to eject any unwanted particles in your lungs, you are likely to be coughing a lot if you have active tuberculosis. As the bacteria continue to attack your lung tissues, the damage and inflammation becomes more extensive, and you may even begin to cough up blood.

4. Symptoms

Many of the worst symptoms of active tuberculosis arise as a direct result of the extensive tissue damage that the bacteria do to your lungs. Typical signs and symptoms of active tuberculosis include a bad dry cough lasting for more than three weeks that may cause you to cough up bloody sputum. You are also likely to experience night sweats, fever and weight

loss (the reason why historically tuberculosis was called “consumption”) as your body tries to fight off the infection.

For about one in five people, the infection is so severe that cavities begin to form within the lung tissue. If these areas start to bleed, tuberculosis bacteria are able to enter the bloodstream. If this happens, they can travel to other parts of your body, causing additional symptoms. A tuberculosis infection outside of the lungs is called an extra-pulmonary tuberculosis infection and most commonly occurs in your lymphatic system, your genitourinary system, and/or in your bones and joints. However, in some cases extra-pulmonary tuberculosis is disseminated, which means the infection has spread widely throughout your whole body.⁹

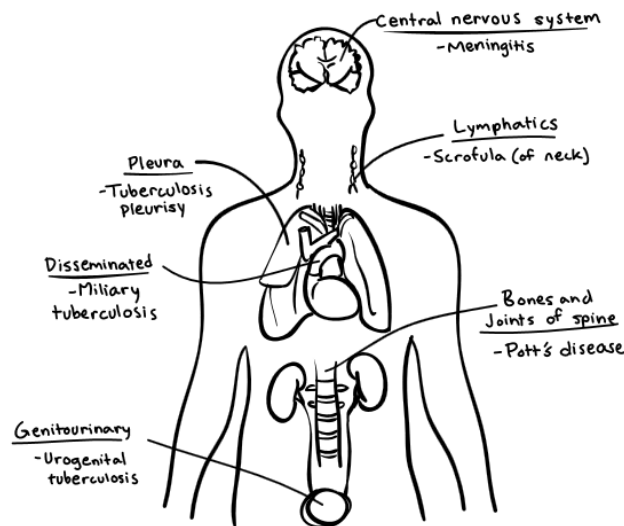


Figure 3 Image illustrating the effects of extra-pulmonary tuberculosis.

5. What puts you at risk of catching tuberculosis?

Tuberculosis is contagious, meaning that you can catch it from other people, especially if you live with someone who is infected. However, there are many other situations that can also increase your chances of getting tuberculosis. These include times of life when your immune system is weaker; for example when you are very young or very old, or when you have certain diseases that reduce immune function, such as HIV/AIDS, diabetes or cancer, or are receiving immunosuppressive medications for these or other diseases. The risk of catching tuberculosis is also linked to crowded, poorly ventilated living conditions. This is a common situation for people living in poverty, for whom malnutrition, lack access to medical care, and

substance abuse may all contribute to an increased risk of becoming infected. It is worth noting that poverty is not the only driver of crowding and inadequate living conditions. In many countries, prisons also make transmission of tuberculosis very efficient, for these reasons. Finally, drug resistant tuberculosis has been reported in 100 countries worldwide, including sub-Saharan Africa, India, China and Pakistan.¹⁰ Around 10% of people are infected with this form, which is very hard to treat.¹⁰ Your chances of catching tuberculosis is higher if you live in or travel to these regions, where it is becoming a major public health problem.

6. How likely are you to get tuberculosis?

Tuberculosis is the world’s second most deadly infectious disease after HIV/AIDS. In 2015, around 10.4 million people got active tuberculosis and 1.4 million people died of the disease, mainly in low- and middle-income countries.¹¹ HIV (human immunodeficiency virus) attacks and weakens your immune system. This reduces your ability to fight off other infections including tuberculosis, making it around 30 times more likely you will become infected with both HIV and tuberculosis.¹² This type of coinfection is often very serious, and tuberculosis is a leading cause of death of people with HIV infection.

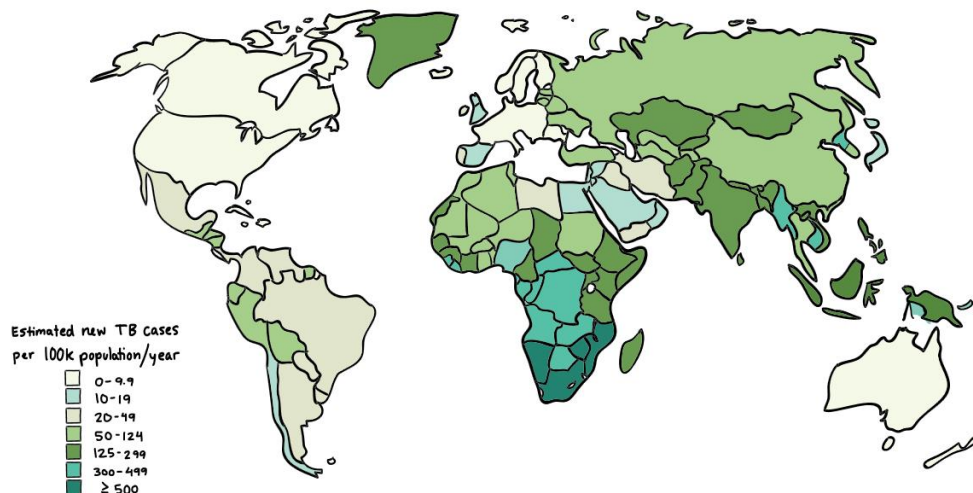


Figure 4 Map illustrating TB prevalence around the world.

7. How is tuberculosis treated?

Tuberculosis is a treatable and curable disease. There are at least 10 anti-tuberculosis drugs available to treat tuberculosis infection. However, unlike many other bacterial

infections, which only require a short course of medicine, tuberculosis drugs generally need to be taken for at least six to nine months. This is because the bacteria can remain latent, or dormant in your lungs for long periods of time without making you sick. It is very important to get treated properly to eliminate both latent and active tuberculosis bacteria. Your healthcare provider will choose the antibiotics you need based on whether or not your infection is latent or active, where the infection is in your body (lungs or elsewhere), your general state of health, and whether or not you have a drug resistant strain.

Treatment of latent tuberculosis - if you have tested positive for latent tuberculosis, your healthcare provider may recommend that you take either **isoniazid** or **rifampin** to prevent a first or recurrent episode of active tuberculosis. This approach is typically used to help people who are at particularly high risk of developing active tuberculosis including infants and young children, people with a recent infection (within the last 2 years), people infected with tuberculosis and HIV, and people who may have a weak immune system brought about by another disease, such as diabetes, or chronic kidney failure.

Treatment of active, drug-sensitive tuberculosis - most cases of active, drug-sensitive tuberculosis are treated with a standard six-month course (short course) of four anti-tuberculosis drugs. The most common ones are **isoniazid**, **rifampin**, **ethambutol** and **pyrazinamide** (first line drugs). These drugs are very effective; however, the infection will only be cured if the drugs are taken properly, and for the prescribed length of time. If you stop taking the drugs early, or skip doses, the tuberculosis bacteria may mutate and become resistant to the drugs. Drug resistant tuberculosis is much more difficult to treat, and is more likely to be spread from one person to the next.

Treatment of drug resistant tuberculosis - if you are infected with a drug-resistant strain of tuberculosis, you will likely need a different combination of antibiotics, and you may have to take them for 2 years or more.⁹

For multidrug-resistance (MDR) and extensively drug resistance (XDR) are used the combination of first line drugs and seconde line drugs as **aminoglycosides** (amikacyn and kanamicyn), **polypeptides** (capreomicyn, viomycin, envyomicin), **fluoroquinolones** (ofloxacin, levofloxacin, moxifloxacin, gatifloxacin), **thioamides** (ethionamide,

prothionimide), cycloserine, terizidone and para-aminosalicylic acid. This chemotherapy is less effective, longer, expensive and very toxic to your liver than the short course therapy and may cause serious side effects.¹³

Third line drugs include rifabutin, macrolides (clarithromycin), linezolid, thiacetazone, thioridazine, arginine, vitamin D are still being developed, have less or unproven efficacy and are very expensive.¹⁴

8. Intrinsic or acquired drug resistance?

Intrinsic resistance - refers to the innate ability of a bacterium to resist the activity of a particular antimicrobial agent through its inherent structural or functional characteristics. Intrinsic drug resistance in *M. tuberculosis* has been attributed to its unique cell wall properties, including the presence of mycolic acids, which are high-molecular-weight α -alkyl, β -hydroxy fatty acids covalently attached to arabinogalactan, and which constitute a very hydrophobic barrier responsible for resistance to certain antibiotics.¹⁵ In addition, *M. tuberculosis* possesses β -lactamase enzymes, which confer intrinsic resistance to β -lactam antibiotics, while efflux mechanisms appear to play an important role in resistance to antibiotics such as tetracycline and the aminoglycosides.

Acquired drug resistance - occurs when a microorganism obtains the ability to resist the activity of a particular antimicrobial agent to which it was previously susceptible. Acquired drug resistance in *M. tuberculosis* is caused mainly by spontaneous mutations in chromosomal genes, and the selective growth of such drug-resistant mutants may be promoted during suboptimal drug therapy.¹⁶ The rate of genetic mutations leading to resistance varies somewhat among anti-tuberculosis drugs, from a frequency of $\sim 10^{-5}$ - 10^{-6} organisms for isoniazid to $\sim 10^{-7}$ - 10^{-8} organisms for rifampin.¹⁷ Since the bacterial burden typically present in pulmonary cavities does not exceed 10^{12} bacilli,¹⁸ combination therapies is highly effective for drug-susceptible disease, and the risk for development of acquired drug resistance is minimized.

9. Investigation of Anti-TB Drugs structure

As a part of our ongoing studies in developing of new active compounds with anti-mycobacterial activity we report here a fragment-based screening. Here, we took advantage of the similarity structure of small molecules bound with drug target to define new group that

interact with the protein and discovered several binding azoles chemotypes. Where, this will help us to identify lead compounds for our future work.

Anti-tuberculosis activities of compounds possessing azoles heterocyclic. Which, containing a nitrogen atom and at least one other non-carbon atom (i.e. nitrogen, sulfur, or oxygen) as part of the ring have been reported in numerous studies.¹⁹⁻²⁵

Fragment screening and target screening are complementary approaches that combine with structural biology to explore the binding capabilities of an active site.

Sterol 14 α -demethylation as a general part of sterol biosynthetic pathways in eukaryotes has been known and studied for more than 30 years. The enzyme catalysing this reaction was first purified from yeast in 1984 (*Sacharomyces cerevisiea*), and following determination of its primary structure the cytochrome P450 sterol 14 α -demethylases were placed into the CYP51 family, a number reserved for fungal sequences. In 1986 the orthologous mammalian P450 was purified from rat liver microsomes, in 1996 the first sterol 14 α -demethylase was found in plants (*Sorghum bicolor*), and in 2000 the orthologous nature of a CYP51-like gene from *Mycobacterium tuberculosis* to eukaryotic CYP51s was confirmed.

CYP51 is also of great practical importance as a drug target. Inhibition of sterol 14 α -demethylase activity blocks sterol biosynthesis, which is lethal in unicellular organisms. The demands for CYP51 inhibitors are increasing continuously because of drug resistance, worldwide increase in the incidence of opportunistic fungal infections as a consequence of the rising number of immunocompromised hosts (HIV-infections, cancer chemotherapy, organ and bone marrow transplantation) and patients with primary infections such as tuberculosis, etc.

Azoles are the most broadly known CYP51 inhibitors. They coordinate to the heme iron through a basic nitrogen and inhibit activity preventing substrate binding and metabolism. Azoles are less toxic, inexpensive and broadly available, yet have several disadvantages. Their long term usage can inhibit other P450 enzymes and leads to resistance allowing the drugs tolerance in the pathogen. It is well known that affinities of different CYP51 orthologs to the same azole drug may vary significantly (up to 3-4 orders of magnitude). Also, it is well known that the lower drug susceptibility a TB strain has, the more frequently and rapidly resistance develops. Besides, selecting the most powerful CYP51 inhibitors would help to shorten treatment time and lower the necessary doses.²⁶

CHAPTER II

Computer-Assisted Drug Design

What is computer-assisted drug design (CADD), and why is it important? There is no clear definition, although a consensus view has emerged. Simply, CADD is the coalescence of information on chemical structures, their properties, and their interactions with biological macromolecules. Further, these data are transformed into knowledge intended to aid in making better decisions for drug discovery and development.

These are representative of some questions facing the current drug-design community and significant applications of CADD.

Of the compounds included in our dataset, how many could be predicted to lack drug like properties based on similarity in properties to known orally active drugs?

How many would be predicted to be inactive based on the known structure–activity data available on *M. tuberculosis* H37Rv inhibitors?

Given the structure–activity relationships (SARs) available on the inhibitors, what could one determine regarding the active site of *M. tuberculosis* H37Rv?

What novel classes of compounds could be suggested based on the SAR of inhibitors, or based on the new crystal structure of the complex?

Do the most potent compounds share a set of properties that can be identified and used to optimize a novel lead structure?

Can a predictive equation relating properties and affinity for the isolated enzyme be established?

1. Predictive Quantitative Structure–Activity Relationship Modeling

At the beginning of its over 40 years of existence as an independent area of research, quantitative structure–activity relationship (QSAR) modeling was viewed strictly as analytical physical chemical approach applicable only to small congeneric series of molecules. The technique was first introduced by Hanschet al.²⁷ on the basis of implications from linear free-energy relationships in general and the Hammett equation in particular.²⁸

It is based upon the assumption that differences in physicochemical properties account for the differences in biological activities of compounds. According to this approach, the changes in physicochemical properties that affect the biological activities of a set of congeners are of three major types: electronic, steric, and hydrophobic.²⁹

The quantitative relationships between biological activity (or chemical property) and the structural parameters could be conventionally obtained using multiple linear regression (MLR) analysis. The fundamentals and applications of this method in chemistry and biology

have been summarized by Hansch and Leo.²⁹ This traditional QSAR approach has generated many useful and, in some cases, predictive QSAR equations and led to several documented drug discoveries.^{30–32}

Many years of active research in QSAR have dramatically changed the breadth and the depth of this field in all its components including the diversity of target properties, descriptor types, data modeling approaches, and applications. The most important changes in QSAR deal with a substantial increase in the size of data sets available for the analysis and an increasing use of QSAR models as virtual screening tools to discover biologically active molecules in chemical databases and virtual chemical libraries.

2. Key Quantitative Structure–Activity Relationship Concepts

An inexperienced user or sometimes even an avid practitioner of QSAR could be easily confused by the diversity of methodologies and naming conventions used in QSAR studies. 2D or three-dimensional (3D) QSAR, variable selection or artificial neural network (ANN) methods, Comparative molecular field analysis (CoMFA), or binary QSAR present examples of various terms that may appear to describe totally independent approaches, which cannot be generalized or even compared to each other. In fact, any QSAR method can be generally defined as an application of mathematical and statistical methods to the problem of finding empirical relationships (QSAR models) of the form $P_i = k(D_1, D_2, \dots, D_n)$, where P_i are biological activities (or other properties of interest) of molecules, D_1, D_2, \dots, D_n are calculated (or, sometimes, experimentally measured) structural properties (molecular descriptors) of compounds, and k is some empirically established mathematical transformation that should be applied to descriptors to calculate the property values for all molecules.

The relationship between values of descriptors D and target properties P can be linear (e.g., MLR as in the Hansch QSAR approach), where target property can be predicted directly from the descriptor values, or nonlinear (such as ANNs or classification QSAR methods) where descriptor values are used in characterizing chemical similarity between molecules, which in turn is used to predict compound activity.

The differences in various QSAR methodologies can be understood in terms of the types of target property values, descriptors, and optimization algorithms used to relate descriptors to the target properties and generate statistically significant models.

Target properties (regarded as dependent variables in statistical data modeling sense) can generally be of three types:

- (1) continuous, i.e., real values covering certain range, e.g., IC₅₀, MIC values, or binding constants;
- (2) categorical related, classes of target properties covering certain range of values, e.g., active and inactive compounds, frequently encoded numerically for the purpose of the subsequent analysis as 1 (for active) or 0 (for inactive), or adjacent classes of metabolic stability such as unstable, moderately stable, stable; and
- (3) categorical unrelated, classes of target properties that do not relate to each other in any continuum, e.g., compounds that belong to different pharmacological classes, or compounds that are classified as drugs versus non drugs.

Chemical descriptors (or independent variables in terms of statistical data modeling) can be typically classified into two types:

- (1) continuous (i.e., range of real values, e.g., as simple as molecular weight or many molecular connectivity indices); or
- (2) categorical related (i.e., classes corresponding to adjacent ranges of real values, e.g., counts of functional groups or binary descriptors indicating presence or absence of a chemical functional group or an atom in a molecule).

Descriptors can be generated from various representations of molecules, e.g., 2D chemical graphs or 3D molecular geometries, giving rise to the terms of 2D or 3D QSAR, respectively.

Correlation methods (which can be used either with or without variable selection) can be classified into two major categories:

- (1) linear (e.g., linear regression (LR), or principal component regression (PCR), or partial least squares (PLS)) or
- (2) nonlinear (e.g., k nearest neighbor (kNN), recursive partitioning (RP), ANNs, or support vector machines (SVMs)).³³

In some cases, the types of biological data, the choice of descriptors, and the class of optimization methods are closely related and mutually inclusive. For instance, MLR can only be applied when a relatively small number of molecular descriptors are used (at least five to six times less than the total number of compounds) and the target property is characterized by a continuous range of values. The use of multiple descriptors makes it impossible to use MLR

due to a high chance of spurious correlation³⁴ and requires the use of PLS or nonlinear optimization techniques.

3. Molecular Descriptors

It has been said frequently that there are three keys to the success of any QSAR model building exercise: descriptors, descriptors, and descriptors. Many different molecular representations have been proposed in literature, including Hansch-type parameters, topological indices,^{35, 36} quantum mechanical descriptors,³⁷ molecular shapes,³⁸ molecular fields,³⁹ atomic counts,⁴⁰ 2D fragments,⁴¹ 3D fragments,⁴² etc.

Various descriptors have been used to represent molecular identities in our different studies. We discuss below all the types of molecular descriptors used.

3.1. Molecular Size and Shape

Molecular size can be assessed in different ways. The molecular weight is easily calculated from the molecular formula. Also a simple atom count can be seen as a crude measure of molecular size. Other descriptors often used are molecular volume and molecular surface. The solvent-accessible surface calculations are based on a grid method derived by Bodor et al.,⁴³ using the atomic radii of Gavezotti.⁴⁴ For the molecular volume can be defined according to the molecular surface.

Another size descriptor is the molar refractivity (MR), which has often been included as a steric parameter. Tute has aptly dubbed it as the most 'chameleon-like' parameter⁴⁵ and, despite 40 years of usage, it still remains an elusive descriptor which defies easy interpretability in terms of QSAR. Pauling and Pressman first suggested that MR could be used to model the dispersion forces affecting hapten-antibody interactions since MR was directly related to molecular polarizability, α .²⁷

$$MR = \frac{4\pi N\alpha}{3}$$

$$MR = \frac{n^2 - 1}{n^2 + 2} * \frac{MW}{d}$$

MR is usually defined by the Lorentz/Lorenz, where n is the refractive index, d is the density, and MW is the molecular weight of a compound. Since n of organic liquids does not vary much, the molar volume term constitutes from 75% to 80% of MR. Although van de

Waterbeemd and Testa have shown a strong correlation between MR and van der Waals volume,⁴⁶ MR has been shown to provide superior correlations, particularly in ligand–receptor interactions where it is not adequately replaced by molar volume.^{47, 48} This suggests that polarizability is important when dealing with interactions in polar space. This has been borne out in extensive molecular graphics studies by Hansch and Blaney with various ligand–receptor systems.⁴⁹

Shape descriptors are also often highly correlated to molecular size. Flexibility measures, e.g., the number of rotatable bonds, can be interpreted as information about both size and variable shape of the molecule. It was suggested that less flexibility as measured by the number of rotatable bonds improves oral bioavailability.⁴⁸

Molecular size and shape descriptors are usually part of every descriptor set used in QSAR modeling, although they are not necessarily important in the final model. This does not imply that molecular size does not influence the target property in question, but rather that molecular size may be considered implicitly in other descriptors like lipophilicity or polar surface area.

3.2. Lipophilicity and Hydrophobicity

Lipophilicity, the ‘love of fat,’ and hydrophobicity, the ‘fear of water,’ are often taken as synonyms, but do not exactly describe the same property: hydrophobicity considers the interaction between the compound and water, whereas lipophilicity is a measure of the interaction with a lipid. It has been suggested that hydrophobicity may be a component of lipophilicity^{50, 51}:

$$\textit{lipophilicity} = \textit{hydrophobicity} - \textit{polarity}$$

and that lipophilicity may consist of a cavity (volume or size related) and a polarity term (the combination of hydrogen bonding and dipolarity/polarizability)⁵²:

$$\log P = aV + \Lambda$$

$$(V = \textit{molecular volume}, \Lambda = \textit{polarity term})$$

It has long been assumed that molecular size in general and hydrogen bonding or polarity together are largely able to explain lipophilicity.^{53, 54} In summary, hydrophobicity can be seen as a (mostly) size- or cavity-related term, i.e., only dependent on the molecule itself,

whereas lipophilicity includes a polarity factor and depends additionally on the lipid used. Lipids with different polar properties will give different lipophilicity values for the same compound, a phenomenon that is used for assessment of hydrogen bonding.^{52, 55, 56} Lipophilicity, as the ability of a molecule to mix with an oily phase rather than with water, is usually measured as partition coefficient, P , between the two phases and is often expressed as $\log P$.⁵⁷

Due to the importance of lipophilicity, different ways to assess the value experimentally and to calculate $\log P$ have been developed. Since it has been found that $\log P_{\text{oct}}$, the logarithm of the partition coefficient between *n*-octanol and water, can be calculated from the sum of the contributions (π) of the molecular fragments, various fragmental approaches for calculating $\log P$ have been developed.⁵⁸

Nowaday, both experimentally obtained and calculated $\log P$ values usually refer to the partitioning between *n*-octanol and water, if nothing else is stated. This parameter is sometimes also termed $\log K_{\text{OW}}$.⁵⁹ However, it is important to distinguish between the pH-independent partition coefficient, P , and the pH-dependent distribution coefficient, D . The former expresses the quotient of the concentrations of the neutral compound in both phases, whereas the latter expresses the quotient of the concentration of all ionized and unionized species of the compound in both phases. It is generally assumed that (almost) only the unionized species can partition into the lipid phase.⁶⁰ Although ionized species are probably able to partition into the lipid phase, at least together with a counter ion,⁶¹ the partition coefficient of such an ionic species is usually about three orders of magnitude lower than the partition coefficient of the neutral species (i.e., if $\log P_{\text{neutral}}$ is 4, $\log P_{\text{ion}}$ is about 1).⁶² It is, thus, easily understandable that $\log D$ will become lower the more of the ionized species is present at the investigated pH.

However, it is likely that $\log D$ at physiological pH is actually the more interesting parameter, since it gives the lipophilicity at a relevant pH. The pH to consider is 7.4 if blood/body tissue conditions are studied and around 6.0–8.0 in order to mimic the conditions along the gastrointestinal tract. pH varies from very acidic in the stomach, around pH 6.0–6.5 in the proximal small intestine to slightly basic in the colon, pH 8.0.⁶³ pH varies also with food intake.⁶⁴

3.3. Hydrogen Bonding

Hydrogen bonding has been found to be an important part in structure permeation relationships.⁶⁵⁻⁶⁸ Hydrogen bonds are also important for molecular recognition and thus will not only determine a compound's activity but also its metabolism or transport properties. Van de Waterbeemd et al.,⁶⁶ suggested that the calculated polar surface area (PSA) might be a more easily accessible descriptor of hydrogen bonding ability. Since then, various different definitions for polar surface area have been used.^{66, 69, 70} The value for PSA will differ depending on what type of surface is calculated (e.g., Van der Waals surface, solvent-accessible surface,⁷¹ or Connolly surface^{72,73}) and which atoms are used to define the surface. Nitrogen, oxygen and attached hydrogen atoms usually define a polar surface area, although sulfur atoms have been suggested as well.⁶⁵ It has also been proposed that an indicative PSA can be derived from the 2D structure alone.⁷⁴

It has been found that simple counting descriptors may give a good enough correlation to interesting ADME properties, e.g., to permeability.⁶⁵ Such counting descriptors for hydrogen bonding are the number of hydrogen bond donors and acceptors, which can be defined either as donor and acceptor atoms⁷⁵ or as donor hydrogen atom and acceptor electron pair.⁷⁶

3.4. Quantum Chemical Descriptors

Quantum chemically derived descriptors include also descriptors like highest occupied molecular orbital (HOMO), lowest unoccupied molecular orbital (LUMO), hardness (LUMO-HOMO)/2, dipole moment, atomic charges, polarizability, polarity, ionization potential, electrostatic potentials, molecular energy values, and others. Quantum chemical descriptors and their use in QSAR/QSPR studies were reviewed some time ago.⁷⁷

4. Quantitative Structure–Activity Relationship Modeling Approaches

4.1. General Classification

Many different approaches to QSAR have been developed since Hansch's seminal work. As briefly discussed above, the major differences between these methods can be analyzed from two viewpoints:

- (1) the types of structural parameters that are used to characterize molecular identities starting from different representation of molecules, from simple chemical formulas to 3D conformations, and
- (2) the mathematical procedure that is employed to obtain the quantitative relationship between these structural parameters and biological activity.

Based on the origin of molecular descriptors used in calculations, QSAR methods can be divided into three groups.

One group is based on a relatively small number (usually many times smaller than the number of compounds in a data set) of physicochemical properties and parameters describing hydrophobic, steric, electrostatic, etc. effects. Usually, these descriptors are used as independent variables in multiple regression approaches. In the literature, these methods are typically referred to as Hansch analysis.

A more recent group of methods is based on quantitative characteristics of molecular graphs (molecular topological descriptors). Since molecular graphs or structural formulas are ‘two-dimensional,’ these methods are described as 2D QSAR. Most of the 2D QSAR methods are based on graph theoretical indices. Although these structural indices represent different aspects of molecular structures, and, what is important for QSAR, different structures provide numerically different values of indices, their physicochemical meaning is frequently unclear.

The third group of methods is based on descriptors derived from spatial (3D) representation of molecular structures. Correspondingly, these methods are referred to as 3D QSAR; they have become increasingly popular with the development of fast and accurate computational methods for generating 3D conformations and alignments of chemical structures. Perhaps the most popular example of 3D QSAR is CoMFA, developed by Cramer et al.,⁷⁸ which has combined the power of molecular graphics and PLS technique and has found wide applications in medicinal chemistry and toxicity analysis.⁷⁹

4.2. Transforming the Bioactivities

The main advantage of transforming data is to guarantee linearity, to achieve normality, or to stabilize the variance. Several simple nonlinear regression relationships can be made linear through the appropriate transformations. The simplest and most common method of transforming⁸⁰ bioactivity data is to take the log or negative log of the bioactivities to reduce the range of the data.

4.3. Training and Test Set Creation

The method of creating Training and Test Sets that are representative of the population is to choose molecules that represent all the molecules of interest based on molecular structure and bioactivity. The number of molecules in the Test Set is determined (20% of the total molecules in this study) and then all the molecules are placed in a table and ordered based on bioactivities. With the table prepared, the extraction of the molecules for the Test Set can begin through an iterative process starting at the top of the table.

4.4. Determination of the Best Set of Descriptors Approaches

Both 2D and 3D QSAR studies have focused on the development of optimal QSAR models through variable selection. This implies that only a subset of available descriptors of chemical structures, which are the most meaningful and statistically significant in terms of correlation with biological activity, is selected.

The Stepwise Method Search selects a model by adding or removing individual descriptors, a step at a time, based on their statistical significance. The end result of this process is a single regression model, which makes it nice and simple.

The p-value for each term tests the null hypothesis that the coefficient is equal to zero (no effect). A low p-value (< 0.05) indicates that you can reject the null hypothesis. In other words, a descriptor that has a low p-value is likely to be a meaningful addition to your model because changes in the descriptor's value are related to changes in the response variable (bioactivity). Conversely, a larger (insignificant) p-value suggests that changes in the descriptor are not associated with changes in the response.

5. Building Predictive Quantitative Structure–Activity Relationship Models: The Approaches to Model Validation

5.1. The Importance of Validation

The process of QSAR model development is divided into three key steps: (1) data preparation, (2) data analysis, and (3) model validation. The implementation and relative merit of these steps is generally determined by the researcher's interests and experience, and the availability of software. The resulting models are then frequently employed, at least in theory, to design new molecules based on chemical features or trends found to be statistically significant with respect to underlying biological activity.

The first stage includes the selection of a data set for QSAR studies and the calculation of molecular descriptors. The second stage deals with the selection of a statistical data analysis technique, either linear or nonlinear such as MLR, PLS or ANN. A variety of different algorithms and computer software are available for this purpose. In all approaches, descriptors are considered as independent variables, and biological activities as dependent variables.

Typically, the final part of QSAR model development is model validation,^{81, 82} in which estimates of the predictive power of the model are calculated. This predictive power is one of the most important characteristics of QSAR models.

Ideally, it should be defined as the ability of the model to predict accurately the target property (e.g., biological activity) of compounds that were not used in model development.

Here, we are going to discuss about the validation parameters for the QSAR models which are developed by multiple linear regression (MLR). Four tools of assessing validity of QSAR models⁸³ are (i) cross-validation, (ii) bootstrapping, (iii) randomization of the response data, and (iv) external validation. Where we are using the data that created the model (an internal method) and using a separate data set (an external method) (Fig.5).

The methods of least squares fit (R^2), cross validation (Q^2)⁸⁴⁻⁸⁶, adjusted R^2 (R^2_{adj}), chi-squared test (χ^2), rootmean-squared error ($RMSE$), bootstrapping and scrambling (Y-Randomization)^{87, 88} are internal methods of validating a model. The best method of validating a model is an external method, such as evaluating the QSAR model on a test set of compounds.

5.2. Internal Validation

5.2.1. Least Squares Fit

The most common internal method of validating the model is least squares fitting. This method of validation is similar to linear regression and is the R^2 (squared correlation coefficient) for the comparison between the predicted and experimental activities. An improved method of determining R^2 is the robust straight line fit, where data points are away from the central data points (essentially data points a specified standard deviation away from the model) are given less weight when calculating the R^2 . An alternative to this method is the removal of outliers (compounds from the training set) from the dataset in an attempt to optimize the QSAR model and is only valid if strict statistical rules are followed. The difference between the R^2 and R^2_{adj} value is less than 0.3 indicates that the number of

descriptors involved in the QSAR model is acceptable. The number of descriptors is not acceptable if the difference is more than 0.3.

$$R^2 = 1 - \frac{PRESS}{\sum_{i=1}^n (y_i - y_m)^2}$$

$$PRESS = \sum_{i=1}^n (\hat{y}_i - y_i)^2$$

Where, y and \hat{y} are the experimental and predicted bioactivity for an individual compound in the training set, y_m is the mean of the experimental bioactivities, and n is the number of molecules in the set of data being examined. *PRESS* is the predictive residual sum of the squares.

5.2.2. Fit of the Model

Fit of the QSAR models can be determined by the methods of chi-squared (χ^2) and root-mean squared error (*RMSE*). These methods are used to decide if the model possesses the predictive quality reflected in the R^2 . The use of *RMSE* shows the error between the mean of the experimental values and predicted activities. The chi squared value exhibits the difference between the experimental and predicted bioactivities:

$$\chi^2 = \sum_{i=1}^n \left(\frac{(y_i - \hat{y}_i)^2}{\hat{y}_i} \right)$$

$$RMSE = \sqrt{\sum_{i=1}^n \frac{(\hat{y}_i - y_m)^2}{n-1}}$$

Large chi-square or *RMSE* values (≥ 0.5 and 1.0 , respectively) reflect the model's poor ability to accurately predict the bioactivities even the model is having large R^2 value (≥ 0.7). For good predictive model the chi and *RMSE* values should be low (< 0.5 and < 0.3 , respectively). These methods of error checking can also be used to aid in creating models and are especially useful in creating and validating models for nonlinear data sets, such as those created with Artificial Neural Network (ANN) ⁸⁹.

However, excellent values of R^2 , χ^2 and *RMSE* are not sufficient indicators of model validity. Thus, alternative parameters must be provided to indicate the predictive ability of models. In principle, two reasonable approaches of validation can be envisaged one based on

prediction and the other based on the fit of the predictor variables to rearranged response variables.

5.3. External validation

Several authors have suggested that the only way to estimate the true predictive power of a QSAR model is to compare the predicted and observed activities of an (sufficiently large) external test set of compounds that were not used in the model development ^{90, 91, 92-94}. The problem in external validation is how can we select the training and test set? Roy et al. clearly discussed that how we can solve this problem in one of their article. ⁹⁵

To estimate the predictive power of a QSAR model, Golbraikh and Tropsha recommended use of the following statistical characteristics of the test set ⁹⁶: (i) correlation coefficient R between the predicted and observed activities; (ii) coefficients of determination (R^2) (predicted vs. observed activities r_0^2 , and observed vs. predicted activities $r_0'^2$); (iii) slopes k and k' of the regression lines through the origin. They consider a QSAR model is predictive, if the following conditions are satisfied ⁹⁶:

$$R_{test}^2 > 0.6 ;$$

$$r^2 - \frac{r_0^2}{r^2} < 0.1 \quad ; \quad r'^2 - \frac{r_0'^2}{r'^2} < 0.1 \quad \text{and}$$

$$0.85 \leq k \leq 1.15 \quad \text{or} \quad 0.85 \leq k' \leq 1.15$$

The predictive ability of the selected model was also confirmed by external R_{test}^2 . A value of R_{test}^2 is greater than 0.6 may be taken as an indicator of good external predictability.

$$R_{test}^2 = 1 - \frac{\sum_{i=1}^{test} (y_{exp} - y_{pred})^2}{\sum_{i=1}^{test} (y_{exp} - \bar{y}_{tr})^2}$$

Where \bar{y}_{tr} is the average value for the dependent variable for the training set. Kubinyi et al. ⁹⁰, Novellino et al. ⁹², Norinder ⁹³, and Golbraikh and Tropsha ⁹⁶ demonstrated that all of the above-mentioned criteria are necessary to adequately assess the predictive ability of a QSAR model. Norinder suggest ⁹³ that the external test set must contain at least five compounds, representing the whole range of both descriptor and activities of compounds included into the training set.

6. Applicability Domain

Activity of the entire universe of chemicals can not be predicted even by a robust and validated QSAR model. The prediction of a modeled response using QSAR is valid only if the compound being predicted is within the applicability domain of the model. The applicability domain is a theoretical region of the chemical space, defined by the model descriptors and modeled response and, thus, by the nature of the training set molecules. It is possible to check whether a new chemical lies within applicability domain using the leverage approach. A compound will be considered outside the applicability domain when the leverage value is higher than the critical value of $3p/n$, where p is the number of model variables plus 1 and n is the number of objects used to develop the model.

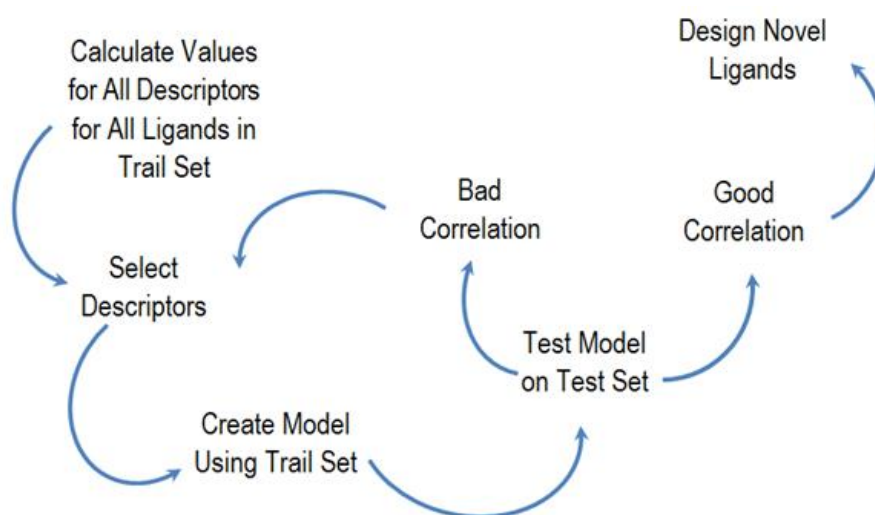


Figure 5 General methodology of a QSAR Study.

7. Molecular Modeling Techniques

A key requirement in molecular modeling is to be able to calculate the energy of an arrangement of atoms and/or molecules in 3D space. There exist a variety of methods that can be used to perform such calculations.

The most ‘fundamental’ way to tackle this problem is to use *quantum mechanics*, where in the Schrödinger equation is solved for the distribution of electrons and atoms in the system in order to derive a wave function from which other properties can be derived. As will be described elsewhere in this chapter, a variety of different quantum mechanical methods are applicable to the systems and problems typically encountered in drug design. Quantum

mechanical methods have some clear advantages in that they are much less reliant on empirical parameters for the system being studied and they are also able to provide information on some key properties (e.g., electric multipoles, electrostatic potentials, ionization potentials, etc.) that are dependent upon a knowledge of the electronic distribution and which cannot be calculated using other techniques. However, they do have the significant drawback of being relatively time consuming to perform and so are rarely used for calculations involving large systems and/or for those on large numbers of molecules.

Empirical force field methods^{97, 98} (also known as *molecular mechanics*) ignore the electronic motions in the system and calculate the energy solely as a function of the positions of the atoms. The method uses a very simple model of the intra- and intermolecular interactions within a molecular system with the energy being partitioned into contributions from processes such as the stretching of bonds, bending of angles, rotations about single bonds, and steric and electrostatic interactions between pairs of non-bonded atoms (Fig.6). The simplest type of force field encountered in drug design applications contains just these four contributions; a common functional form is as follows:

$$E = \sum_{\text{bonds}} \frac{k_i}{2} (l_i - l_{i,0})^2 + \sum_{\text{angles}} \frac{k_i}{2} (\theta_i - \theta_{i,0})^2 + \sum_{\text{torsions}} \frac{V_n}{2} (1 + \cos(n\omega - \gamma))$$

$$+ \sum_{i=1}^N \sum_{j>i}^N \left(4\epsilon_{ij} \left[\left(\frac{\sigma_{ij}}{r_{ij}} \right)^{12} - \left(\frac{\sigma_{ij}}{r_{ij}} \right)^6 \right] + \frac{q_i q_j}{4\pi\epsilon_0 r_{ij}} \right)$$

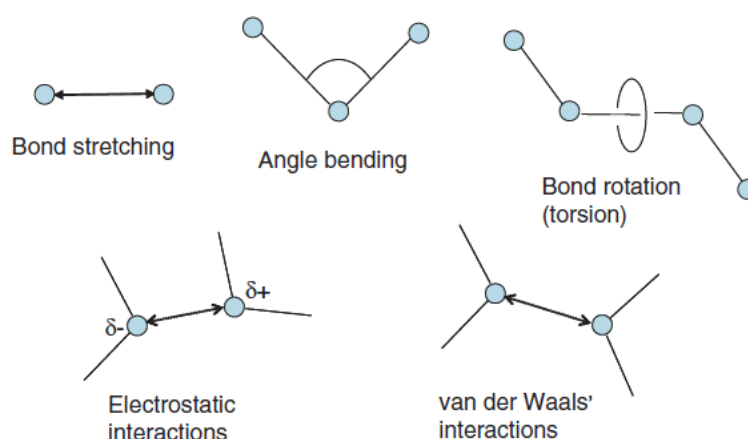


Figure 6 An illustration of the various terms that contribute to a typical force field.

The greatest appeal of quantum mechanical methods is that they can, in principle, be used to calculate the entire range of properties that are necessary to understand the characteristics of a molecule which are responsible for all its properties and that allow its recognition by and activation of receptors.

Quantum mechanical calculations are also able to extrapolate and predict properties of basically any compound without prior knowledge or parameterization, as mentioned above. This is in contrast to other computational methods like for example the classical force fields, which require extensive and complex parameterization and can only be interpolated within the boundaries of that parameterization. However, quantum mechanics techniques are computationally very intensive and require significantly more specialist expertise for the correct and meaningful interpretation of the data they generate than do conventional molecular mechanics or force field methods.⁹⁸ This significant difference in required expertise combined with a lack of understanding of the potential of quantum mechanical calculations in the wider chemistry community and particularly in medicinal chemistry may perhaps be responsible for the apparent under utilization of these very powerful methods.

8. Theoretical Background for Quantum Mechanical Calculations

Although the purpose of this chapter is to review applications of quantum mechanical calculations relevant to medicinal chemistry and drug design. These introductions are however kept to a minimum, focus on the main differences between methods and their known strengths and weaknesses in relation to medicinal chemistry applications, and will contain only one mathematical equation, probably much to the relief of most readers.

For a more background on quantum mechanical calculations we refer to my Master thesis,⁹⁹ such as : ab initio calculations, density functional calculations, and semiempirical as well as molecular mechanical methods.

The Schrödinger equation forms the basis of quantum mechanics and has the simple form for an eigenvalue problem:

$$H\psi = E\psi$$

This famous equation cannot be solved explicitly for anything larger than hydrogen, even with modern computer power.

Therefore, several approximations were introduced in order to enable the quantum mechanical treatment of molecules of more immediate interest to most chemists. These are for

example the Born–Oppenheimer approximation, treating the nuclei of atoms as fixed, and the Hartree–Fock (HF) approximation where an effective potential replaces the true electron–electron potential description, effectively eliminating electron correlation. Another is the introduction of basis sets, designed to mimic the structure of orbitals, in place of actual electron integrals. The quality of these basis sets is essential for ab initio calculations, and as a general rule the larger they are and the more individual Gaussian functions they contain the better. Rather than discussing them here in detail we will refer to my Master thesis⁹⁹ for further reading. The usefulness and accuracy of calculations using these approximations is mostly confirmed by comparison with experiment, particularly for molecular geometries and properties like for example dipole moments, and despite the use of these simplifications, the results are often surprisingly accurate.

However, some approximations are more questionable and the magnitude of error introduced is often unclear. Despite using a number of approximations, quantum mechanical calculations are generally very accurate and useful in practically answering questions and describing molecular structures, properties, and interactions important for medicinal chemistry. It also has to be emphasized that for some of these questions, for example those relating to chemical reactivity, molecular properties like nucleophilicity, electrophilicity, charge distribution, spin–orbit coupling, dipole and higher multipole moments relating to polarizability, infrared, Raman and NMR chemical shifts, circular dichroism, and magnetic susceptibility,¹⁰⁰ quantum mechanical calculations are the only available option to the computational and medicinal chemist to obtain accurate predictions.

As pointed out above, the focus of this chapter is to review the application of quantum mechanical calculations in medicinal chemistry and drug design rather than to deal in detail with the theory of the methods. For that, there are short summaries for the most important approaches below (Sections 8.1- 8.4). Then Section 9 discusses the applications of quantum mechanical calculations.

Quantum mechanical calculations, in contrast to the molecular mechanics approach, are directly derived from the physical principles that govern molecular structure, by solution of the Schrödinger equation in an approximate way. The techniques can be divided into ab initio, DFT methods and semiempirical methods. While ab initio and density functional methods do not resort to parametrization to solve the Schrödinger equation, semiempirical methods contain parameters that avoid the computation of some time-consuming integrals required in ab initio and DFT calculations. Moreover, the semiempirical techniques take into account only the valence electrons. Although there are far fewer parameters in semiempirical

methods, they are also less intuitive than those in molecular mechanics methods. All three methods (ab initio, DFT, and semiempirical) provide a wave function from which all electronic properties can be computed.¹⁰¹

8.1. Ab Initio Methods

This category of methods based on HF theory utilizing the self-consistent-field procedure (SCF), is the most widely used type of quantum mechanics calculation. It scales with about N^4 , which means that when doubling the number of electrons in a calculation that it will take 16 times as long. This of course immediately sets a limit to the scope of this type of approach in terms of the size of molecule that can be calculated on a reasonable time scale in terms of medicinal chemistry and drug design, i.e., in a matter of a couple of days at best. Over the last 15 years, this size limit for molecules that are amenable to ab initio calculations has increased from about 10–15 heavy atoms at a moderate basis set (3-21G) to about 40–50 heavy atoms currently on even a high-end desktop computer. However, if larger time scales and more compute power is invested, very significant results can be achieved. Recently, a full geometry optimization on a 126-atom chain of 12 alanines has been performed at the HF 3-21G level.¹⁰² Although it is unclear whether this level of theory provides an accurate enough description of the system in terms of for example hydrogen bonding geometries, it is certainly an important realization that calculations of this size are not only possible but also practical for addressing medicinal chemistry problems. It is also clear that for example the treatment of electron correlation, that would be provided by methods like perturbation methods like MP2 (Møller–Plesset level 2) is rather less practical, since they scale with N^5 , which is also the case for the higher level correlation methods like coupled cluster methods, scaling with N^7 .¹⁰³ Although these higher level methods provide excellent accuracy and agreement with experiment in terms of geometries and relative energies, they are rather less useful for applications in computational chemistry and medicinal chemistry on pharmacologically relevant molecular systems, and will therefore not be discussed further in this chapter. However, there are methods that enable the treatment of electron correlation while remaining fast enough to be used for larger systems. They are the DFT methods and this approach will be discussed in the next section.

8.2. Density Functional Theory Methods

DFT is the latest addition to the field of quantum chemistry. It is probably an understatement to state that DFT has strongly influenced the evolution of quantum chemistry

during the last 15 years, the term revolutionized is perhaps more appropriate.¹⁰⁴ DFT is based on the Hohenberg–Kohn paradigm,¹⁰⁵ which states that the electron density and electronic Hamiltonian have a functional relationship, which allows the computation of all ground-state molecular properties without a wave function. This means that it is possible to obtain the properties of a molecule after determination of only three coordinates, regardless of molecular size. However, we do not know exactly what the nature of this functional relationship is. The only approach is to build trial exchange–correlation functionals and assess their relevance and accuracy. In its current Kohn–Sham formulation DFT is a method still very much underdevelopment, and although it is a long way away from its promise, the modern-day Kohn–Sham DFT has still massive computational advantages over *ab initio* methods and can be applied just as easily via implementations in modern day commercial software packages. Current implementations are for example the functionals B3LYP^{106, 107} and BP86^{108, 109} which have been shown to have significant advantages over *ab initio* approaches since their performance is roughly equivalent to the electron correlation MP2 method at the cost of only a HF/SCF level calculation.¹⁰³ Another way of utilizing this advantage is to use lower-level density functional equivalent in performance to HF/SCF approaches and trade off advantages in speed against increase in quality of for example size of basis sets to allow more accurate description of molecular systems. In addition to the above-mentioned advantages in speed and performance of DFT over traditional *ab initio* methods, it is also differentiated by its ability to accurately describe the electronic properties of transition metals and their complexes.¹¹⁰

8.3. Semiempirical Methods

This category of methods has been developed in parallel with *ab initio* methods based on the realization that further simplifications were needed in order to be able to perform calculations on larger molecular systems and reactions. The main difference between semiempirical and *ab initio* as well as DFT is the additional use of parameters derived either empirically or from high-level *ab initio* calculations in place of the explicit calculation of some molecular integrals.¹⁰³

This has the obvious benefit of speeding up the calculations but comes at a significant cost in terms of accuracy of the results. Methods like AM1¹¹¹ and PM3¹¹² perform very well compared to *ab initio* and DFT methods for properties like atomic charges, electrostatic potentials, dipole moments and highest occupied molecular orbit/lowest unoccupied molecular orbit (HOMO/LUMO) energies. However, they have significant deficits in terms of accuracy of molecular structures, particularly hydrogen bond geometries (AM1) as well as the

hybridization of for example nitrogen atoms in amide bonds and also heterocyclic aromatic ring systems.¹¹³ Nevertheless, they are a very valuable addition to the tools available to computational chemists, particularly when dealing with larger molecular systems.

8.4. Molecular Mechanics or Force Field Methods

Molecular mechanics have virtually nothing in common with any of the methods described so far. They describe chemical bonds as a spring between two spheres and build a model of a molecular system based on classical mechanics and some empirical corrections.¹⁰³ Parameters and parameter sets, often called ‘force fields,’ are derived based on a training set to provide a best fit for specific bond types or molecular classes. Some examples for molecular force fields are the MM2/MM3/MM4¹¹⁴ series, which is generalized for large organic systems, whereas others like AMBER¹¹⁵ are specialized for certain classes of macromolecules like proteins. Others are the Tripos force field¹¹⁶ and the Merck molecular force field (MMFF).¹¹⁷ It has to be pointed out at this stage that some if not all force fields are developed by using quantum mechanical calculations to derive bond and torsion parameters. As an example, the parameterization of the MM3 force field makes extensive use of high-level ab initio calculations and the results of the force field calculations are compared with high-level ab initio calculations to assess the quality of the results.¹¹⁸

9. Application of Quantum Mechanical Calculations to Medicinal Chemistry and Drug Design

One of the major challenges for computer-aided drug design is that it is not governed by the clear-cut rules of design in engineering, and hence, these methods do not produce a finished product by a fully prescribed procedure. The limitations of the rational computer-aided drug design approach arise because of the complexity of the biological processes involved in drug actions and metabolism at the molecular level and the level of approximation that must be used in describing molecular properties.¹⁰¹ However, there is clear evidence in the literature that molecular modeling and computer-aided drug design methods and also data analysis and chemoinformatics approaches have become very important tools for drug discovery and that they have been successfully applied to medicinal chemistry,¹¹⁹ particularly hit and lead generation as well as at the lead development stages.¹²⁰⁻¹²² Accepting that molecular modeling and chemoinformatics are useful techniques does however not sufficiently explain why one needs quantum mechanical methods. This has been done by

Clark in a recent review, where he indicates that calculational techniques used to describe molecules should be able to describe the intermolecular interactions adequately.¹²³ He points out that this can only be achieved if the molecular electrostatics and the molecular polarizability are described well. The former is responsible for strong interactions and the latter is directly related to dispersion and other weak interactions. Therefore, following this argument, molecular interactions of any type can only be described adequately and accurately by using quantum mechanical calculations.

We will divide the application of quantum mechanical calculations to answer medicinal chemistry related questions in a drug design environment into a total of four sections on:

- (1) the accurate calculation of molecular structure,
- (2) the calculation of quantum mechanical descriptors for prediction of molecular properties and QSAR,^{124, 125}
- (3) applications to chemical reactivity and the investigation of enzyme mechanisms, and
- (4) the calculation of interactions and binding energies of small molecules with proteins.

This selection of topics is meant to reflect the main areas of interest to medicinal chemists working in the field of drug discovery. It is noted that although there are a great number of publications on the use of quantum mechanical calculations to medicinal chemistry, however, a large number of them are retrospective studies concerned with the validation of new technology rather than the prospective application to problem solving and design of new chemical entity (NCEs).

10. Computational Docking

Computational docking is used to predict the binding modes of two or more molecules. Building on two decades of research, many successful methods for docking of ligands to macromolecular targets have been developed¹²⁶⁻¹³³. Computational docking relies on two methods: first, a force field to estimate the free energy of binding of the complex, typically estimated based on a particular bound conformation, and second, a search method to explore the conformational space available to the ligand and target. Often, many approximations must be built into the method, both in the force field and in the conformation search, to allow docking with a reasonable computational effort. These may include use of simplified force fields, restriction of the search space, or limitations to the conformational flexibility of the ligand and/or target.

AutoDock Vina, relies on a number of approximations to predict the conformation and free energy of binding during a docking simulation. Generally, it is assumed that much or all of the receptor is rigid and the ligand is treated as flexible, but unlike traditional molecular mechanics methods, only torsional degrees of freedom are explored, holding bond angles and bond lengths constant. This allows very rapid transformations of coordinates during the search.

The empirical free energy force field is based on a molecular mechanics force field, which includes typical terms for dispersion/repulsion (Steric interaction), hydrophobic interaction, hydrogen bonding, and the number of active rotatable bonds between heavy atoms in the ligand. The force field has been calibrated against a PDBbind data set of complexes with known structure and binding constant, allowing the force field to predict binding free energies.

Several search methods are available in Vina, including genetic algorithms, simulated annealing, and local search. All of these methods are stochastic, so repeated docking simulations are often used to validate the exhaustiveness of the search and the solution.

11. Virtual Screening

Today, virtual screening is widely used to predict the binding of a large database of ligands to a particular target, with the goal of identifying the most promising compounds from the database for further study^{130, 134-140}. Hundreds of thousands of compounds may be evaluated in a virtual screen, so two aspects of the search are critical. First, we must be confident that the docking method will find a relevant conformation. Docking methods are typically validated by “redocking” experiments, where a series of known complexes are separated and then redocked, ensuring that the docking algorithm can reproduce the observed binding mode. Second, the predicted free energy of binding must be accurate enough to allow ranking of compounds, ensuring that compounds that are predicted to bind most strongly actually do bind when tested experimentally. Most computational docking techniques, including Vina, have an accuracy of free energy prediction of about 2–3 kcal/mol standard deviation¹⁴¹. This is not sufficient, unfortunately, to provide confident ranking. Rather, we typically refer to the process of “enrichment,” where the set of compounds that are predicted to bind tightly are enriched in compounds that actually show strong binding upon testing.

CHAPTER III

Results and Discussion

PART I

In Silico Modeling of Substitution-
Induced Effect and Structure
Property/Activity Relationship Profile
of 1, 3, 4-Oxadiazole Derivatives

Oxadiazole is a nitrogen heterocyclic nucleus that attracted a wide attention of the chemist in research for new therapeutic molecules. Out of its four possible isomers, 1, 3, 4-oxadiazoles are widely exploited for various applications¹⁴². Among heterocyclic compounds, 1, 3, 4-oxadiazoles have become an important construction motif for the development of new drugs. Compounds containing 1, 3, 4-oxadiazole cores have a broad biological activity spectrum including antibacterial, antifungal^{143, 144}, analgesic, anti-inflammatory^{145, 146}, antiviral¹⁴⁵, anticancer¹⁴⁷⁻¹⁴⁹, and anticonvulsant^{145, 150}. Therapeutic significance of these useful drugs as anti-tubercular encouraged the development of more potent and significant compounds. Extensive biochemical and pharmacological studies have confirmed that these molecules are effective as anti-tubercular compounds^{19, 21, 22, 24}. Earlier, it was reported that a number of 2, 5-disubstituted-1, 3, 4-oxadiazoles have been designed, synthesized, and screened for their anti-tuberculosis activity against *M. tuberculosis* H37Rv.¹⁹

The knowledge of the relationship between chemical structure and biological activity is an essential prerequisite for the effective search for biologically active compounds. For example, 2D QSAR¹⁵¹⁻¹⁵⁶ and 2D similarity¹⁵⁷⁻¹⁶⁰ methods can be applied almost immediately. As a part of our ongoing studies in developing new active compounds with anti-mycobacterial activity, we are going to study and understand the structural requirements to substituted-1,3,4-oxadiazole derivatives that cause the anti-tuberculosis activity, which help to identify structural information to derive new lead compounds for our future researches. In this context, the substitution effect study¹⁶¹ was done in order to deepen our understanding of the influence of various substituents on 1, 3, 4-oxadiazole ring. Here, we present the electronic and geometric structure calculations¹⁶²⁻¹⁶⁵ for 1, 3, 4-oxadiazole substituted by two functional groups of different strengths using the conceptual DFT¹⁶⁶ descriptors.

Nowadays, various approaches to simultaneously optimize many factors in drug design are broadly described under the term ‘multi-parameter optimization’ (MPO)¹⁶⁷. In this paper, we use rules of thumb and calculated metrics methods¹⁶⁸ to guide the exploration of this new anti-tuberculosis agent to identify new chemistries with a high probability of achieving the required property profile.

Starting with rules of thumb, we use Lipinski¹⁶⁹, Veber¹⁷⁰ and Petrauskas¹⁷¹ rules to study the high oral bioavailability at the target site. The latter is often an important factor for the development of bioactive molecules, as therapeutic agents and any attempt to predict or

study the bioavailability would require that both properties absorption and metabolism must be taken into account.

The main factor of drugs' absorption and metabolism is the lipophilicity which offers a critical information that enable us to better interpret our results since it's a major structural factor that influences the pharmacokinetic (permeation of physiological membranes, plasma protein binding and volume of distribution) and pharmacodynamic (target recognition, target affinity and target specificity) behavior of our anti-tuberculosis compounds.

Afterward, we extended our study towards calculated metrics methods. In this respect, we applied a Per cent Efficiency Index (PEI) and Group Efficiency (GE) analysis¹⁷²⁻¹⁷⁵ to guide the selection of best anti-tubercular compounds that use their atoms most efficiently.

1. Methods validation

Molecular geometry is determined by the quantum mechanical behavior of the electrons. It can be specified in terms of bond lengths, bond angles and dihedral angles. 1, 3, 4-oxadiazole is relatively simple systems from the computational point of view, since they are planar, symmetric (they belong to the C_{2v} point group symmetry), and do not contain large numbers of atoms. As shown from (Table.1), all the 1, 3, 4-oxadiazole geometries obtained from B3LYP and Hartree-Fock models are very similar and generally improved over geometries obtained from MP2 models. With the DFT method, the mean absolute error is smaller comparing to MP2 and HF methods, which mean that it is in a good agreement with experimental data. This demonstrates that to describe an accurate ground state configuration, the electron correlation effects that play an important role in such molecules should be taken into account. Consequently, we have chosen the DFT method to perform the substitution effect study of 1, 3, 4-oxadiazole ring (Fig.7). All the calculated results are performed by Gaussian 09 software.¹⁷⁶

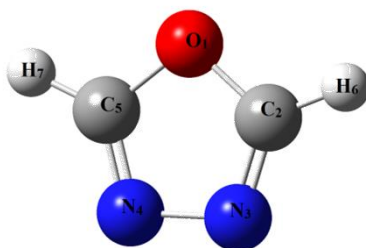


Figure 7 3D structure of 1, 3, 4-oxadiazole.

Table 1 Bond lengths and valence angles of 1, 3, 4-oxadiazole.

| Parameters | | Exp ¹⁷⁷ | HF 6-31G++(d,p) | PM2 6-31G++(d,p) | DFT/B3LYP 6-31G++(d,p) |
|---------------------------------|----------|--------------------|--------------------|---------------------|---------------------------|
| Length of bond (Angstroms) | O1-C2 | 1.348 | 1.363 | 1.337 | 1.361 |
| | C2-N3 | 1.297 | 1.304 | 1.264 | 1.291 |
| | N3-N4 | 1.399 | 1.404 | 1.383 | 1.403 |
| | C2-H6 | 1.075 | 1.074 | 1.068 | 1.078 |
| mean absolute error | | – | 0.007 | 0.0167 | 0.0065 |
| Angle of valence (Degrees) | O1-C2-N3 | 113.4 | 113.5 | 112.8 | 113.2 |
| | C2-N3-N4 | 105.6 | 105.7 | 106.0 | 105.9 |
| | C5-O1-C2 | 102.0 | 101.5 | 102.2 | 101.7 |
| | O1-C2-H6 | 118.1 | 118.0 | 118.7 | 118.1 |
| | N3-C2-H6 | - | 128.5 | 128.4 | 128.7 |
| mean absolute error | | – | 0.25 | 0.4 | 0.2 |
| Dipole moments μ (Debye) | | 3.04 | 3.43 | 3.29 | 3.24 |

2. Substitution effects on 1, 3, 4-oxadiazole

The main objective of this study is to produce two series of derivatives of 1, 3, 4-oxadiazole (Fig.8) to explore the substitution effect on this core. Where, the substitution of our groups will be at one carbon atom of 1, 3, 4-oxadiazole ring because of the C_{2v} symmetry.

Our focus was placed on modifications of the polar or the electronic effects exerted by different electron donating and withdrawing groups (“series 1 & 2” analogs, Fig.8), which is a combination of the inductive and the mesomeric effect.

Several criteria have been put forward in attempts to rationalize and quantify this effect. These can be roughly divided into two categories: energetic and reactivity-based measures. Many of these properties are available through quantum chemical calculations.

Ionization potentials and electron affinities are related in that both involve transfer of an electron between a molecular orbital and infinity: in one case (IP) we have removal of an electron from an occupied orbital and in the other (EA) addition of an electron to a virtual (or a half-occupied) orbital.

The EA of a molecule is positive for all derivatives of 1, 3, 4-oxadiazole it means that the accepted electron is bound, i.e. it is not spontaneously ejected; if the new electron is ejected in microseconds or less (is unbound), the molecule has a negative EA. For, the electron affinity which states that a compounds B_4 and B_3 with a big positive value than the other

derivatives is called an electron acceptor, and the A₃, A₄ and B₁ are less positive and electron donor. In general, the EA decreases by the addition of the alkyls groups, NH₂ and OH and increases for CN and OCH groups compared to ODZ.

Following the ionization potential values we can see that they decrease for all the derivatives just for the COH group which it stays the same as for ODZ and it increases for the CN group. Further, the NH₂ substituent shows the lower IP than the alkyl derivatives and the OH substituents. This suggests that the systems with these substituents contribute more towards electron donating character.

Similar conclusion can be drawn from the frontier molecular orbitals (FMOs), HOMO-LUMO gaps (HLG's), chemical potential, softness and hardness parameters reported in (Table.2).

The electronic chemical potential (μ) and the chemical hardness (η) determine the resistance of the chemical species to lose electrons and measure their global response to changes in the number of electrons since they are independent of the position.

Thus, the chemical potential of DFT is equivalent to the negative of the concept of electronegativity, and the principle of electronegativity equalization follows readily from this identification.

$$\mu = -\frac{IP + EA}{2} = -\chi$$

All compounds have a negative chemical potential, which means that they have a weaker tendency of the electrons to escape from the system. That is, electrons flow from the regions with higher chemical potential to the regions with lower chemical potential, up to the point in which μ becomes constant throughout the space.

The global descriptor of hardness has been an indicator of overall stability of the system. It has been customary to use a finite difference approximation for η using the energies of N , $(N + 1)$ and $(N - 1)$ electron systems; we get the operational definition of η as,

$$\eta = (IP - EA)/2$$

Where, IP and EA are the first vertical ionization energy and electron affinity of the chemical species respectively. The inverse of the hardness is expressed as the global softness,^{178, 179}

$$\sigma = \frac{1}{2\eta}$$

When using the Pearson's Hard and Soft, Acids and Bases theory¹⁸⁰ as a guide for predicting the behavior of our derivatives. On the basis of, the HSAB concept, reactive molecules are divide by their respective polarizability, such that electrophiles and nucleophiles, are classified as either soft (relatively polarizable) or hard (relatively nonpolarizable).

Whereas the HSAB theory initially described hardness and softness in terms of the experimental ionization potential and electron affinity of the reacting molecules, these parameters also can be related (e.g., by Koopmans theorem) to the respective energies of the FMOs.¹⁸¹

HSAB concept stat that a hard base (nucleophile) is characterized by a low value for the energy of the occupied frontier orbital HOMO, a soft base by a higher value of HOMO. Accordingly, the hardness of a base increases with the decrease of HOMO.

A hard acid on the contrary is characterized by a high value for the energy of the empty frontier orbital LUMO, and its hardness will decrease with the decrease of LUMO.¹⁸²

The identification of the global hardness with the HLG of molecular orbital theory has been richly rewarding in terms of measuring stability.

(Fig.9) shows an orbital energy diagram for 1, 3, 4-oxadiazole derivatives for only the HOMO and LUMO orbitals. Substitution of donor and acceptor functional groups affects the energy levels of the frontier orbitals. Where the HOMO and LUMO are going up in energy in compounds A₁, A₂, A₃ and A₄ where the HLG and the hardness η are little affected compared to ODZ ring. But for the compounds B₁ and B₂ the HOMO is going up in energy and the LUMO is little affected where the HLG is smaller than for ODZ ring so B₁ and B₂ are becoming softer with increasing the basic character in contrast to ODZ.

As for compounds B₃ and B₄ the HOMO and LUMO has decrease in energy in which they have the smallest gaps in all compounds with the biggest values of the softness character. So, much more soft acidic character in contrast to ODZ.

In contrast to the Bronsted-Lowry definition of acids and bases, Lewis defined the species in terms of electron transfer rather than hydrogen cation. Hence, a Lewis base is a species that donates an electron pair to a Lewis acid, which accepts the donated electron pair.

The electronic interactions involved are the donation of electrons from the highest occupied molecular orbital (HOMO) of the subsequently known base to the lowest unoccupied molecular orbital (LUMO) of the second species, then known as the acid. The interaction is usually governed by the relative strengths of the acid and base, which can be either hard or soft.

Hard acids and bases are usually small species that are difficult to polarize, in contrast, soft acids and bases are usually large species that are easily polarized, e.g. soft acids: B_3 and B_4 ; soft bases: B_1 and B_2 this is an important distinction as hard acids tend to bind to hard bases, as they both exhibit high ionic character so the stability constant (K) is high, and soft acids tend to bind to soft bases, which both exhibit significant covalent character and, again, K is high. Any soft-hard interaction will have a low K as the interaction will be poor.

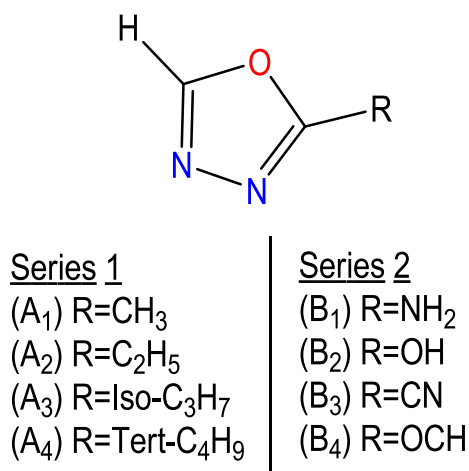


Figure 8 1, 3, 4-oxadiazole systems.

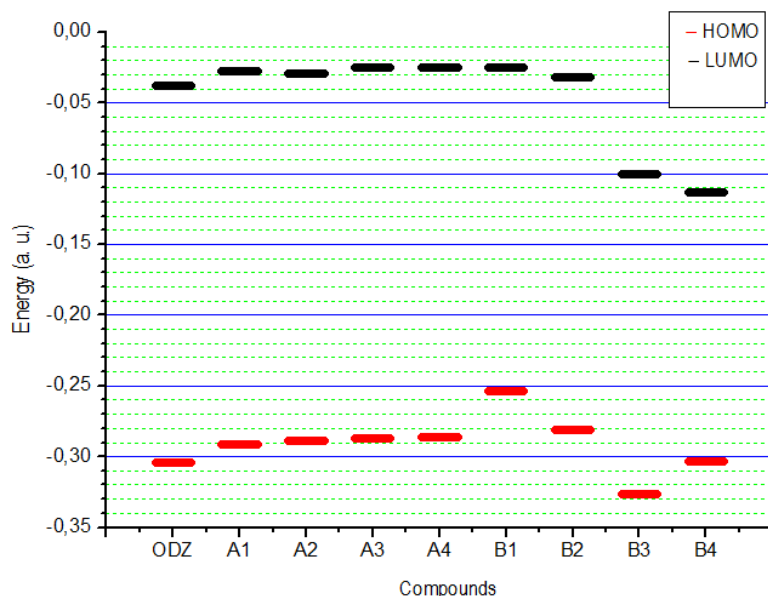


Figure 9 Changes in the energy levels of HOMO–LUMO orbital of 1, 3, 4-oxadiazole derivatives.

Table 2 Density based descriptors of 1, 3, 4-oxadiazole systems.

| COMPOSE | HOMO | LUMO | HLG's | IP | EA | η | μ | σ | χ |
|---|--------|--------|-------|-------|-------|--------|---------|----------|--------|
| ODZ | -0.304 | -0.038 | 0.266 | 0.304 | 0.038 | 0.133 | -0.171 | 3.759 | 0.171 |
| A ₁ CH ₃ | -0.291 | -0.028 | 0.263 | 0.291 | 0.028 | 0.1315 | -0.1595 | 3.802 | 0.1595 |
| A ₂ C ₂ H ₅ | -0.289 | -0.029 | 0.260 | 0.289 | 0.029 | 0.130 | -0.159 | 3.846 | 0.159 |
| A ₃ Iso-C ₃ H ₇ | -0.287 | -0.025 | 0.262 | 0.287 | 0.025 | 0.131 | -0.156 | 3.816 | 0.156 |
| A ₄ Tert-C ₄ H ₉ | -0.286 | -0.025 | 0.261 | 0.286 | 0.025 | 0.1305 | -0.1555 | 3.831 | 0.1555 |
| B ₁ NH ₂ | -0.254 | -0.025 | 0.229 | 0.254 | 0.025 | 0.1145 | -0.1395 | 4.366 | 0.1395 |
| B ₂ OH | -0.281 | -0.032 | 0.249 | 0.281 | 0.032 | 0.1245 | -0.1565 | 4.016 | 0.1565 |
| B ₃ CN | -0.326 | -0.100 | 0.226 | 0.326 | 0.100 | 0.113 | -0.213 | 4.424 | 0.213 |
| B ₄ OCH | -0.303 | -0.113 | 0.190 | 0.303 | 0.113 | 0.095 | -0.208 | 5.263 | 0.208 |

*All the density based descriptors are in u. a. of energy (Hartree), just σ which is in (Hartree⁻¹).

3. Structure Activity/Property Relationships Studies

Molecular structure properties are usually the first and the simplest calculated values to produce information that can be used to predict the behavior of the compounds in the body. For this, we have choosing these criteria to characterize the compounds of this series: molecular weight (MW), lipophilicity (log D and log P), number of hydrogen-bond donors and acceptors (NHBD and NHBA), polar surface area (PSA), number of rotatable bonds (nrotb) and ionization state (dissociation constant pKa).

3.1. Drug-like properties of rule of thumb

The successful design of new drugs requires optimization of many parameters simultaneously. The absorption is predominantly a function of solubility and permeability. Solubility is perhaps the most basic requirement of an orally available drug. In general, it is desirable for a drug candidate to have high enough water solubility to dissolve in body fluids in adequate concentrations, and at the same time to have high enough lipophilicity to permeate across various biological membranes.

One way to screen out compounds with probable absorption problems is known as Lipinski's "rule of five". According to Lipinski and al.¹⁶⁹, these four parameters are thought to be associated with solubility, permeability and binding efficiency of drugs which are the basic requirements for any drug to have good pharmacokinetic properties. As most of the drug candidates are designed to be administered to human body via oral route and thus absorbed from the intestine, the first barrier they meet on their way to systemic circulation is the gut wall. The most usual way of permeation across the gut wall is passive transcellular permeation through the cells, but absorption of many compounds is also affected by ATP-driven efflux pumps (efflux transporters, e.g. P-glycoprotein, BCRP, MRD-family) or active cell uptake (influx) transporters, located on various cell membranes in the body.

Generally, passive transport is governed by physicochemical properties whereas active transport involves specific binding of a molecule to a binding site on a transport protein.¹⁸³

Lipinski used these molecular properties in formulating his rule. The rule states that most molecules with good membrane permeability have $\log P \leq 5$, $MW \leq 500$, $NHBA \leq 10$, and $NHBD \leq 5$. A compound that fulfils at least three out of the four criteria is said to adhere to Lipinski's 'rule of 5'.

Veber¹⁷⁰ suggest that compounds which meet only the two criteria of (1) 10 or fewer rotatable bonds and (2) polar surface area equal to or less than 140 \AA^2 (or 12 or fewer H-bond donors and acceptors) will have a high probability of good oral bioavailability in the rat.

The above mentioned parameters were calculated for all the series of the anti-tubercular agents (Table.3). From the data obtained, it was observed that all the derivatives of the series were found to obey the Lipinski rule and Veber's. TPSA and Volume are inversely proportional to %ABS. TPSA was used to calculate the percentage of absorption (%ABS) according to the equation: $\%ABS = 109 \pm 0.345 \cdot TPSA$.¹⁸⁴ From all these parameters, it can

be observed that all the title compounds exhibited a great %ABS ranging from 72.14% to 84.30%.

Overall permeability, both in vitro and in vivo can be considered to be the sum of passive (diffusion driven) and active (transporter mediated) processes. The latter can affect both influx and efflux. In particular P-glycoprotein (PGP) mediated efflux is widely known to have a significant effect on absorption and distribution potential. Considering active efflux alone, Petrauskas has proposed the ‘rule of four’,^{171, 185} which states that compounds are likely to be efflux substrates if they have a hydrogen bond acceptor count (sum of N and O atoms) ≥ 8 , MW > 400 and an acid with a pKa > 4. Conversely, compounds are likely to be non-substrates if they have an acceptor count ≤ 4 , MW < 400 and a base with a pKa < 8. In which, all most our compounds are seems to satisfy the unlikely efflux substrates criteria just for compounds 14 which is likely to be efflux substrate for the P-glycoprotein.

Table 3 Drug-likeness parameters of anti-tuberculosis compounds.

| Comps | %ABS | MW | Log P | NHB D | NHB A | Nrotb | PSA | Acidic pKa | Basic pKa | Δ pKa |
|--------------------|-------|--------|-------|----------|----------|-------|--------|---------------|--------------|-----------------|
| Rules | - | <500 | <5 | <5 | <10 | <10 | <140 | - | - | - |
| 1 _(2a) | 75.32 | 271.28 | -0.14 | 2 | 7 | 3 | 97.610 | 11.27 | 1.12 | 10.15 |
| 2 _(2b) | 75.32 | 299.33 | 0.89 | 2 | 7 | 3 | 97.610 | 11.27 | 1.33 | 9.94 |
| 3 _(2c) | 75.32 | 285.31 | 0.37 | 2 | 7 | 3 | 97.610 | 11.27 | 1.29 | 9.98 |
| 4 _(2d) | 72.14 | 363.38 | 1.36 | 2 | 8 | 5 | 106.84 | 11.27 | -1.86; 1.10 | 10.17 |
| 5 _(2e) | 75.32 | 305.72 | 0.46 | 2 | 7 | 3 | 97.610 | 11.27 | -1.88; 0.66 | 10.61 |
| 6 _(3a) | 84.30 | 288.32 | 0.78 | 0 | 6 | 3 | 71.590 | 6.68 | 0.96 | 5.72 |
| 7 _(3b) | 84.30 | 316.38 | 1.81 | 0 | 6 | 3 | 71.590 | 6.70 | 1.18 | 5.52 |
| 8 _(3c) | 84.30 | 302.35 | 1.30 | 0 | 6 | 3 | 71.590 | 6.69 | 1.13 | 5.56 |
| 9 _(3d) | 81.12 | 380.42 | 2.28 | 0 | 7 | 5 | 80.820 | 6.61 | 0.98 | 5.63 |
| 10 _(3e) | 84.30 | 322.77 | 1.39 | 0 | 6 | 3 | 71.590 | 6.61 | 0.54 | 6.07 |
| 11 _(4a) | 80.15 | 347.38 | 2.13 | 1 | 7 | 5 | 83.620 | 7.62 | 1.30 | 6.32 |
| 12 _(4b) | 80.15 | 375.43 | 3.16 | 1 | 7 | 5 | 83.620 | 7.62 | 1.45 | 6.17 |
| 13 _(4c) | 80.15 | 361.40 | 2.64 | 1 | 7 | 5 | 83.620 | 7.62 | 1.44 | 6.18 |
| 14 _(4d) | 76.97 | 439.47 | 3.63 | 1 | 8 | 7 | 92.850 | 7.62 | 1.26 | 6.36 |
| 15 _(4e) | 80.15 | 381.82 | 2.73 | 1 | 7 | 5 | 83.620 | 7.62 | 0.92 | 6.7 |

3.2. Lipophilicity profile and the ionization state

Lipophilicity is a critical information that enable us to better interpret our results since it's a major structural factor that influences the pharmacokinetic (permeation of physiological membranes (absorption and distribution), plasma protein binding and volume of distribution) and pharmacodynamic (target recognition, target affinity and target specificity) behavior of our anti-tuberculosis compounds. LogP (also known as Kow or Pow) and logD are the most

descriptors of the lipophilicity. There is no constant pH in the body and it is therefore essential that we consider an appropriate pH when predicting the behavior of this anti-tuberculosis compounds. For that we have decided to study the lipophilic character of this new series of anti-tuberculosis. Generally Log P is measured in the pH where the compound exist in their neutral form. From (Table.4 & Fig.10) we can see that the compounds 1-5 have the values of Log D equal to Log P in almost the range of physiologically relevant pH (1-8) for these compounds we can predict their behavior only from examining the Log P profile. The predicted Log P values are -0.14, 0.89, 0.37, 1.36 and 0.46 for compounds 1-5 respectively. The conclusion we draw from this is that the compounds 2-5 show a preference to be associated with the lipid phase, and by extension will likely permeate biological membranes spontaneously, unlike the compound 1, which has negative values, it would be more susceptible to higher aqueous solubility and for lower lipophilicity in the body. As a result, we would expect membrane permeability to be poor for the compound 1 and acceptable for the other compounds 2-5. Log $D_{7.4}$ is equal to Log P for these compounds, so, all these compounds will exist in their neutral form and it's often quoted to give an indication of the lipophilicity of a drug at the pH of blood plasma. High values of Log $D_{7.4}$, the compounds will tend to be metabolized by P450 enzymes in the liver and increasing its value above 0 will decrease renal clearance and increase metabolic clearance.

Whereas, for the compounds 6-15 the difference between the basic and the acidic pKa values is too small (ΔpK_a value about 6, Table.3) which means that the neutral form of these anti-tuberculosis compounds is existent at a very small range of the physiologically relevant pH, we can see that, in the (Table.4 & Fig.10) of Log P and Log D values. For that, we are going to examine the Log D profile to better predict the behavior of our anti-tuberculosis compounds. Where, the Log D value for these compounds is changing within the range of 0.06 and 3.62. Which, lead us to deduce that all the compounds prefer to be associated with the lipid phase, and by extension will likely permeate biological membranes spontaneously.

Table 4 Log D and Log P profile of the anti-tuberculosis compounds.

| pH | Compounds | | | | | | | | | | | | | | |
|------|-------------------|-------------------|-------------------|-------------------|-------------------|-------------------|-------------------|-------------------|-------------------|--------------------|--------------------|--------------------|--------------------|--------------------|--------------------|
| | 1 _(2a) | 2 _(2b) | 3 _(2c) | 4 _(2d) | 5 _(2e) | 6 _(3a) | 7 _(3b) | 8 _(3c) | 9 _(3d) | 10 _(3e) | 11 _(4a) | 12 _(4b) | 13 _(4c) | 14 _(4d) | 15 _(4e) |
| 0 | -0.99 | -0.20 | -0.65 | 0.47 | -0.09 | -0.22 | 0.60 | 0.13 | 1.25 | 0.75 | 0.79 | 1.67 | 1.17 | 2.34 | 1.77 |
| 0.5 | -0.76 | 0.08 | -0.39 | 0.71 | 0.11 | 0.19 | 1.04 | 0.57 | 1.67 | 1.07 | 1.25 | 2.14 | 1.64 | 2.79 | 2.18 |
| 1 | -0.49 | 0.40 | -0.08 | 0.98 | 0.29 | 0.50 | 1.41 | 0.92 | 1.99 | 1.26 | 1.64 | 2.56 | 2.06 | 3.17 | 2.47 |
| 1.5 | -0.30 | 0.65 | 0.16 | 1.19 | 0.40 | 0.67 | 1.64 | 1.14 | 2.17 | 1.34 | 1.91 | 2.87 | 2.36 | 3.43 | 2.63 |
| 2 | -0.20 | 0.80 | 0.29 | 1.30 | 0.44 | 0.74 | 1.75 | 1.24 | 2.24 | 1.37 | 2.05 | 3.04 | 2.53 | 3.56 | 2.70 |
| 2.5 | -0.16 | 0.86 | 0.35 | 1.34 | 0.46 | 0.77 | 1.79 | 1.28 | 2.27 | 1.38 | 2.10 | 3.12 | 2.60 | 3.60 | 2.72 |
| 3 | -0.15 | 0.88 | 0.36 | 1.35 | 0.46 | 0.78 | 1.80 | 1.29 | 2.28 | 1.39 | 2.12 | 3.14 | 2.63 | 3.62 | 2.73 |
| 3.5 | -0.14 | 0.88 | 0.37 | 1.36 | 0.46 | 0.78 | 1.81 | 1.29 | 2.28 | 1.39 | 2.13 | 3.15 | 2.64 | 3.63 | 2.73 |
| 4 | -0.14 | 0.89 | 0.37 | 1.36 | 0.46 | 0.78 | 1.81 | 1.29 | 2.28 | 1.39 | 2.13 | 3.15 | 2.64 | 3.63 | 2.73 |
| 4.5 | -0.14 | 0.89 | 0.37 | 1.36 | 0.46 | 0.78 | 1.81 | 1.29 | 2.28 | 1.38 | 2.13 | 3.16 | 2.64 | 3.63 | 2.73 |
| 5 | -0.14 | 0.89 | 0.37 | 1.36 | 0.46 | 0.78 | 1.80 | 1.29 | 2.27 | 1.38 | 2.13 | 3.16 | 2.64 | 3.63 | 2.73 |
| 5.5 | -0.14 | 0.89 | 0.37 | 1.36 | 0.46 | 0.76 | 1.79 | 1.28 | 2.26 | 1.36 | 2.13 | 3.15 | 2.64 | 3.63 | 2.73 |
| 6 | -0.14 | 0.89 | 0.37 | 1.36 | 0.46 | 0.72 | 1.75 | 1.23 | 2.21 | 1.31 | 2.12 | 3.15 | 2.64 | 3.62 | 2.73 |
| 6.5 | -0.14 | 0.89 | 0.37 | 1.36 | 0.46 | 0.61 | 1.64 | 1.12 | 2.08 | 1.18 | 2.11 | 3.13 | 2.62 | 3.61 | 2.71 |
| 7 | -0.14 | 0.89 | 0.37 | 1.36 | 0.46 | 0.38 | 1.42 | 0.90 | 1.84 | 0.94 | 2.06 | 3.09 | 2.57 | 3.56 | 2.67 |
| 7.4 | -0.14 | 0.89 | 0.37 | 1.36 | 0.46 | 0.13 | 0.17 | 0.65 | 1.58 | 0.68 | 1.98 | 3.00 | 2.49 | 3.48 | 2.58 |
| 7.5 | -0.14 | 0.89 | 0.37 | 1.36 | 0.46 | 0.06 | 1.10 | 0.58 | 1.51 | 0.61 | 1.94 | 2.97 | 2.46 | 3.44 | 2.55 |
| 8 | -0.14 | 0.89 | 0.37 | 1.36 | 0.46 | -0.26 | 0.78 | 0.27 | 1.20 | 0.31 | 1.71 | 2.74 | 2.22 | 3.21 | 2.31 |
| 8.5 | -0.14 | 0.89 | 0.37 | 1.36 | 0.46 | -0.48 | 0.56 | 0.04 | 1.00 | 0.11 | 1.37 | 2.40 | 1.88 | 2.87 | 1.97 |
| 9 | -0.14 | 0.89 | 0.37 | 1.36 | 0.46 | -0.58 | 0.45 | -0.07 | 0.91 | 0.01 | 1.02 | 2.04 | 1.53 | 2.52 | 1.62 |
| 9.5 | -0.14 | 0.88 | 0.37 | 1.36 | 0.46 | -0.62 | 0.40 | -0.11 | 0.87 | -0.02 | 0.75 | 1.78 | 1.26 | 2.25 | 1.35 |
| 10 | -0.15 | 0.88 | 0.36 | 1.35 | 0.45 | -0.64 | 0.39 | -0.12 | 0.86 | -0.03 | 0.61 | 1.63 | 1.12 | 2.11 | 1.21 |
| 10.5 | -0.17 | 0.85 | 0.34 | 1.33 | 0.43 | -0.64 | 0.39 | -0.13 | 0.86 | -0.04 | 0.55 | 1.57 | 1.06 | 2.05 | 1.15 |
| 11 | -0.24 | 0.79 | 0.27 | 1.26 | 0.36 | -0.64 | 0.38 | -0.13 | 0.86 | -0.04 | 0.53 | 1.55 | 1.04 | 2.03 | 1.13 |
| 11.5 | -0.39 | 0.63 | 0.12 | 1.11 | 0.21 | -0.64 | 0.38 | -0.13 | 0.86 | -0.04 | 0.52 | 1.55 | 1.03 | 2.02 | 1.12 |
| 12 | -0.65 | 0.37 | -0.14 | 0.85 | -0.05 | -0.64 | 0.38 | -0.13 | 0.86 | -0.04 | 0.52 | 1.55 | 1.03 | 2.02 | 1.12 |
| 12.5 | -0.95 | 0.08 | -0.44 | 0.55 | -0.35 | -0.64 | 0.38 | -0.13 | 0.86 | -0.04 | 0.52 | 1.54 | 1.03 | 2.02 | 1.12 |
| 13 | -1.18 | -0.15 | -0.66 | 0.32 | -0.57 | -0.64 | 0.38 | -0.13 | 0.86 | -0.04 | 0.52 | 1.54 | 1.03 | 2.02 | 1.12 |
| 13.5 | -1.29 | -0.27 | -0.78 | 0.21 | -0.69 | -0.64 | 0.38 | -0.13 | 0.86 | -0.04 | 0.52 | 1.54 | 1.03 | 2.02 | 1.12 |
| 14 | -1.34 | -0.31 | -0.83 | 0.16 | -0.74 | -0.64 | 0.38 | -0.13 | 0.86 | -0.04 | 0.52 | 1.54 | 1.03 | 2.02 | 1.12 |

Green: physiologically relevant pH ; Yellow: Log P values, and red: Log D at blood pH.

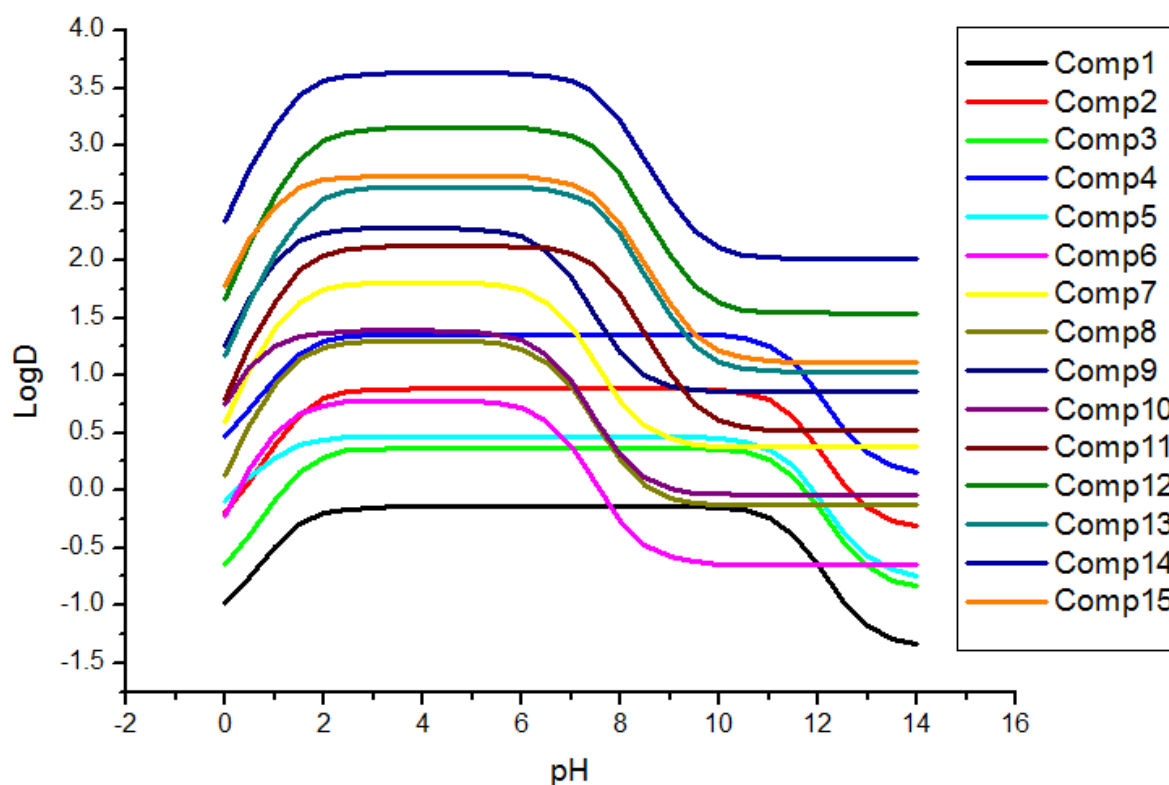


Figure 10 Lipophilicity profiles for the anti-tuberculosis compounds.

Fig.11 & .12 and Table.3 show the pKa values of our compounds, we see that they are ampholytes i.e. they have the basic and acidic character and can exist as an un-ionized form, or as an anion depending on the pH value, but because the difference between $pK_{a_{acidic}}$ and $pK_{a_{basic}}$ is > 3 , there will be no simultaneous ionization of the two groups. In contrast to other ionizable drugs with only an acidic or basic group, an amphoteric drug exhibits unique physicochemical and pharmacokinetic properties. Usually, their volume of distribution is lower than that of a basic drug, which suggests that the amphoteric drug tends to stay in the blood. Unlike normal ionizable molecules, which at some pH can be predominantly chargeless, many ampholyte can transition between several different charge states, without ever becoming chargeless; thus their lipophilicity tends to be low to moderate. These properties would be better suited for the drug targets located in the plasma, since the distribution into tissues/organs is not favorable for ampholytes.

According to the pH-partition Hypothesis, absorption is favored for the chargeless form of the drug molecule. Transporters expressed in the intestinal surface, such as Pgp and OAT (organic anion transporter), could affect efflux/active uptake of the compound. It is thought that the development of amphoteric compounds into a drug is likely to be more challenging

than compounds of other charge types, may be partly due to the lack of understanding of the factors governing their membrane permeability. Given that ampholytes are expected to be poorly absorbed by transmembrane passive diffusion processes, absorption via the paracellular route may be important. In the latter route, small solvated zwitterions could diffuse through water-filled channels between cells. Such channels are known to be capacity-limited, size-restricted, and cation-selective, thus attenuating free diffusion in the water phase.

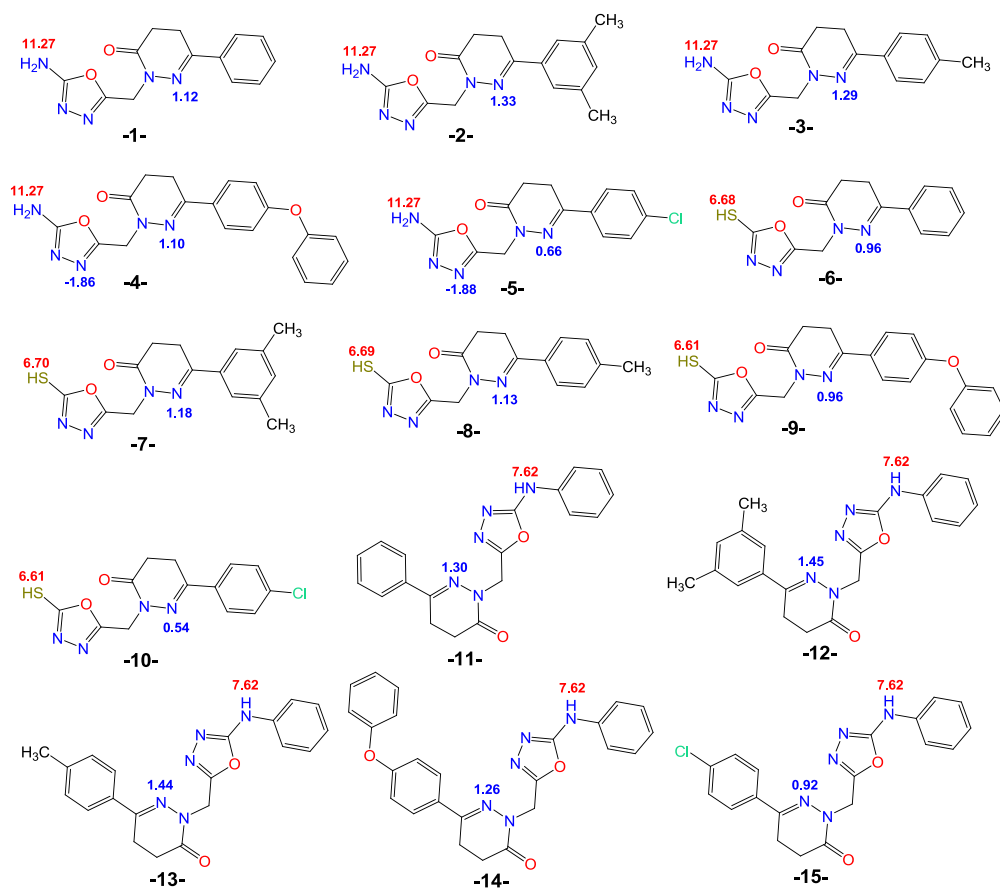


Figure 11 The multiprotic acid/base sites of anti-tuberculosis compounds.

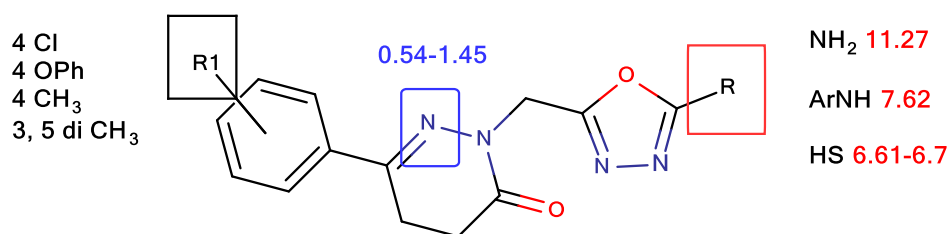


Figure 12 Changes of pKa values of anti-tuberculosis compounds; red atoms denote acidic groups, and blue atoms indicate basic groups.

3.3. Structure Activity/Affinity Relationships (PEI and GE analysis)

Our antitubercular activity was obtained by measurement of percentage inhibition against *M.tuberculosis* H37Rv at a single concentration (6.25 µg/ml). A simple efficiency index, PEI, can be introduced to guide the selection of the best compounds that use their atoms most efficiently. The idea of Per cent Efficiency Index is derived from Ligand Efficiency, which is defined as: $LE = \Delta G/N$

Where: $\Delta G = -RT \ln K$, is the free energy of binding and, N, is the number of non-hydrogen atoms which can be seen as a measure of molecular size. Hence, it is simpler and more straightforward to calculate MW. In addition, MW is superior in dealing with the contribution of different heteroatoms. Abad-Zapatero and Metz¹⁷³ introduced the Per cent Efficiency Index (PEI) defined as the fractional (0 – 1 scale) inhibition of a compound divided by the MW in kDa.

As we can see in our results that our compounds divide in two groups where the first one have the biggest values of PEI in the range of 2.32-3.17, all these compounds are the most active with %in between 84-91. Moreover, the second with the low values of PEI in the range of 1.11-1.96 where the %in is between 45-56.

The hall purpose of PEI is instead of considering the efficiency of the whole compound, the average efficiency contribution per atom is taken into account. For the compound1 with the biggest value of PEI 3.17. Which it is not the most potent compound but it has a combination between a good potency and the small size.

The group efficiency (GE) metric introduced by Verdonk and Rees¹⁷⁴ represents the binding efficiency of a functional group that has been added to an existing molecule “A” to form molecule “B”, it is defined as

$$GE = -\frac{\Delta\Delta G}{\Delta HA}$$

$$\Delta\Delta G = \Delta G(B) - \Delta G(A)$$

$$\Delta HA = HA(B) - HA(A)$$

Where the affinity gained by molecule “B”, through the introduction of additional non-hydrogen atoms ΔHA to molecule “A”, is expressed as the difference of the free energies of binding ($-\Delta\Delta G$).¹⁷⁵

The PEI analysis show that compounds 1, 5, 6, 10, 11 and 15 with the highest values, are favored because this allows atoms to be added to modulate in vivo properties while still ending up with a candidate with a molecular weight that fits the Lipinski guidelines.

(Fig.13) shows GE analysis of the efficiency of various parts of those anti-tuberculosis compounds where it's clear in compounds 5, 10 and 15 that the additions of 4-chloro substituent decrease the molecular efficiency. The addition of phenyl ring to compound 1, it improves potency by 5%, and raise molecular size by about 77.104 Da has a good GE equal to 0.65. The latter has decreased to GE=0.27 by adding Cl group. Moreover, the GE of the NH₂ substitution group with SH group is the most effective addition (GE=1.17) for anti-tubercular activity.

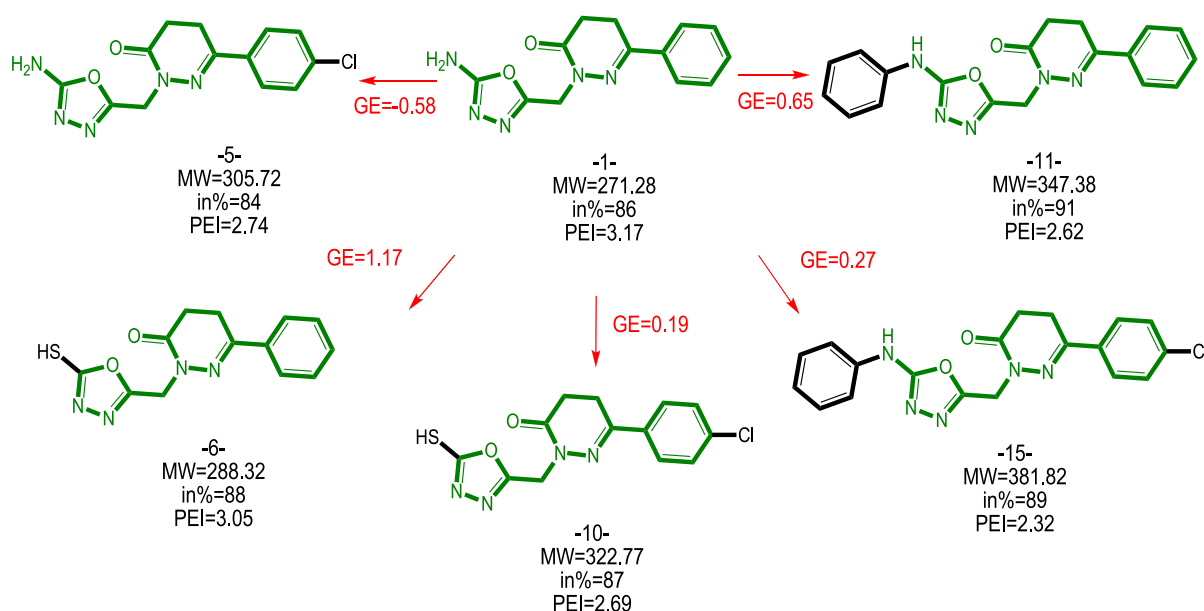


Figure 13 Group Efficiency analysis of the most efficient compounds of studied series.

4. Conclusion

It is now understood that 1, 3, 4-oxadiazole characters changes with regard to substitution groups. These behaviors are based on electronic and structural characteristics that constitute the soft and hard classifications of the HSAB theory. In this present study, we analyze the electronic properties of 1, 3, 4-oxadiazole ring and its derivatives, in order to deepen our understanding of its various therapeutic significance in general. The alkyl, amine and hydroxyl substitution at the 2-position of 1, 3, 4-oxadiazole ring increases the hardness of the system, while the cyanide and ketone one decreases it.

With regard to the anti-tuberculosis series, the lipophilicity balance and ionization state seem to play an important role. Where they reveal their ampholytes character, which lead us to explore the Log D profile that shows they have good permeability.

And all compounds followed Lipinski's rule as they have a molecular weight under 500 Da, a limited lipophilicity (expressed by $\text{Log P} < 5$), far less than 5 H-bond donors (expressed as the sum of OHs and NHs), and also far less than 10 H-bond acceptors (expressed as the sum of Os and Ns) and Viber's rules also. In addition, they present a high percentage of absorption (%ABS), with all of the compounds being potentially able to cross biological membranes and to have a good oral bioavailability.

The correlation between the size and %inhibition of this anti-tuberculosis series was expressed by Per cent Efficiency Index (PEI). The calculated PEI suggests that compound 1 could be adopted as lead to locate a potential active anti-tuberculosis compound. Moreover, the Group Efficiency (GE) show the quality of SH and phenyl added group to maintain (or increase) the optimization of the anti-tubercular activity.

PART II

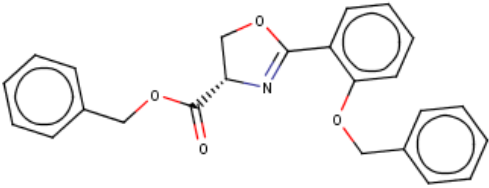
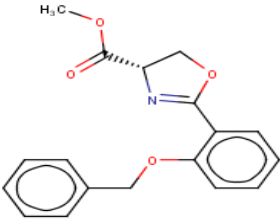
Quantitative Structure- Antituberculosis Activity Relationships Study in a series of Oxazoline and Oxazole benzyl esters Derivatives

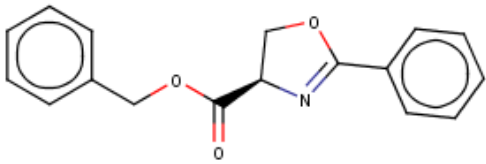
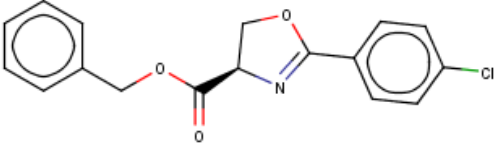
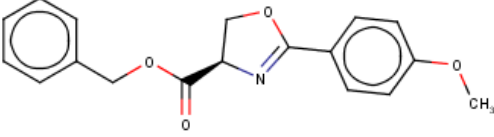
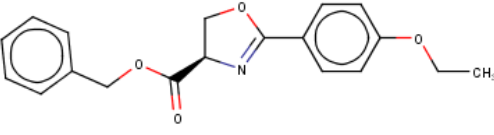
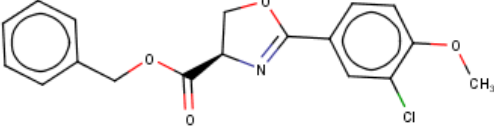
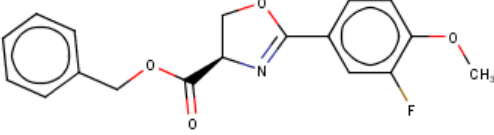
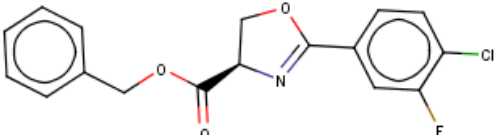
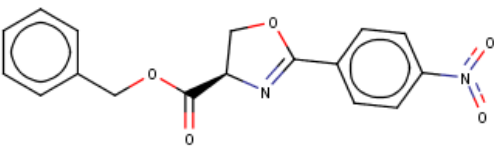
Years ago, the investigation of the idea of using deep learning to make predictions for ligand binding activity was developing rapidly. Where, the started basic idea was very simple: many known molecules and their biological activity to specific receptors. The sum of information of all these molecules to a specific receptor is like a negative of the receptor itself. Training a multilinear regression with the information of many oxazoline and oxazole benzyl esters derivatives to a single receptor (MT P450_{14DM}) would make the MLR itself a negative of the receptor, by discovering more potent inhibitors.

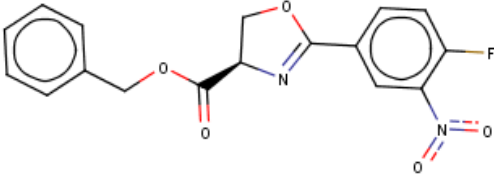
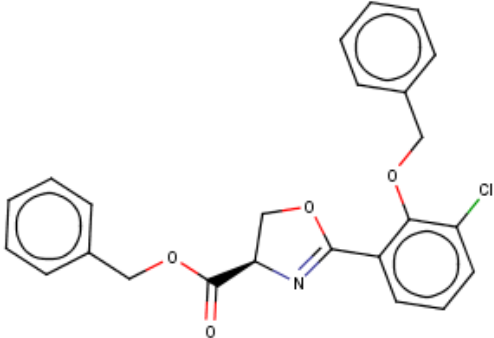
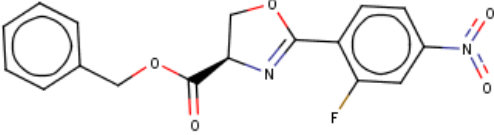
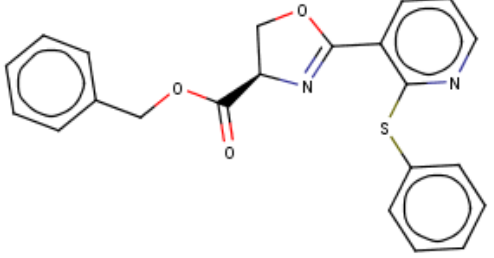
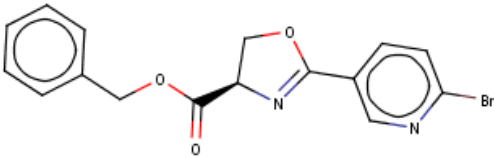
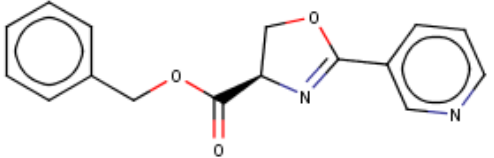
1. Biological Data

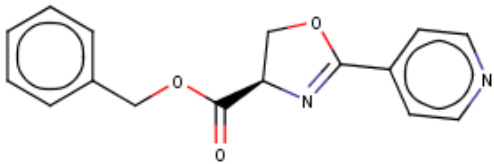
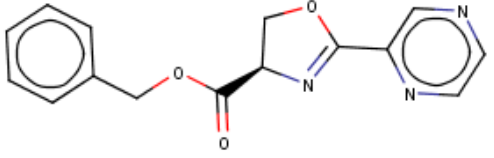
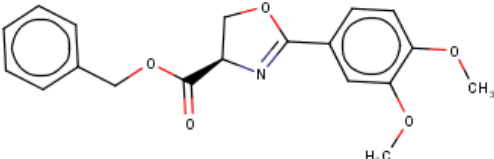
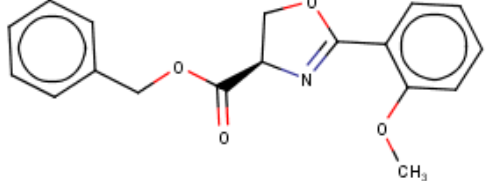
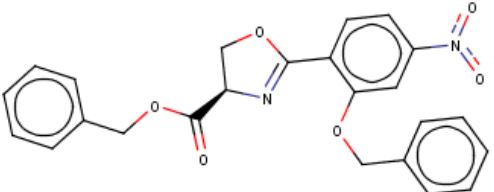
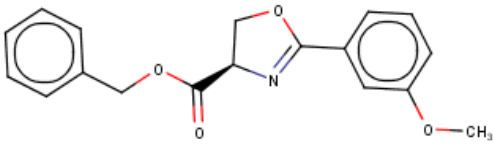
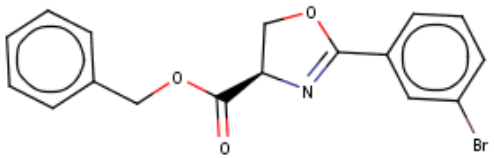
In the present work, a group of 82 oxazoline and oxazole benzyl esters derivatives display growth inhibitory activity against *M. tuberculosis* H37Rv, ²⁵ was investigated to predict a QSAR model using MLR correlation method. Activity data [MIC (μ M)] for each molecule was converted to logarithmic scale [pMIC (M)] to guarantee linearity, and to achieve normality. To detect outliers that have an undue influence on the multiple regression model, a group of 59 representative compounds with a residual value under 0.55 was selected for the study. We suggest a rational approach, based on the distribution of structure diversity and the activity ranking, to divide our experimental SAR dataset into a training and test set, which are used for model development and validation, considering the ratio of 80% and 20% respectively. The chemical structures of studied molecules with their corresponding activity data were listed in (Table.5).

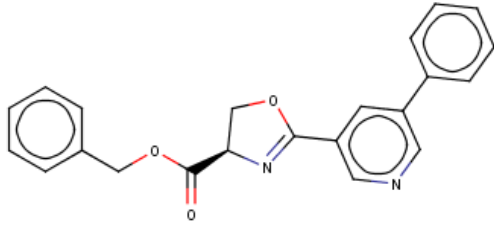
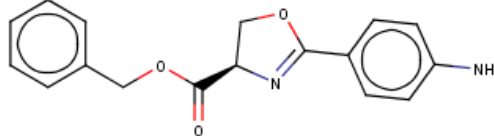
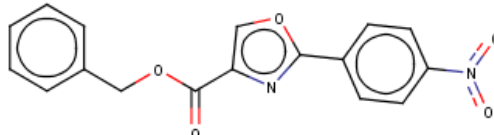
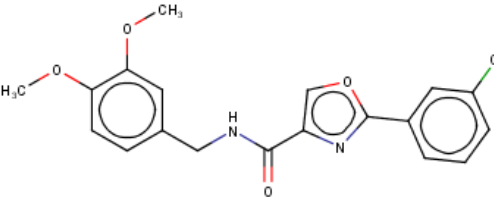
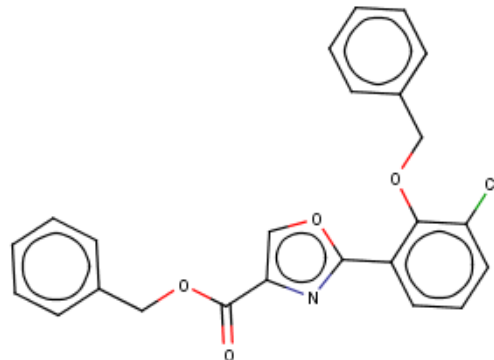
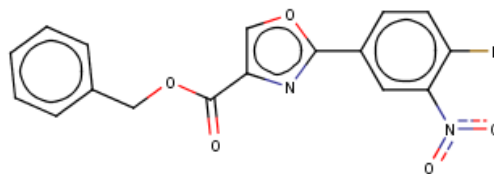
Table 5 The chemical structures of studied molecules with their corresponding activity data.

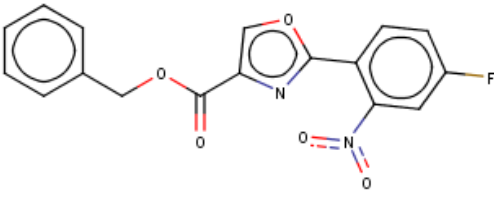
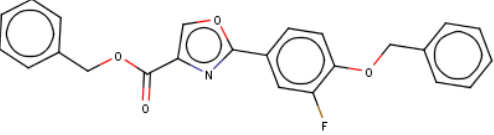
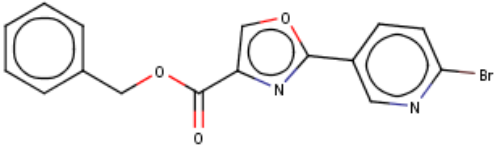
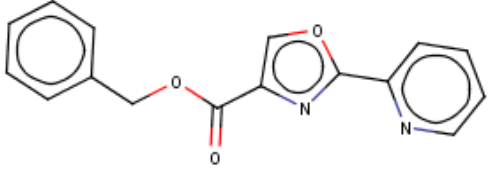
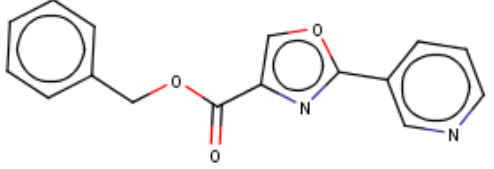
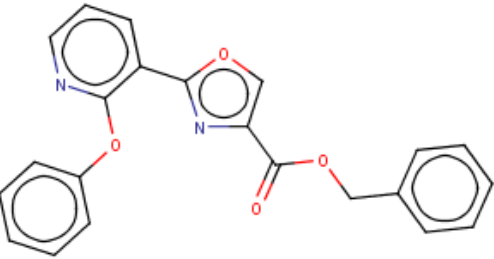
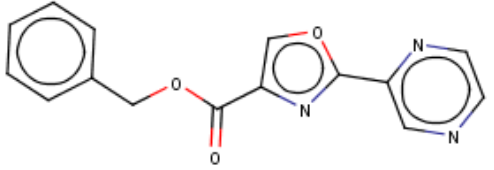
| Comp. | Structure | pMIC _{exp} ²⁵ | pMIC _{Pred} | Residu |
|-------|---|-----------------------------------|----------------------|--------|
| 3 |  | 4.900 | 4.408 | -0.492 |
| 12 |  | 3.928 | 4.033 | 0.105 |

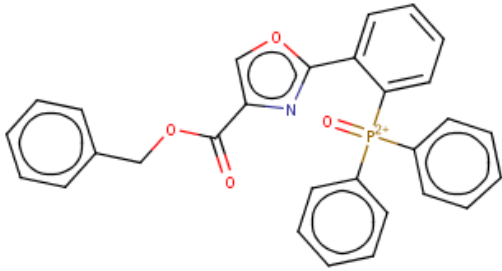
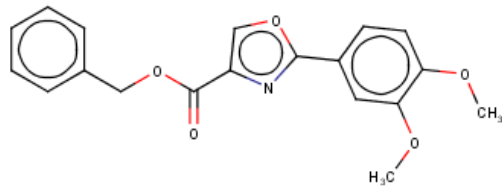
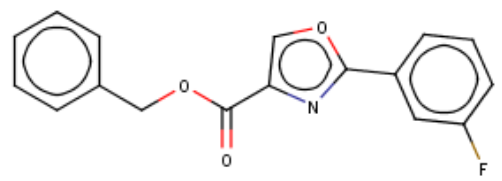
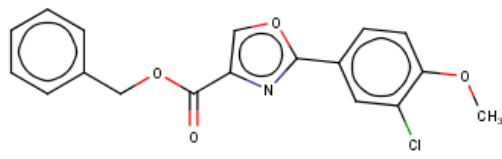
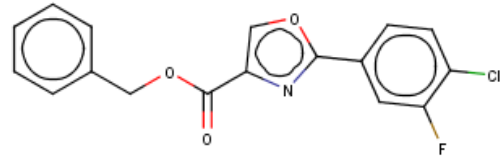
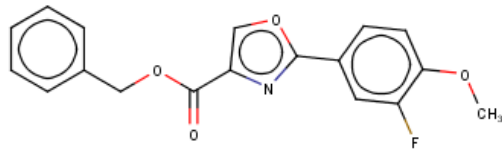
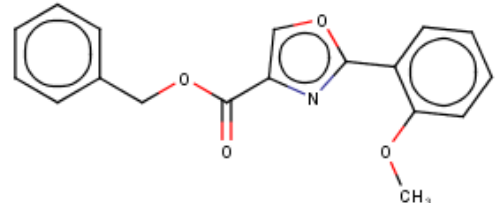
| | | | | |
|----|---|-------|-------|--------|
| 15 |  | 5.143 | 4.889 | -0.253 |
| 18 |  | 4.215 | 4.293 | 0.078 |
| 21 |  | 4.583 | 4.565 | -0.017 |
| 22 |  | 4.218 | 4.424 | 0.206 |
| 23 |  | 4.217 | 4.231 | 0.014 |
| 24 |  | 4.297 | 4.424 | 0.127 |
| 26 |  | 4.284 | 4.325 | 0.041 |
| 28 |  | 4.514 | 5.014 | 0.500 |

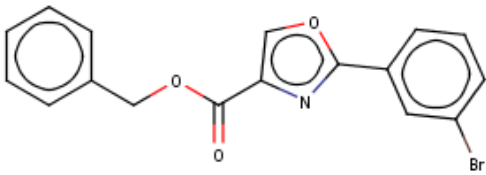
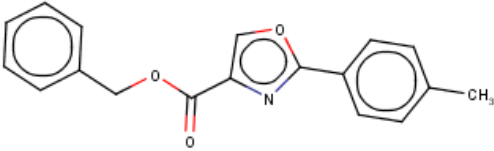
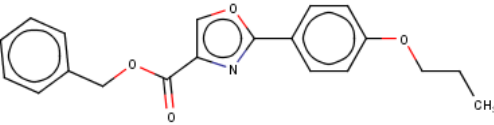
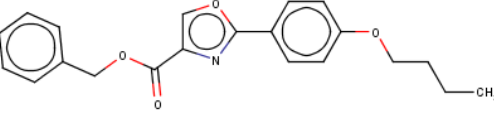
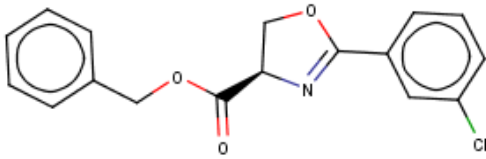
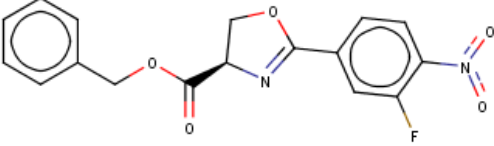
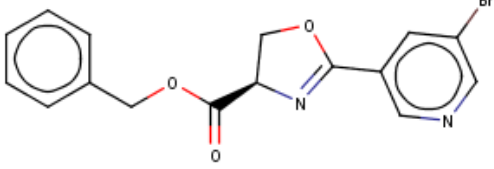
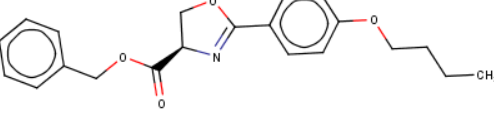
| | | | | |
|----|---|-------|-------|--------|
| 29 |  | 5.205 | 4.835 | -0.370 |
| 31 |  | 5.201 | 4.872 | -0.329 |
| 33 |  | 4.886 | 5.050 | 0.164 |
| 34 |  | 4.750 | 4.855 | 0.105 |
| 37 |  | 4.640 | 4.344 | -0.296 |
| 39 |  | 4.273 | 4.482 | 0.209 |

| | | | | |
|----|---|-------|-------|--------|
| 40 |  | 4.255 | 4.810 | 0.555 |
| 41 |  | 4.213 | 4.815 | 0.602 |
| 42 |  | 4.409 | 4.214 | -0.195 |
| 45 |  | 4.432 | 4.619 | 0.187 |
| 50 |  | 4.807 | 4.895 | 0.088 |
| 52 |  | 4.606 | 4.553 | -0.053 |
| 54 |  | 4.616 | 4.761 | 0.145 |

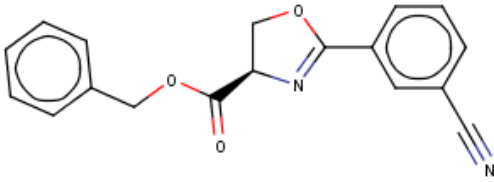
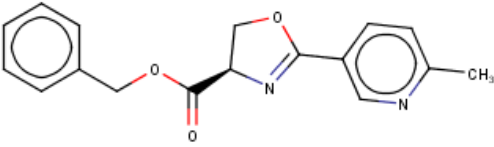
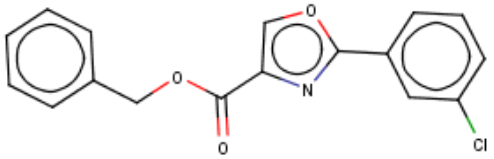
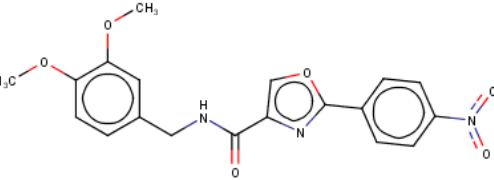
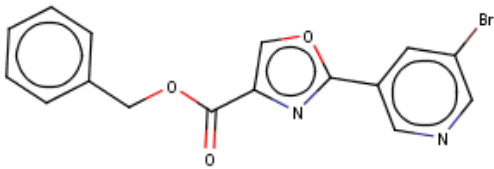
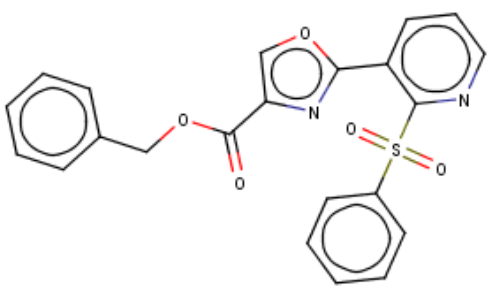
| | | | | |
|----|---|-------|-------|--------|
| 56 |  | 4.903 | 4.428 | -0.475 |
| 57 |  | 4.595 | 5.104 | 0.509 |
| 58 |  | 5.747 | 5.944 | 0.197 |
| 62 |  | 3.928 | 3.825 | -0.103 |
| 64 |  | 5.268 | 4.851 | -0.417 |
| 66 |  | 5.959 | 5.838 | -0.121 |

| | | | | |
|----|---|-------|-------|--------|
| 69 |  | 5.620 | 5.544 | -0.076 |
| 72 |  | 5.519 | 5.350 | -0.169 |
| 74 |  | 5.595 | 5.295 | -0.299 |
| 76 |  | 5.699 | 5.674 | -0.025 |
| 77 |  | 5.418 | 5.480 | 0.062 |
| 82 |  | 5.164 | 5.121 | -0.043 |
| 83 |  | 5.135 | 5.110 | -0.025 |

| | | | | |
|----|---|-------|-------|--------|
| 84 |  | 4.209 | 4.979 | 0.770 |
| 85 |  | 4.796 | 4.529 | -0.267 |
| 89 |  | 6.041 | 5.567 | -0.474 |
| 90 |  | 5.629 | 4.934 | -0.694 |
| 91 |  | 5.542 | 5.112 | -0.430 |
| 92 |  | 5.256 | 4.996 | -0.260 |
| 93 |  | 5.411 | 5.268 | -0.143 |

| | | | | |
|-----------------|---|-------|-------|--------|
| 96 |  | 5.714 | 5.500 | -0.214 |
| 97 |  | 4.891 | 4.573 | -0.317 |
| 98 |  | 5.458 | 5.531 | 0.073 |
| 100 |  | 5.754 | 5.770 | 0.016 |
| 17 ^a |  | 4.936 | 4.456 | -0.479 |
| 30 ^a |  | 4.520 | 4.909 | 0.389 |
| 36 ^a |  | 4.559 | 4.370 | -0.189 |
| 48 ^a |  | 5.565 | 4.834 | -0.731 |

In Quantitative Structure-Antituberculosis Activity Relationships Study in a series of Oxazoline and Oxazole benzyl esters Derivatives

| | | | | |
|-----------------|---|-------|-------|--------|
| 53 ^a |  | 4.326 | 3.974 | -0.352 |
| 55 ^a |  | 4.137 | 4.023 | -0.114 |
| 59 ^a |  | 5.903 | 5.376 | -0.526 |
| 61 ^a |  | 4.446 | 4.389 | -0.057 |
| 73 ^a |  | 5.625 | 5.246 | -0.379 |
| 80 ^a |  | 4.179 | 3.769 | -0.410 |
| 94 ^a |  | 5.219 | 5.233 | 0.014 |

^a test set

2. Descriptors Generation

All the 82 investigated molecules were pre-optimized using the Molecular Mechanics Force Field (MM+) method. Then the resultant minimized structures were further refined using the semiempirical PM3 method. Both methods included in HyperChem version 8.08 package.¹⁸⁶ The gradient norm limit of 0.01 kcal/Å was chosen for the geometry optimization.

QSAR Properties module in HyperChem was used to calculate and estimate a variety of molecular descriptors such as:

- Surface Area (Grid) (S), the grid calculation of solvent accessible surface areas is much slower than the approximate calculation, but is more accurate for a given set of atomic radii. The grid method used is that described by Bodor and al.,¹⁸⁷ using the atomic radii of Gavezotti.¹⁸⁸
- Molecular volumes (V), bounded by solvent accessible surfaces, using a grid method.
- Refractivity (R), also using an atom-based fragment method due to Ghose and Crippen.¹⁸⁹ For a sample of organic molecules, the method yields a correlation coefficient (r) with experimental values of 0.995 and a standard error of 1.1.
- Polarizability (Pol), using an atom-based method due to K. J. Miller.¹⁹⁰ For a sample of organic molecules, the method yields a correlation coefficient (r) with experimental values of 0.991 and a standard error of 9.3.
- The dipole moment (μ) can be calculated from the partial atomic charges. The molecular dipole moment is perhaps the simplest experimental measure of charge density in a molecule. The accuracy of the overall distribution of electrons in a molecule is hard to quantify, since it involves all of the multipole moments. Experimental measures of accuracy are necessary to evaluate results.

Here are some of the properties we have calculated using MarvinSketch software:^{191, 192}

- Log P (the log of the octanol-water partition coefficient), a hydrophobicity indicator, using Log P Consensus; this method uses a consensus model built on the ChemAxon and Klopman et al. models and the PhysProp database.¹⁹³

- Acceptor Count (AC) = the sum of the acceptor atoms. An acceptor atom always has a lone electron pair/lone electron pairs that is capable of establishing a H bond.
- Acceptor Sites (AS)= the sum of the lone pairs on the acceptor atoms.
- Rotatable Bond Count (RotBC) is number of rotatable bonds in the molecule. Unsaturated bonds, and single bonds connected to hydrogens or terminal atoms, single bonds of amides, sulphonamides and those connecting two hindered aromatic rings (having at least three ortho substituents) are considered non-rotatable.

Table 6 Molecular descriptors used in the regression analysis.

| Comps. | MW | S | V | R | Plo | μ | LogP | AS | AC | RotBC |
|--------|--------|--------|---------|--------|-------|-------|------|----|----|-------|
| 3 | 387.43 | 606.05 | 1091.52 | 121.18 | 42.92 | 3.536 | 4.94 | 5 | 3 | 8 |
| 12 | 311.34 | 544.44 | 919.24 | 92.43 | 33.26 | 1.391 | 3.21 | 5 | 3 | 6 |
| 15 | 281.31 | 531.52 | 857.55 | 86.06 | 30.79 | 1.440 | 3.37 | 3 | 2 | 5 |
| 17 | 315.76 | 553.83 | 900.52 | 90.78 | 32.72 | 1.562 | 3.97 | 3 | 2 | 5 |
| 18 | 315.76 | 551.01 | 900.83 | 90.78 | 32.72 | 1.745 | 3.97 | 3 | 2 | 5 |
| 21 | 311.34 | 573.66 | 934.20 | 92.43 | 33.26 | 2.127 | 3.21 | 5 | 3 | 6 |
| 22 | 325.36 | 603.47 | 991.46 | 97.18 | 35.10 | 2.202 | 3.57 | 5 | 3 | 7 |
| 23 | 345.78 | 590.99 | 971.66 | 97.15 | 35.19 | .908 | 3.82 | 5 | 3 | 6 |
| 24 | 329.33 | 579.15 | 942.89 | 92.56 | 33.17 | .925 | 3.35 | 5 | 3 | 6 |
| 26 | 333.75 | 557.90 | 907.88 | 90.90 | 32.63 | 2.473 | 4.12 | 3 | 2 | 5 |
| 28 | 326.31 | 562.56 | 919.27 | 92.28 | 32.63 | 6.086 | 3.31 | 8 | 4 | 6 |
| 29 | 344.30 | 568.96 | 929.27 | 92.41 | 32.54 | 6.095 | 3.45 | 8 | 4 | 6 |
| 30 | 344.30 | 570.46 | 929.31 | 92.41 | 32.54 | 6.821 | 3.45 | 8 | 4 | 6 |
| 31 | 421.88 | 670.72 | 1154.23 | 125.90 | 44.85 | 1.691 | 5.54 | 5 | 3 | 8 |
| 33 | 344.30 | 570.54 | 927.16 | 92.41 | 32.54 | 5.385 | 3.45 | 8 | 4 | 6 |
| 34 | 390.46 | 678.31 | 1121.63 | 119.29 | 42.74 | .925 | 4.93 | 4 | 3 | 7 |
| 36 | 361.19 | 556.02 | 905.68 | 90.10 | 32.71 | 2.313 | 2.92 | 4 | 3 | 5 |
| 37 | 361.19 | 557.76 | 907.38 | 90.07 | 32.71 | 2.949 | 3.13 | 4 | 3 | 5 |
| 39 | 282.30 | 521.81 | 845.00 | 82.56 | 30.08 | 2.113 | 2.15 | 4 | 3 | 5 |
| 40 | 282.30 | 527.63 | 844.30 | 82.49 | 30.08 | 2.715 | 2.15 | 4 | 3 | 5 |
| 41 | 283.29 | 523.75 | 834.29 | 80.34 | 29.37 | 1.533 | 1.32 | 5 | 4 | 5 |
| 42 | 341.36 | 614.01 | 1009.88 | 98.81 | 35.73 | 3.424 | 3.05 | 7 | 4 | 7 |
| 45 | 311.34 | 574.20 | 933.80 | 92.43 | 33.26 | 2.376 | 3.21 | 5 | 3 | 6 |
| 48 | 353.42 | 668.84 | 1098.54 | 106.31 | 38.77 | 2.285 | 4.54 | 5 | 3 | 9 |
| 50 | 432.43 | 713.17 | 1208.20 | 127.40 | 44.76 | 5.676 | 4.88 | 10 | 5 | 9 |
| 52 | 311.34 | 574.87 | 935.36 | 92.43 | 33.26 | 1.974 | 3.21 | 5 | 3 | 6 |
| 53 | 306.32 | 561.79 | 914.35 | 91.04 | 32.64 | 3.613 | 3.22 | 4 | 3 | 5 |
| 54 | 360.21 | 565.37 | 918.17 | 93.59 | 33.41 | 1.615 | 4.14 | 3 | 2 | 5 |
| 55 | 296.33 | 554.82 | 898.44 | 88.35 | 31.91 | 1.750 | 2.28 | 4 | 3 | 5 |
| 56 | 358.40 | 633.50 | 1048.48 | 111.08 | 39.74 | 2.207 | 3.80 | 4 | 3 | 6 |
| 57 | 396.33 | 552.70 | 893.28 | 89.61 | 32.14 | 2.750 | 2.54 | 4 | 3 | 5 |
| 58 | 324.29 | 559.29 | 904.77 | 93.16 | 32.44 | 4.014 | 3.79 | 8 | 4 | 6 |
| 59 | 313.74 | 548.44 | 884.49 | 91.66 | 32.52 | 1.551 | 4.46 | 3 | 2 | 5 |
| 61 | 383.36 | 619.75 | 1044.79 | 107.86 | 38.10 | 4.691 | 2.75 | 12 | 6 | 7 |

| | | | | | | | | | | |
|-----------------|--------|--------|---------|--------|-------|-------|------|----|---|---|
| 62 | 372.81 | 609.33 | 1024.79 | 106.36 | 38.18 | 3.070 | 3.41 | 7 | 4 | 6 |
| 64 | 419.86 | 605.41 | 1105.19 | 126.79 | 44.66 | 1.942 | 6.02 | 5 | 3 | 8 |
| 66 | 342.28 | 565.51 | 913.49 | 93.29 | 32.35 | 4.112 | 3.94 | 8 | 4 | 6 |
| 69 | 342.28 | 558.99 | 912.89 | 93.29 | 32.35 | 3.790 | 3.94 | 8 | 4 | 6 |
| 72 | 403.41 | 682.90 | 1142.82 | 122.20 | 42.64 | 1.429 | 5.56 | 5 | 3 | 8 |
| 73 | 359.18 | 549.86 | 889.73 | 90.98 | 32.51 | .502 | 3.40 | 4 | 3 | 5 |
| 74 | 359.18 | 555.24 | 893.15 | 90.95 | 32.51 | .887 | 3.61 | 4 | 3 | 5 |
| 76 | 280.28 | 521.23 | 832.46 | 84.65 | 29.89 | 2.911 | 3.02 | 4 | 3 | 5 |
| 77 | 280.28 | 518.77 | 829.67 | 83.45 | 29.89 | 1.209 | 2.64 | 4 | 3 | 5 |
| 80 | 420.44 | 644.71 | 1120.20 | 121.02 | 40.69 | 5.527 | 4.19 | 8 | 5 | 7 |
| 82 | 372.38 | 653.58 | 1078.17 | 113.73 | 40.19 | 2.372 | 4.73 | 4 | 3 | 7 |
| 83 | 281.27 | 511.85 | 819.66 | 80.23 | 29.18 | 1.836 | 1.80 | 5 | 4 | 5 |
| 84 | 479.47 | 688.80 | 1262.19 | 153.81 | 50.87 | 2.879 | 6.56 | 5 | 3 | 8 |
| 85 | 339.35 | 601.15 | 997.36 | 99.69 | 35.54 | 2.170 | 3.54 | 7 | 4 | 7 |
| 86 | 323.35 | 602.59 | 977.64 | 98.07 | 34.90 | 3.571 | 4.05 | 5 | 3 | 7 |
| 89 | 297.29 | 531.10 | 851.38 | 87.07 | 30.51 | 1.153 | 4.00 | 3 | 2 | 5 |
| 90 | 343.77 | 587.59 | 960.60 | 98.03 | 35.00 | 2.350 | 4.30 | 5 | 3 | 6 |
| 91 | 331.73 | 551.81 | 893.41 | 91.79 | 32.43 | .635 | 4.60 | 3 | 2 | 5 |
| 92 | 327.31 | 568.54 | 928.17 | 93.45 | 32.98 | 1.591 | 3.84 | 5 | 3 | 6 |
| 93 | 309.32 | 565.46 | 919.37 | 93.32 | 33.07 | 3.660 | 3.70 | 5 | 3 | 6 |
| 94 | 309.32 | 564.29 | 918.98 | 93.32 | 33.07 | 2.129 | 3.70 | 5 | 3 | 6 |
| 96 | 358.19 | 558.25 | 903.62 | 94.48 | 33.22 | 1.408 | 4.62 | 3 | 2 | 5 |
| 97 | 293.32 | 548.93 | 894.13 | 91.23 | 32.43 | 2.728 | 4.37 | 3 | 2 | 5 |
| 98 | 337.38 | 632.09 | 1030.20 | 102.59 | 36.74 | 3.587 | 4.58 | 5 | 3 | 8 |
| 100 | 351.40 | 664.84 | 1083.36 | 107.19 | 38.57 | 3.605 | 5.02 | 5 | 3 | 9 |
| 17 ^a | 315.76 | 553.83 | 900.52 | 90.78 | 32.72 | 1.562 | 3.97 | 3 | 2 | 5 |
| 30 ^a | 344.3 | 570.46 | 929.31 | 92.41 | 32.54 | 6.821 | 3.45 | 8 | 4 | 6 |
| 36 ^a | 361.19 | 556.02 | 905.68 | 90.1 | 32.71 | 2.313 | 2.92 | 4 | 3 | 5 |
| 48 ^a | 353.42 | 668.84 | 1098.54 | 106.31 | 38.77 | 2.285 | 4.54 | 5 | 3 | 9 |
| 53 ^a | 306.32 | 561.79 | 914.35 | 91.04 | 32.64 | 3.613 | 3.22 | 4 | 3 | 5 |
| 55 ^a | 296.33 | 554.82 | 898.44 | 88.35 | 31.91 | 1.75 | 2.28 | 4 | 3 | 5 |
| 59 ^a | 313.74 | 548.44 | 884.49 | 91.66 | 32.52 | 1.551 | 4.46 | 3 | 2 | 5 |
| 61 ^a | 383.36 | 619.75 | 1044.79 | 107.86 | 38.1 | 4.691 | 2.75 | 12 | 6 | 7 |
| 73 ^a | 359.18 | 549.86 | 889.73 | 90.98 | 32.51 | 0.502 | 3.4 | 4 | 3 | 5 |
| 80 ^a | 420.44 | 644.71 | 1120.2 | 121.02 | 40.69 | 5.527 | 4.19 | 8 | 5 | 7 |
| 94 ^a | 309.32 | 564.29 | 918.98 | 93.32 | 33.07 | 2.129 | 3.7 | 5 | 3 | 6 |

^a test set

3. Regression Analysis

Multiple linear regression analysis was carried out using the stepwise strategy in SPSS version 19 for Windows.¹⁹⁴ Our regression analysis generates an equation to describe the

statistical relationship between one or more predictor variables (descriptors) and the response variable (bioactivity).

The Stepwise Method Search selects a model by adding or removing individual descriptors, a step at a time, based on their statistical significance. The end result of this process is a single regression model, which makes it nice and simple.

The p-value for each term tests the null hypothesis that the coefficient is equal to zero (no effect). A low p-value (< 0.05) indicates that you can reject the null hypothesis. In other words, a descriptor that has a low p-value is likely to be a meaningful addition to your model because changes in the descriptor's value are related to changes in the bioactivity.

Conversely, a larger (insignificant) p-value suggests that changes in the descriptor are not associated with changes in the response. In our output, we found that the five descriptors of the equation are statistically significant because their p-values are less than 0.05. Typically, we use the coefficient p-values to determine which terms to keep in the regression model.

4. QSAR model validation

Stepwise Method Search was used to select the most appropriate descriptors. Based on the selected descriptors, multiple linear regression analysis was performed on the training set (47 comps) and then, evaluated by test set (11 comps). The five descriptors, which were selected, are: in which contribute to the inhibition activity.

Here our coefficients are OK so our regression equation would be:

$$pMIC = 8.549 + 0.006 * M + 0.051 * S - 0.064 * V + 0.206 * RM + 0.940 * RotBC$$

$$n_{train} = 47, R_{train}^2 = 0.722, R_{adj}^2 = 0.688, F_{train} = 21.271$$

Table 7 Statistical results.

| Set | N | PRESS | SSY | PRESS/SSY | R | R ² | RMSE | F |
|----------|----|-------|--------|-----------|-------|----------------|-------|--------|
| Training | 47 | 4.475 | 15.687 | 0.285 | 0.845 | 0.715 | 0.308 | 21.271 |
| Test | 11 | 1.681 | 3.954 | 0.425 | 0.762 | 0.581 | 0.374 | 4.106 |

Where N is the number of compounds in training and test set; R² is the squared correlation coefficient, R²adj is adjusted R² and F is Fisher F statistic. The statistical parameters of stepwise-MLR model are shown in (Table.6). It is obvious that, the built model showed better results for the training set, is referred to calculated R² values in both sets. The

higher R^2 and F values with lower root mean square error (RMSE) values ($RMSE_{\text{train}}=0.308$, and $RMSE_{\text{test}}=0.374$) show the predictive capability of the built model. The predicted inhibitory activities for whole molecules were listed in (Table.5). The plot of predicted pMIC values against the experimental pMIC values was demonstrated in (Fig.14).

We used F-tests to test the overall significance for a regression model, to compare the fits of different models, to test specific regression terms, and to test the equality of means. The F-test values ($F_{\text{training}}=21.271$, and $F_{\text{test}}=4.106$) indicates that the model is useful for predicting the biological activity.

R is the correlation coefficient measuring the strength of the linear relationship. So, what does the correlation of ($R_{\text{training}}=0.845$, and $R_{\text{test}}=0.762$) between the pMIC and the five descriptors tell us? It tells us:

- The relationship is positive and linear
- The relationship is quite strong (since the value is pretty close to 1)

R^2 square is the coefficient of determination, more usually expressed as a percentage. Here it tells us that 71.5% of the variability in pMIC can be explained by the variability in the five descriptors: Mass, Surface, Volume, Molar Refractivity and Rotatable Bond Count.

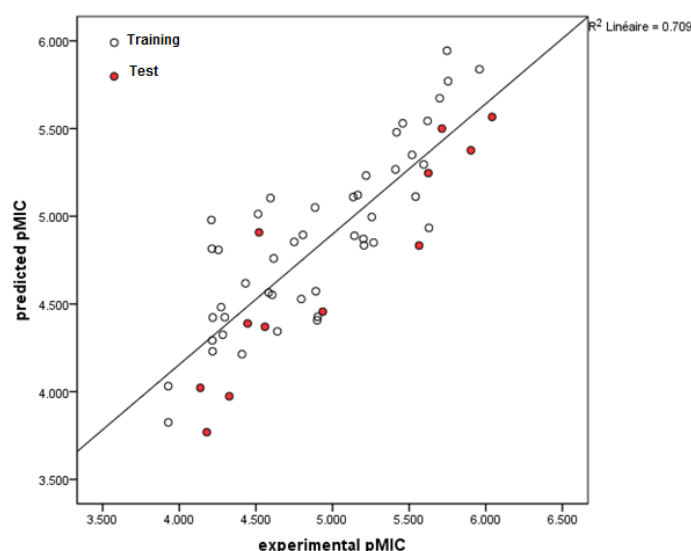


Figure 14 The plot of predicted pMIC values against the experimental pMIC values.

To evaluate the data set for any possible outliers, William plot (the plot of standardized residuals versus leverage values) was employed to visualize the applicability domain. The Williams plot was shown in (Fig.15). As it can be seen, all compounds were inside the domain of built model and have the leverage lower than warning $h=3p/n$ value (the

warning leverage limit is 0.55), where p is the number of model variables plus 1 and n is the number of objects used to develop the model. As it is obvious from (Fig.15), all the compounds in the training and test sets have standardized residuals smaller than three standard deviation units (3δ). Therefore, there are no outliers for the developed model and prediction results of the developed model can be confirmed.

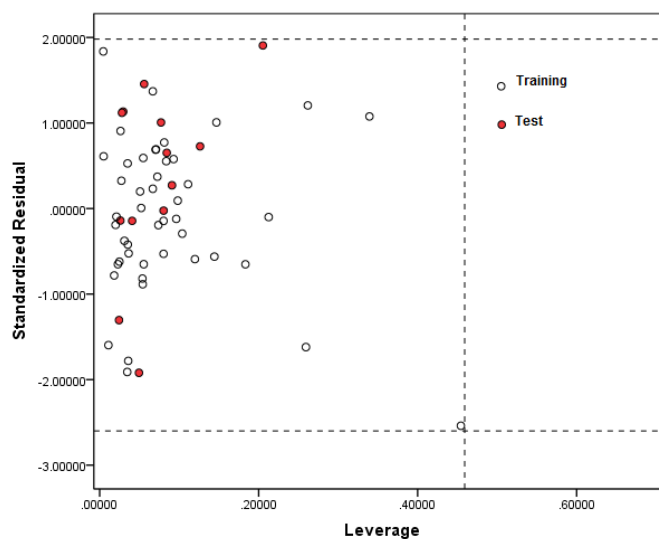


Figure 15 The plot of standardized residuals versus leverage values.

5. Interpretation of descriptors

By interpreting the selected descriptors with their corresponding effects on inhibitory activities, some useful chemical insight can be provided to understand the mechanism of inhibitory activity, and consequently, the new drugs can be designed with higher inhibitory activities. Hence, an acceptable interpretation of the QSAR results is provided below.

Firstly, at it appears, all the selected descriptors are size- and shape-based descriptors. There are many examples of applications of computational methods using shape. For example, Ekin et al. have elucidated substrate recognition in visualizing differences in inhibitors for human cytochrome P450 (CYP) 51.¹⁹⁵

The **shape** of an object located in some space refers to the part of space occupied by the object as determined by its external boundary. However, the definition of shape in molecular pharmacology does encompass structural features like depth, size and surface. the importance of shape comes into play when a small molecule is desired to fit into a binding site on a protein surface, where size and shape complementarity may be essential in addition to

favorable electrostatic and steric interactions, to fulfill the “lock and key” or “induced fit” hypotheses.¹⁹⁶

All of Mass, Surface, Molar Refractivity and Rotatable Bond Count display a positive sign, which indicates that the pMIC is directly related to these descriptors, and increasing the atomic mass of some specific substituents and fragments in molecule would result in higher inhibitory activity.

Volume displays a negative sign, which indicates that the pMIC value is inversely correlated to this descriptor. Therefore, it can be concluded that by increasing the volume of compounds the pMIC values will be reduced.

This result explores the various definitions of shape generally used when describing a ligands or interaction between ligands-receptor and provides an example of biological systems (P450_{14DM}) where the concept of shape plays a major role. Thus, the presence of structurally compatible regions between the receptor and its ligand is required for the functioning of these compounds.

6. Conclusion

In this work, the QSAR analyses of a series of compounds as P450_{14DM} inhibitors were carried out using multiple linear regressions. The most relevant descriptors were selected based on stepwise method search. The performed validation methods (external validation) demonstrate the accuracy and strength of the built model.

Using stepwise method as a selection tool presented five descriptors correlated with the inhibitory activity. By interpretation of the selected descriptors, it can be concluded that the activity of studied molecules increases by decreasing the molecular volume. In this study, the developed QSAR models can be useful to predict the activity of new compounds as P450_{14DM} inhibitors, and can provide a better insight to design new potent P450_{14DM} inhibitors.

PART III

Docking-Based Virtual Screening for Lead Optimization

In target based screening, compounds are tested with purified macromolecules (usually a protein) to find lead compounds that make intended macromolecular changes. For a lead compound to become a drug, it needs to be able to reach a site of action in the body, bind to its target macromolecule, and elicit the desired biological effect.

Compared to large biological molecule therapeutics, such as insulin or antibodies, which are administered through injection, small molecules can be taken orally and are better at reaching different sites in the body. This is why the majority of approved and experimental drugs are small molecules. Small molecules are also better suited for virtual molecular screening, which is the main subject to a target macromolecule to find compounds with the best binding affinity.¹⁹⁷

In all cases, finding the right target is very important for virtual screening to succeed. When the 3D (three-dimensional) structure of a target is available, through X-ray crystallography, NMR spectroscopy, or any other means, we can apply docking algorithms to search for the best binding mode between target macromolecule and ligand.

In this chapter, we perform a virtual screening experiment with PyRx open source software. We use the 3D structure of the mycobacterial cytochrome P450-dependent sterol 14 α -demethylase in the sterol biosynthesis pathway. Importantly, the P450_{14DM} encoded by the CYP51 gene of *M. tuberculosis* has also been shown to be highly susceptible to azole derivatives, suggesting the potential use of these compounds as alternative TB therapeutic agents.

1. Materials

PyRx version 0.8¹⁹⁸ is Virtual Screening software for Computational Drug Discovery that can be used to screen libraries of compounds against potential drug targets, which, is written in Python programming language and it can run on nearly any modern computer, from PC (personal computer) to supercomputer. HyperChem¹⁸⁶ was used for geometry optimization; and for LigPlot⁺ v.1.4.5¹⁹⁹ was used to generate schematic 2-D representations for interaction visualization.

2. Input files

To start with structure-based virtual screening, we need structures of the target macromolecule and small molecules as input files. Here we are using:

1. 33 oxadiazolone-,²² 38 oxadiazole-,¹⁹⁻²¹ and 82 oxazoline- and oxazole-related²⁵ chemical compounds, all classified as azole, sharing structural similarities (nitrogen heterocyclic ring compounds); which showed an interesting antimycobacterial activity against the reference strain of *Mycobacterium tuberculosis* H37Rv. This approach, is called the fragment-based screening technique, which has the advantage of finding lead molecules based on a set of fragment elements derived from a specific functional ligand family (azoles) and;
2. Protein Data Bank²⁰⁰ to get 3D structures of the mycobacterial protein: cytochrome P450-dependent sterol 14 α -demethylase in the sterol biosynthesis pathway (PDB ID: 2W0B) (Fig.16). Importantly, the MT P450_{14DM} has also been shown to be highly susceptible to **azole derivatives**, suggesting the potential use of these compounds as alternative TB therapeutic agents.

The reason for choosing these particular molecules is; that they are as mentioned above, all classified as azole (nitrogen heterocyclic ring compounds) with same anti-TB inhibitory activity. Selection of ligands depends whether virtual screening is used for lead discovery or lead optimization. For lead discovery, it is advised to include as many ligands with diverse shapes, sizes, and composition as possible. For lead optimization, our main work here, ligands are selected to closely match the lead compound (Azoles class).²⁰¹ One of the advantages of the virtual screening is that we are not limited to commercially available compounds; we can also use a ligand file for a novel compound not found in any of the databases.

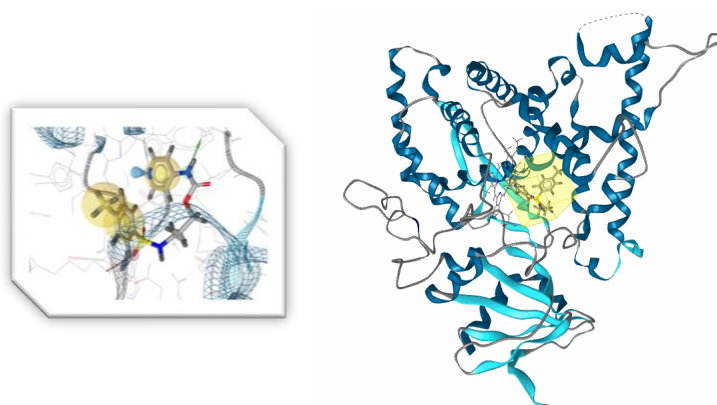


Figure 16 Cristal structure complexe (2W0B) interactions.

3. Methods

1- Prepare Input Files for Docking

Before we can use input files for virtual screening, we need to convert them to PDBQT file format suitable for docking with AutoDock Vina.

1. Initially we filter of these 33 oxadiazolone derivatives good MT P450_{14DM} inhibitory activity ones, by choosing 11 compounds with interesting MIC values of 4 µg/ml. Where these 33 oxadiazolone derivatives have been already docked with P450_{14DM}. The molecular structures of all (38+82+11) ligand molecules were built and subjected to an initial energy minimization, using force field MM+ in HyperChem. The convergence criterion was set to 0.01 kcal/(mol Å);
2. Load all the molecules to PyRx and then;
3. Create pdbqt files, using Convert All to AutoDock Ligand.
4. In this step, the X-ray structure of cytochrome P450 14 α -sterol demethylase in complex with CMW (PDB ID: 2W0B) was used as the reference complex. Then it was prepared for molecular docking by removing off water molecules using UCSFCHIMERA. Then, adding the polar hydrogen atom and Gasteiger charges using Auto Dock Tools (pdbqt file).

2- Run Virtual Screening Using Vina Wizard

1. This is the last step, where the ligand is docked onto the receptor using PyRx Virtual Screening Tool (Vina Wizard). The grid box parameters for the active site are given as: centre (X= -18.3, Y= -1.9, Z= 67.0) and dimension (X= 22.8, Y= 22.5, Z= 21.0).
2. After virtual screening is completed, PyRx automatically advances to Analyze Results page, where we can see results of virtual screening computation. AutoDock Vina, by default, outputs 10 best binding modes for each docking run. Left-click on Binding Affinity (kcal/mol) table header cell under Analyze Results tab to sort this table by predicted binding affinity.
3. Then, the interactions are checked using LigPlot (Fig.18 & .19). From the 10 best binding modes generated by Vina for each compound we choose the first one with low binding affinity (kcal/mol).

4. Docking method validation

First, we must be confident that the docking method will find a relevant conformation. Docking methods are typically validated by “redocking” experiments, where the PDB complex (2W0B) is separated and then redocked, ensuring that the docking algorithm can reproduce the observed binding mode. So the validation of molecular docking was done by superimposing each of the CMW docked poses (blue color) with the PDB crystal structure (PDB ID: 2W0B). The result of the best pose superimposition is shown in (Fig.17).

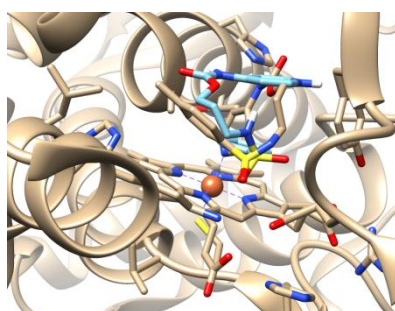


Figure 17 CMW_pose1_-8.4 kcal/mol (pose1_blue).

5. Free binding energy calculations

The main project to be carried out is to investigate all the necessary features of our 11 oxadiazolone, 38 oxadiazole, and 82 oxazoline and oxazole derivatives. During docking runs, 3D structure of the target is fixed while ligand is moved and rotated to find the best binding modes.²⁰² The binding affinity between the target and the small molecule was evaluated by the binding free energy approximation (ΔG_b , kcal/mol) using AutoDock Vina. The best scored conformation of each compound predicted by AutoDock Vina was selected and further ranked (Table.7). The docking score was used to predict the strength of the non-covalent interactions between two molecules after they have been docked (also referred to as binding energy). The docking score is a mathematical approximation of the binding free energy between the ligand and its target, which includes typical terms for dispersion/repulsion (steric interaction), hydrophobic interaction, hydrogen bonding, and the number of active rotatable bonds between heavy atoms in the ligand.

The main results from virtual screening runs are the best predicted binding modes and corresponding binding affinity. The negative values for binding affinity (or binding free

energy) indicate that all our ligands are predicted to bind to a target macromolecule. In this particular case of screening MT P450_{14DM} with:

- the most potent 11 comps of 33 oxadiazolone. Where these 33 oxadiazolone derivatives have been already docked with P450; and
- 38 oxadiazole, and 82 oxazoline and oxazole derivatives

Out of (82+38) compounds, only 18 oxadiazole, and 26 oxazoline and oxazole derivatives were showing better binding affinity than 11 oxadiazolone and CMW (reference ligand). From the top 6 compounds with binding free energy more then -11kcal/mol, we have 1 oxadiazole, and 5 oxazoline and oxazole derivatives. On the other hand, compound 72 exhibited a relatively lowest binding energy of (-12.1 kcal/mol), therefore, the highest binding affinity.

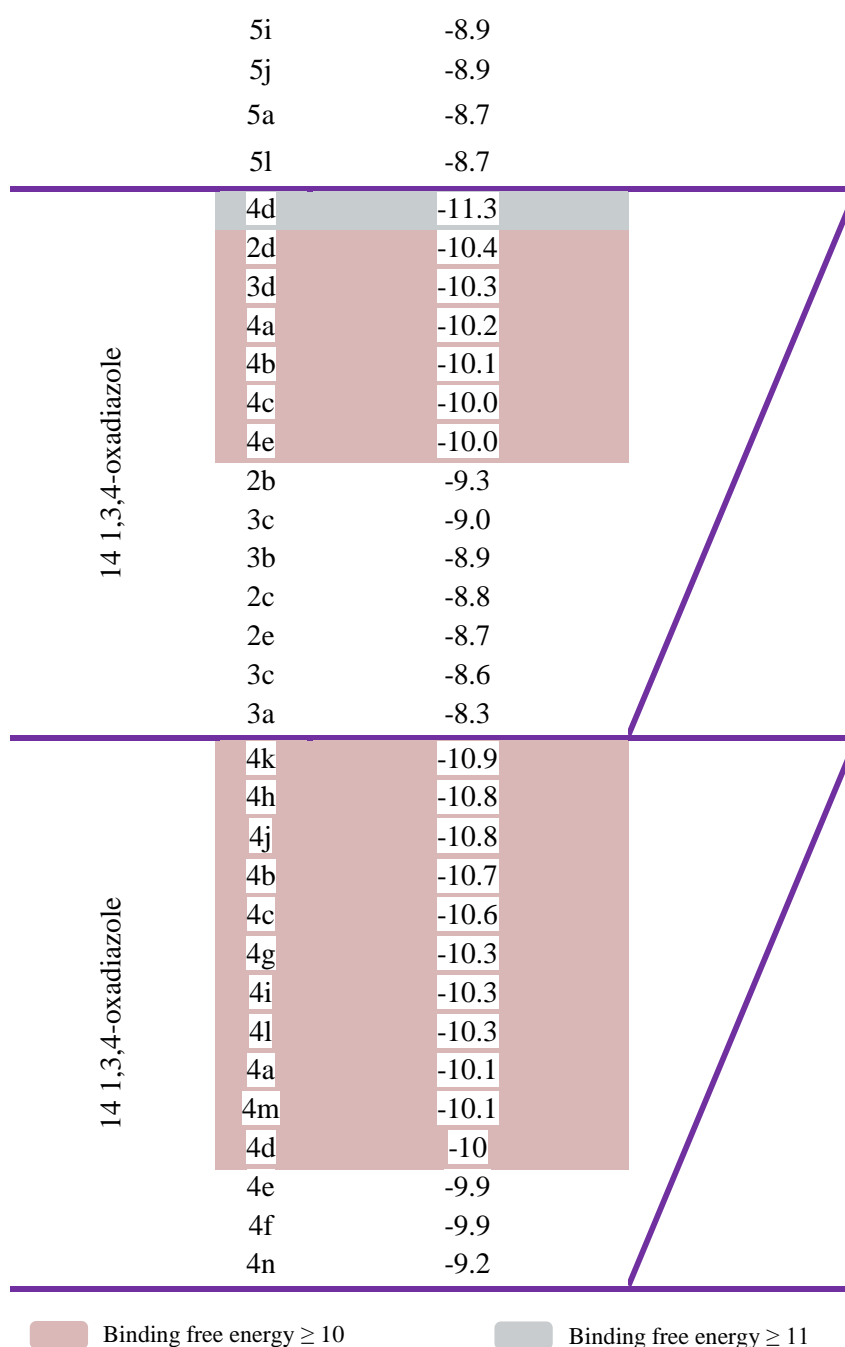
Nevertheless, small molecule virtual screening by docking is very valuable in silico method that can rank small molecules according to their predicted binding affinity to a target macromolecule. The cost of running virtual screening experiments is minuscule compared to real screening experiments.

Table 8 Free binding energy calculations.

| Compounds | | Binding Free Energy (kcal/mol) | MIC and K _D (μM) |
|---|----|--------------------------------|-----------------------------|
| CMW | | -8.4 | K _D =58.3-+4.6 |
| The most potent 11 comps of 33 oxadiazolone | 3i | -9.9 | 4 μg/ml |
| | 3m | -9.9 | |
| | 3h | -9.6 | |
| | 3j | -9.6 | |
| | 3l | -9.6 | |
| | 4h | -9.0 | |
| | 4i | -8.9 | |
| | 4g | -8.6 | |
| | 4j | -8.6 | |
| | 4f | -6.6 | |
| | 3a | -6.2 | |
| 82 oxazoline and oxazole benzyl esters | 72 | -12.1 | 3.03 |
| | 84 | -11.9 | 61.8 |
| | 51 | -11.6 | 0.77 |
| | 56 | -11.3 | 12.5 |
| | 64 | -11.0 | 5.4 |

| | | |
|-----|-------|-------|
| 50 | -10.9 | 15.6 |
| 78 | -10.8 | 1.49 |
| 63 | -10.7 | 62.6 |
| 31 | -10.4 | 6.3 |
| 80 | -10.4 | 66.2 |
| 81 | -10.4 | 8 |
| 34 | -10.3 | 17.8 |
| 99 | -10.3 | 1.95 |
| 33 | -10.1 | 13 |
| 35 | -10.1 | 58.8 |
| 62 | -10.1 | 118 |
| 67 | -10.1 | 35.4 |
| 70 | -10.1 | 0.7 |
| 82 | -10.1 | 6.86 |
| 95 | -10.1 | 25.2 |
| 3 | -10.0 | 12.6 |
| 26 | -10.0 | 52 |
| 86 | -10.0 | 15.5 |
| 88 | -10.0 | 1.98 |
| 92 | -10.0 | 5.55 |
| 98 | -10.0 | 3.48 |
| 28 | -9.9 | 30.6 |
| 49 | -9.9 | 15.5 |
| 66 | -9.9 | 1.1 |
| 68 | -9.9 | 0.73 |
| 90 | -9.9 | 2.35 |
| 91 | -9.9 | 2.87 |
| 97 | -9.9 | 12.84 |
| 100 | -9.9 | 1.76 |
| 18 | -9.8 | 61 |
| 24 | -9.8 | 50.5 |
| 61 | -9.8 | 35.8 |
| 69 | -9.8 | 2.4 |
| 89 | -9.8 | 0.91 |
| 12 | -9.7 | 118 |
| 25 | -9.7 | 60.7 |
| 53 | -9.7 | 47.2 |
| 58 | -9.7 | 1.79 |
| 59 | -9.7 | 1.25 |
| 60 | -9.7 | 1.72 |
| 85 | -9.7 | 16 |

| | | | |
|---------------------|----|------|------|
| | 96 | -9.7 | 1.93 |
| | 57 | -9.6 | 25.4 |
| | 17 | -9.5 | 11.6 |
| | 21 | -9.5 | 26.1 |
| | 22 | -9.5 | 60.6 |
| | 47 | -9.5 | 3.2 |
| | 65 | -9.5 | 0.47 |
| | 23 | -9.4 | 60.7 |
| | 29 | -9.4 | 6.24 |
| | 30 | -9.4 | 30.2 |
| | 32 | -9.4 | 30.7 |
| | 87 | -9.4 | 18.9 |
| | 93 | -9.4 | 3.88 |
| | 94 | -9.4 | 6.04 |
| | 15 | -9.3 | 7.2 |
| | 46 | -9.3 | 2.97 |
| | 52 | -9.3 | 24.8 |
| | 54 | -9.2 | 24.2 |
| | 55 | -9.2 | 73 |
| | 37 | -9.1 | 22.9 |
| | 76 | -9.1 | 2 |
| | 79 | -9.1 | 1.42 |
| | 38 | -9.0 | 110 |
| | 16 | -8.9 | 49.9 |
| | 42 | -8.9 | 39 |
| | 73 | -8.9 | 2.37 |
| | 77 | -8.9 | 3.82 |
| | 83 | -8.9 | 7.32 |
| | 45 | -8.8 | 37 |
| | 48 | -8.8 | 2.72 |
| | 74 | -8.8 | 2.54 |
| | 75 | -8.8 | 3.01 |
| | 40 | -8.7 | 55.6 |
| | 36 | -8.6 | 27.6 |
| | 39 | -8.5 | 53.3 |
| | 41 | -8.1 | 61.2 |
| 10 1,3,4-oxadiazole | 5e | -9.2 | |
| | 5b | -9.1 | |
| | 5c | -9.1 | |
| | 5g | -9.1 | |
| | 5h | -9 | |
| | 5f | -8.9 | |



6. Binding Interactions

The active site residues of proteins are important for their functioning; therefore it is important to understand the interactions of these potential inhibitors with the functional amino acids in the protein. ²⁰³ LigPlot analysis was used to design a 2D interaction maps to show the predicted interactions of each ligand with the active site residues of the protein.

The 6 compounds (Table.7) with the best interaction affinity than endogenous ligand CMW and the best two oxadiazolones (3i and 3m), were found to interact with the amino acid residues participated in interacting with CMW, 3i and 3m given in Table.8.

Different binding modes were revealed for all 6 best compounds. Where, the hydrophobic interactions play the most important role in almost all the docked compounds.

The Gln 72, Tyr 76, Lys 94, and Ala 256 residues interactions are the most responsible for the ligand-protein binding in almost our compounds (Table.8 & Fig.19). Where, they interact with the compounds by forming both hydrogen bond and hydrophobic interactions.

The best interacting three compounds are:

- Compound 72 with (-12.1) lowest binding energy formed only hydrophobic interactions with 48% of the active site residues shown in Fig.19 & Table.8;
- Compound 84 scored (-11.9) formed the hydrogen bond with Lys 97 residue and hydrophobic interactions with 60% of all the active site residues as shown in Fig.19 & Table.8; and
- Compound 51 scored (-11.6) also found to interact hydrophobically with 48% of the active site amino acid residues and formed H-bond with Arg 96 as shown in Fig.19 & Table.8.

Computational analysis suggested that all compounds interacted in a similar manner of CMW within the binding pocket of P450_{14DM}. The compounds attained similar binding orientation occupying the common amino acids within the binding site (Fig.18 & .19).

All of compounds 72 & 51 are similar in structure except of oxazole & oxazoline moieties respectively. The compound 72 (oxazole derivative) got the best binding affinity.

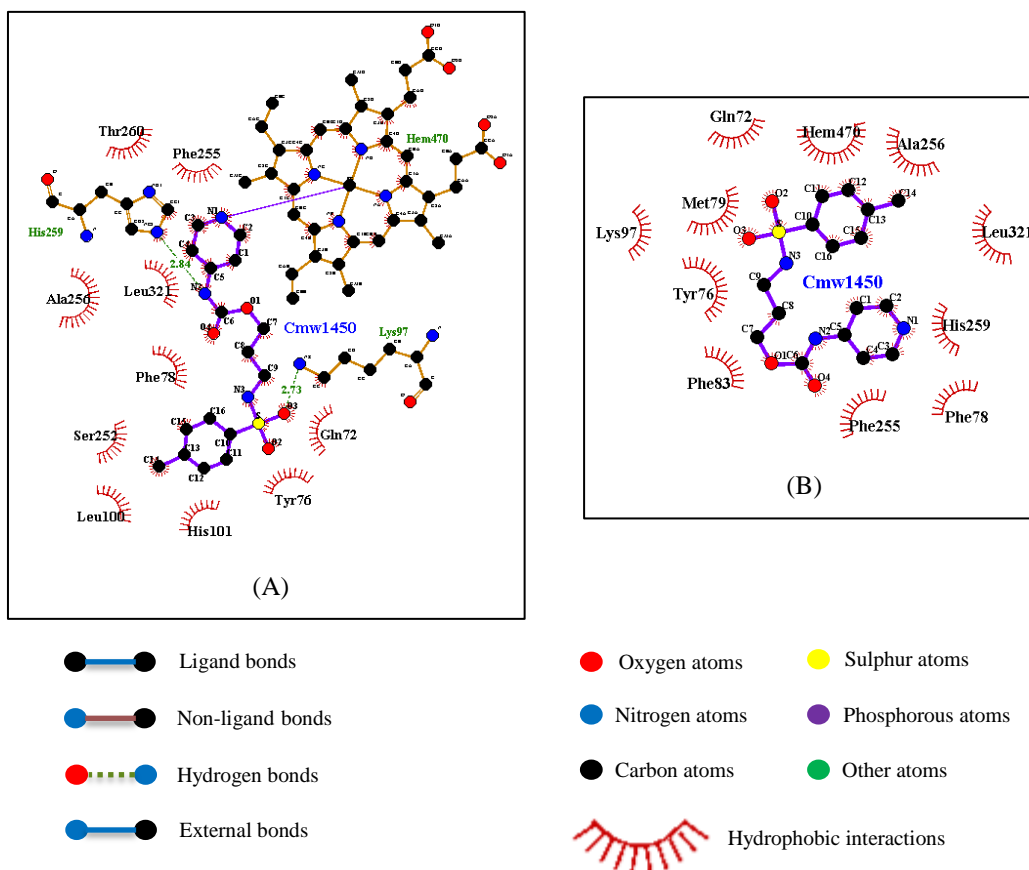


Figure 18 Binding forces between the CMW and the protein active site residues. (A) CMW crystal structure. (B) CMW docked pose 1.

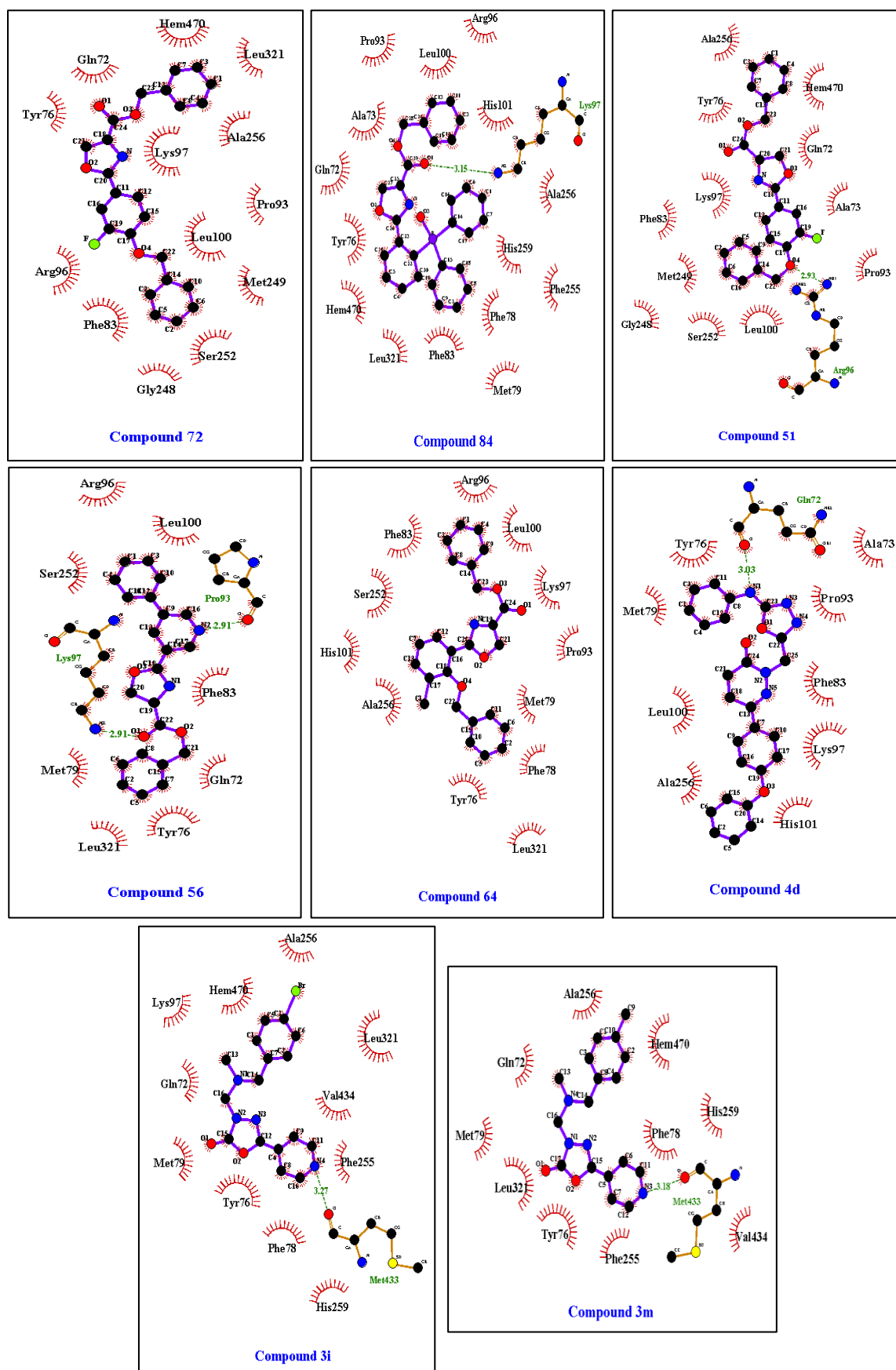


Figure 19 Binding forces between the 6 best binding affinity compound and the protein active site residues.

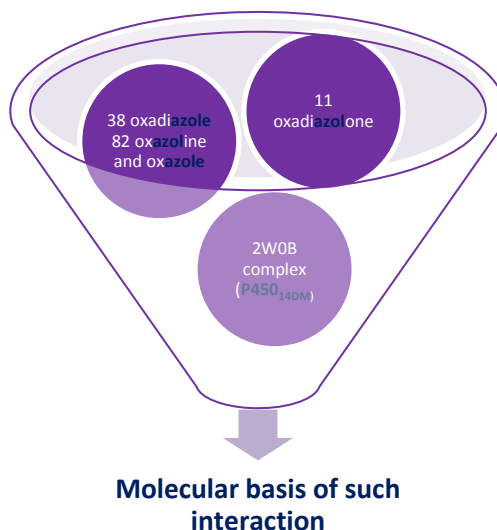
Table 9 Interaction residues of better scoring compounds.

| The active site residues | Compounds | | | | | | | | | |
|--------------------------|--------------------|---------------------|----|----|----|----|----|----|----|----|
| | CMW _{exp} | CMW _{pred} | 72 | 84 | 51 | 56 | 64 | 4d | 3i | 3m |
| Gln 72 | • | • | • | • | • | • | • | • | • | • |
| Ala 73 | | | | • | • | | | • | | |
| Tyr 76 | • | • | • | • | • | • | • | • | • | • |
| Phe 78 | • | • | | • | | | • | | • | • |
| Met 79 | | • | | • | | • | • | • | • | • |
| Phe 83 | | • | • | • | • | • | • | • | | |
| Pro 93 | | | | • | • | • | • | • | | |
| Arg 96 | | | • | • | • | • | • | | | |
| Lys 97 | • | • | • | • | • | • | • | • | • | • |
| Leu 100 | • | | • | • | • | • | • | • | | |
| His 101 | • | | | • | | | • | • | | |
| Gly 248 | | | • | | • | | | | | |
| Met 249 | | | • | | • | | | | | |
| Ser 252 | • | | • | | • | • | • | | | |
| Phe 255 | • | • | | • | | | | | • | • |
| Ala 256 | • | • | • | • | • | • | • | • | • | • |
| Gly 257 | | | | | | | | | | |
| His 259 | • | • | | • | | | | | • | • |
| Thr 260 | • | | | | | | | | | |
| Leu 321 | • | • | • | • | | • | • | | • | • |
| Cys 394 | | | | | | | | | | |
| Met 433 | | | | | | | | | • | • |
| Val 434 | | | | | | | | | • | |

Hydrophobic interaction • H-bond •

4. Conclusion:

The computational study suggested that all of (82+38) active compounds could interact at the active site of MT P450_{14DM}, and the calculated free energy of binding are in agreement with the corresponding MIC values in almost of the cases. These encouraging results led us to advance in the design, synthesis and evaluation of a second generation of azole derivatives.



GENERAL CONCLUSION

In this present study, the knowledge of the relationship between chemical structure and biological activity is an essential prerequisite for the effective search for biologically active compounds. For example, the substitution effect study, 2D QSAR and 2D similarity methods can be applied almost immediately. As a part of our ongoing studies in developing new active compounds with anti-mycobacterial activity, we have studied the structural requirements to substituted-1,3,4-oxadiazole derivatives that cause the anti-tuberculosis activity, which help to identify structural information to derive new lead compounds for our future researches.

First, we analyze the electronic properties of 1, 3, 4-oxadiazole ring and its derivatives, in order to deepen our understanding of its various therapeutic significance in general. It is now understood that 1, 3, 4-oxadiazole characters changes with regard to substitution groups. These behaviors are based on electronic and structural characteristics that constitute the soft and hard classifications of the HSAB theory. Where it has been found that the alkyl, amine and hydroxyl substitution at the 2-position of 1, 3, 4-oxadiazole ring increases the hardness of the system, while the cyanide and ketone one decreases it.

With regard to the anti-tuberculosis series, the lipophilicity balance and ionization state seem to play an important role. Where they reveal their ampholytes character but because the difference between pKa acidic and pKa basic is > 3 , there will be no simultaneous ionization of the two groups and decrease the transition between several different charge states. Knowing that our compound at some pH can be chargeless, lead us to explore the Log D profile that shows they have good permeability. We found all compounds followed Lipinski's rule as they have a molecular weight under 500 Da, a limited lipophilicity (expressed by $\text{Log } P < 5$), far less than 5 H-bond donors (expressed as the sum of OHs and NHs), and also far less than 10 H-bond acceptors (expressed as the sum of Os and Ns) and Viber's rules also. In addition, they present a high percentage of absorption (%ABS), with all of the compounds being potentially able to cross biological membranes and to have a good oral bioavailability. Considering active efflux alone, Petrauskas has proposed the 'rule of four', where all most our compounds are seems to satisfy the unlikely efflux substrates criteria just for compounds 14 which is likely to be efflux substrate for the P-glycoprotein.

The correlation between the size and %inhibition of this anti-tuberculosis series was expressed by Per-cent Efficiency Index (PEI). The calculated PEI (3.17) suggests that compound 1 could be adopted as lead to locate a potential active anti-tuberculosis compound. Moreover, the Group Efficiency (GE=1.17 and 0.65) show the quality of SH and phenyl

added group to maintain (or increase) the optimization of the anti-tubercular activity respectively.

Quantitative structure activity relationship (QSAR) studies were performed on a series of oxazoline and oxazole benzyl esters as anti-tuberculosis agents, multiple linear regression analysis was performed to derive QSAR models which were further evaluated internally and externally for the prediction of activity. Where the best QSAR model ($R^2_{\text{training}}=0.715$, RMSE =0.308) has acceptable statistical quality and predictive potential as indicated by the value of external validation of a test set ($R^2_{\text{test}}=0.581$, RMSE =0.374). Where, all the selected descriptors are size- and shape-based descriptors.

Finally, molecular docking study showed that all of (82+38) active compounds could interact at the active site of MT P450_{14DM}, and the calculated free energy of binding are in agreement with the corresponding MIC values in almost of the cases. Where, the hydrophobic interactions play the most important role in almost all the docked compounds. And the most important interactions for the ligand-protein binding are with Gln 72, Tyr 76, Lys 94, and Ala 256 residues. For compound 72 with (-12.1) lowest binding energy forms only hydrophobic interactions with 48% of the active site residues. These encouraging results led us to advance in the design, synthesis and evaluation of a second generation of azole derivatives.

APPENDIX

In Silico Modeling of Substitution-Induced Effect and Structure Property/Activity Relationship Profile of 1,3,4-Oxadiazole Derivatives

Imane Benbrahim¹, Salah Belaidi^{1,2,*}, and Ahmed M. Alafeefy³

¹Group of Computational and Pharmaceutical Chemistry, LMCE Laboratory, University of Biskra, BP 145 Biskra 07000, Algeria

²Université de Rennes 1, Institut des Sciences Chimiques de Rennes, UMR 6226 CNRS, Campus de Beaulieu, 35042 Rennes Cedex, France

³Department of Chemistry, Kulliyah of Science, International Islamic University, P.O. Box 141, 25710 Kuantan, Malaysia

Nitrogen heterocycles are among the most significant structural components of pharmaceuticals. Our minimalist design format presents opportunities to reveal the electron density profile of 1,3,4-oxadiazoles a function of the various donating and withdrawing substituent groups using the FMOs energies and the density-based descriptors such as chemical potential (μ), electronegativity (χ), hardness (η) and softness (σ). Where the quantum mechanical geometry optimization were performed using B3LYP function of density functional theory. We discussed the enhancement or diminution in the hardness of 1,3,4-oxadiazole derivatives. Furthermore, *in silico* studies showed that, the anti-tuberculosis 1,3,4-oxadiazole derivatives have a good lipophilicity profile and followed Lipinski and Veber rules. Thus, they are expected to have a high probability of good oral bioavailability.

KEYWORDS: 1,3,4-Oxadiazole, Density-Based Descriptors, PEI and GE Analysis, Log *P* and Log *D* Profile, SAR/SPR.

CONTENTS

| | |
|--|---|
| 1. Introduction | 1 |
| 2. Materials and Methods | 3 |
| 3. Results and Discussion | 3 |
| 3.1. Methods Validation | 3 |
| 3.2. Substitution Effects on 1,3,4-Oxadiazole | 3 |
| 3.3. Structure Activity/Property Relationships Studies | 5 |
| 4. Conclusion | 9 |
| References and Notes | 9 |

1. INTRODUCTION

Oxadiazole is a nitrogen heterocyclic nucleus that attracted a wide attention of the chemist in research for new therapeutic molecules. Out of its four possible isomers, 1,3,4-oxadiazoles are widely exploited for various applications.¹ Among heterocyclic compounds, 1,3,4-oxadiazoles have become an important construction motif for the development of new drugs. Compounds containing 1,3,4-oxadiazole cores have a broad biological activity spectrum including antibacterial, antifungal,^{2,3} analgesic, anti-inflammatory,^{4,5} antiviral,⁴ anticancer,^{6–8}

and anticonvulsant.^{4,9} Therapeutic significance of these useful drugs as anti-tubercular encouraged the development of more potent and significant compounds. Extensive biochemical and pharmacological studies have confirmed that these molecules are effective as anti-tubercular compounds.^{10–13} The main causative agent of tuberculosis (TB) is *Mycobacterium tuberculosis* (*M. tuberculosis*). Every year, approximately 8 million of the infected people develop active TB, and 2 million die.

In recent years, the drug discovery/development process has been gaining in efficiency and rationality because of the continuous progress and application of chemoinformatics methods.¹⁴ Earlier, it was reported that a number of 2,5-disubstituted-1,3,4-oxadiazoles have been designed, synthesized, and screened for their anti-tuberculosis activity against *M. tuberculosis* H37Rv.¹⁰ The knowledge of the relationship between chemical structure and biological activity is an essential prerequisite for the effective search for biologically active compounds. For example, 2D QSAR^{15–20} and 2D similarity^{21–24} methods can be applied almost immediately. As a part of our ongoing studies in developing new active compounds with anti-mycobacterial activity, we are going to study and understand the structural requirements to substituted-1,3,4-oxadiazole derivatives that cause the anti-tuberculosis activity, which help

*Author to whom correspondence should be addressed.
Email: prof.belaidi@gmail.com
Received: 28 July 2016
Accepted: 30 August 2016

to identify structural information to derive new lead compounds for our future researches. In this context, the substitution effect study²⁵ was done in order to deepen our understanding of the influence of various substituents on 1,3,4-oxadiazole ring. Here, we present the electronic and geometric structure calculations^{26,29} for 1,3,4-oxadiazole substituted by two functional groups of different strengths using the conceptual DFT³⁰ descriptors.

Nowadays, various approaches to simultaneously optimize many factors in drug design are broadly described under the term ‘multi-parameter optimization’ (MPO).³¹ In this paper, we use rules of thumb and calculated metrics methods³² to guide the exploration of this new anti-tuberculosis agent to identify new chemistries with a high probability of achieving the required property profile.

Starting with rules of thumb, we use Lipinski,³³ Veber³⁴ and Petrauskas³⁵ rules to study the high oral bioavailability at the target site. The latter is often an important factor for the development of bioactive molecules, as therapeutic agents and any attempt to predict or study the bioavailability would require that both properties absorption and metabolism must be taken into account.

The main factor of drugs absorption and metabolism is the lipophilicity which offers a critical information that enable us to better interpret our results since it's a major structural factor that influences the pharmacokinetic (permeation of physiological membranes, plasma protein binding and volume of distribution) and pharmacodynamic (target recognition, target affinity and target specificity) behavior of our anti-tuberculosis compounds.



Imane Benbrahim is a Ph.D. student in molecular chemistry at the university of Biskra working under the supervision of Professor Salah Belaidi. She is a member of the Group of “Computational and medicinal Chemistry” at the Laboratory of Molecular Chemistry and Environment. She received her master’s degree in pharmaceutical chemistry from the University of Biskra under the guidance of Professor Salah Belaidi. Her main research interests are Molecular modeling and drug design. Where her current research primarily focus on the substitution effect, electronic and geometric properties, SAR/SPR and QSAR study of antituberculosis compounds.



Salah Belaidi is currently a professor and Chairman of the Scientific Council of the Faculty of Exact Sciences, University of Biskra. He is the head of the Group of “Computational and Pharmaceutical Chemistry” at the Laboratory of Molecular Chemistry and Environment. He received his MS and Ph.D. degrees in macrolides Chemistry under the supervision of Professor Alain Botrel and Dr. René Grée from Rennes1 University. He reviewed several manuscripts for some journals such as Journal of Enzyme Inhibition and Medicinal Chemistry, Journal of Molecular Structure and Spectrochimica Acta Part A. Professor Dr. Salah BELAIDI has about 60 publications in reputed international scientific journals. His research interests span the domains of medicinal chemistry and computational chemistry. In particular, he studies the principles of chemical design of biomolecules, multi-parameter optimization (MPO) in drug discovery, docking and rational drug design and QSAR models by means of theoretical and computational methods.



Ahmed M. Alafeefy attended Zagazig University from 1978–1983. Then he received his Ph.D. in Pharmaceutical Sciences [Pharm. Chem.], Helwan University, 2005. Currently, he is an Assistant Professor of Medicinal Chemistry at Chemistry Dept. Kulliyah of Science, International Islamic University, Malaysia. Alafeefy’s current research interest covers the application of modern methods and techniques for the development of drugs to combat cancer and viral diseases. He has been consistently funded by King Abdulaziz City for Science and Technology (KACST) and foundations to develop biochemical rationale for the preparation of antitumor drugs focusing on qualitative differences between normal and cancerous cells has been central point of his research area. The development of some of the biologically active antiviral, anticancer and antioxidants from natural sources constitutes his future plan. For the later purpose he has recently won a fund from the Saudi National

Plan for Science and Technology (NPST). Dr. Alafeefy has about 40 publications in reputed highly ranked international scientific journals in addition to two patents at the European patency office. He has 10 oral presentations in international conferences.

Afterward, we extended our study towards calculated metrics methods. In this respect, we applied a Percent Efficiency Index (PEI) and Group Efficiency (GE) analysis^{36–39} to guide the selection of best anti-tubercular compounds that use their atoms most efficiently.

2. MATERIALS AND METHODS

The geometry of the 1,3,4-oxadiazole was initially optimized at three levels of theory:

- using the Hartree-Fock level (HF),
- using Møller-Plesset second order (PM2) level and
- using density functional theory with the Becke's three-parameter exchange functional and the gradient-corrected functional of Lee, Yang and Parr (DFT/B3LYP). With the standard 6-31G++ (d,p) basis set, i.e., the valence double-r basis set augmented by one set of six d- and one set of p-polarization functions on heavy atoms and hydrogens, respectively. Moreover, additional diffuse functions were placed on all atoms.

In particular, large basis sets are used to calculate the polarization effect accurately, and it is shown that the role of polarization may be systematically underestimated if small basis sets are employed.

In the next step, we have chosen the DFT level to determine and analyze the equilibrium geometries of the studied series of the donating and withdrawing groups of the 1,3,4-oxadiazole nucleus according to the comparison between the experimental and calculated results. The Gaussian 09 program package⁴⁰ was used in all quantum-mechanical calculations (HOMO and LUMO energies). The model building was done using molecular visualization software (Gaussian graphical interface GaussView 5.0.8).

All the parameters for drug-likeness were predicted and calculated according to the Lipinski's rule-of-five, Veber's and Petrauskas's rules using Calculator Plugins⁴¹ of MarvinSketch 6.3.0 software.⁴²

3. RESULTS AND DISCUSSION

3.1. Methods Validation

Molecular geometry is determined by the quantum mechanical behavior of the electrons. It can be specified in terms of bond lengths, bond angles and dihedral angles. 1,3,4-oxadiazole is relatively simple systems from the computational point of view, since they are planar, symmetric (they belong to the C_{2v} point group symmetry), and do not contain large numbers of atoms. As shown from (Table I), all the 1,3,4-oxadiazole geometries obtained from B3LYP and Hartree-Fock models are very similar and generally improved over geometries obtained from MP2 models. With the DFT method, the mean absolute error is smaller comparing to MP2 and HF methods, which mean that it is in a good agreement with experimental data. This demonstrates that to describe an accurate ground state configuration, the electron correlation effects that play an important role in such molecules should be taken into account. Consequently, we have chosen the DFT method to perform the substitution effect study of 1,3,4-oxadiazole ring (Fig. 1).

3.2. Substitution Effects on 1,3,4-Oxadiazole

The main objective of this study is to produce two series of derivatives of 1,3,4-oxadiazole (Fig. 2) to explore the substitution effect on this core. Where, the substitution of our groups will be at one carbon atom of 1,3,4-oxadiazole ring because of the C_{2v} symmetry.

Our focus was placed on modifications of the polar or the electronic effects exerted by different electron donating and withdrawing groups ("series 1 and 2" analogs, Fig. 2), which is a combination of the inductive and the mesomeric effect.

Several criteria have been put forward in attempts to rationalize and quantify this effect. These can be roughly divided into two categories: energetic and reactivity-based measures. Many of these properties are available through quantum chemical calculations.

Table I. Bond lengths and valence angles of 1,3,4-oxadiazole.

| Parameters | Exp ⁴³ | HF 6-31G++ (d,p) | PM2 6-31G++ (d,p) | DFT/B3LYP 6-31G++ (d,p) |
|----------------------------|-------------------|------------------|-------------------|-------------------------|
| Length of bond (Angstroms) | | | | |
| O1–C2 | 1.348 | 1.363 | 1.337 | 1.361 |
| C2–N3 | 1.297 | 1.304 | 1.264 | 1.291 |
| N3–N4 | 1.399 | 1.404 | 1.383 | 1.403 |
| C2–H6 | 1.075 | 1.074 | 1.068 | 1.078 |
| Mean absolute error | – | 0.007 | 0.0167 | 0.0065 |
| Angle of valence (Degrees) | | | | |
| O1–C2–N3 | 113.4 | 113.5 | 112.8 | 113.2 |
| C2–N3–N4 | 105.6 | 105.7 | 106.0 | 105.9 |
| C5–O1–C2 | 102.0 | 101.5 | 102.2 | 101.7 |
| O1–C2–H6 | 118.1 | 118.0 | 118.7 | 118.1 |
| N3–C2–H6 | – | 128.5 | 128.4 | 128.7 |
| Mean absolute error | – | 0.25 | 0.4 | 0.2 |

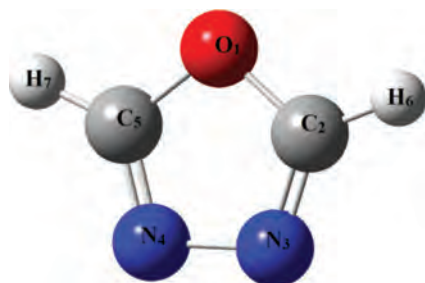


Fig. 1. 3D structure of 1,3,4-oxadiazole.

Ionization potentials and electron affinities are related in that both involve transfer of an electron between a molecular orbital and infinity: in one case (IP) we have removal of an electron from an occupied orbital and in the other (EA) addition of an electron to a virtual (or a half-occupied) orbital.

The EA of a molecule is positive for all derivatives of 1,3,4-oxadiazole it means that the accepted electron is bound, i.e., it is not spontaneously ejected; if the new electron is ejected in microseconds or less (is unbound), the molecule has a negative EA.

For, the electron affinity which states that a compound B_4 and B_3 with a big positive value than the other derivatives is called an electron acceptor and the A_3 , A_4 and B_1 are less positive and electron donor.

In general, the EA decreases by the addition of the alkyl groups, NH_2 and OH and increases for CN and OCH groups compared to ODZ .

Following the ionization potential values we can see that they decrease for all the derivatives just for the COH group which it stays the same as for ODZ and it increases for the CN group. Further, the NH_2 substituent shows the lower IP than the alkyl derivatives and the OH substituents. This suggests that the systems with these substituents contribute more towards electron donating character.

Similar conclusion can be drawn from the frontier molecular orbitals (FMOs), HOMO–LUMO gaps (HLG's),

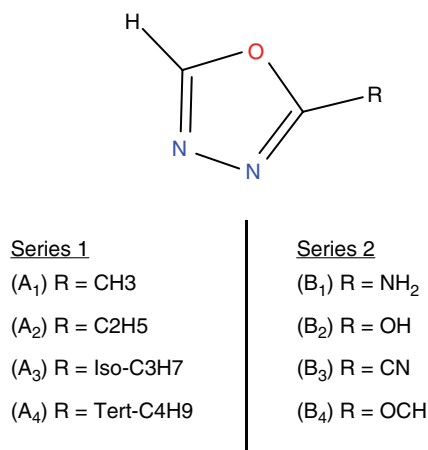


Fig. 2. 1,3,4-oxadiazole systems.

chemical potential, softness and hardness parameters reported in Table II.

The electronic chemical potential (μ) and the chemical hardness (η) determine the resistance of the chemical species to lose electrons and measure their global response to changes in the number of electrons since they are independent of the position.

Thus, the chemical potential of DFT is equivalent to the negative of the concept of electronegativity, and the principle of electronegativity equalization follows readily from this identification.

$$\mu = -(IP + EA)/2 = -\chi$$

All compounds have a negative chemical potential, which means that they have a weaker tendency of the electrons to escape from the system. That is, electrons flow from the regions with higher chemical potential to the regions with lower chemical potential, up to the point in which μ becomes constant throughout the space.

The global descriptor of hardness has been an indicator of overall stability of the system. It has been customary to use a finite difference approximation for η using the energies of N , $(N + 1)$ and $(N - 1)$ electron systems; we get the operational definition of η as,

$$\eta = (IP - EA)/2$$

Where, IP and EA are the first vertical ionization energy and electron affinity of the chemical species respectively. The inverse of the hardness is expressed as the global softness,^{44,45}

$$\sigma = 1/2\eta$$

When using the Pearson's Hard and Soft, Acids and Bases theory⁴⁶ as a guide for predicting the behavior of our derivatives. On the basis of, the HSAB concept, reactive molecules are divided by their respective polarizability, such that electrophiles and nucleophiles, are classified as either soft (relatively polarizable) or hard (relatively nonpolarizable).

Whereas the HSAB theory initially described hardness and softness in terms of the experimental ionization potential and electron affinity of the reacting molecules, these parameters also can be related (e.g., by Koopmans theorem) to the respective energies of the FMOs.⁴⁷

HSAB concept states that a hard base (nucleophile) is characterized by a low value for the energy of the occupied frontier orbital HOMO, a soft base by a higher value of HOMO. Accordingly, the hardness of a base increases with the decrease of HOMO.

A hard acid on the contrary is characterized by a high value for the energy of the empty frontier orbital LUMO, and its hardness will decrease with the decrease of LUMO.⁴⁸

The identification of the global hardness with the HLG of molecular orbital theory has been richly rewarding in terms of measuring stability.

Table II. Density based descriptors of 1,3,4-oxadiazole systems.

| COMPOSE | HOMO | LUMO | HLG's | IP | EA | η | μ | σ | χ |
|---|--------|--------|-------|-------|-------|--------|---------|----------|--------|
| ODZ | -0.304 | -0.038 | 0.266 | 0.304 | 0.038 | 0.133 | -0.171 | 3.759 | 0.171 |
| A ₁ CH ₃ | -0.291 | -0.028 | 0.263 | 0.291 | 0.028 | 0.1315 | -0.1595 | 3.802 | 0.1595 |
| A ₂ C ₂ H ₅ | -0.289 | -0.029 | 0.260 | 0.289 | 0.029 | 0.130 | -0.159 | 3.846 | 0.159 |
| A ₃ Iso-C ₃ H ₇ | -0.287 | -0.025 | 0.262 | 0.287 | 0.025 | 0.131 | -0.156 | 3.816 | 0.156 |
| A ₄ Tert-C ₄ H ₉ | -0.286 | -0.025 | 0.261 | 0.286 | 0.025 | 0.1305 | -0.1555 | 3.831 | 0.1555 |
| B ₁ NH ₂ | -0.254 | -0.025 | 0.229 | 0.254 | 0.025 | 0.1145 | -0.1395 | 4.366 | 0.1395 |
| B ₂ OH | -0.281 | -0.032 | 0.249 | 0.281 | 0.032 | 0.1245 | -0.1565 | 4.016 | 0.1565 |
| B ₃ CN | -0.326 | -0.100 | 0.226 | 0.326 | 0.100 | 0.113 | -0.213 | 4.424 | 0.213 |
| B ₄ OCH | -0.303 | -0.113 | 0.190 | 0.303 | 0.113 | 0.095 | -0.208 | 5.263 | 0.208 |

Note: *All the density based descriptors are in u. a. of energy (Hartree), just σ which is in (Hartree⁻¹).

Figure 3 shows an orbital energy diagram for 1,3,4-oxadiazole derivatives for only the HOMO and LUMO orbitals. Substitution of donor and acceptor functional groups affects the energy levels of the frontier orbitals. Where the HOMO and LUMO are going up in energy in compounds A₁, A₂, A₃ and A₄ where the HLG and the hardness η are little affected compared to ODZ ring. But for the compounds B₁ and B₂ the HOMO is going up in energy and the LUMO is little affected where the HLG is smaller than for ODZ ring so B₁ and B₂ are becoming soft in contrast to ODZ.

As for compounds B₃ and B₄ the HOMO and LUMO has decrease in energy in which they have the smallest gaps in all compounds with the biggest values of the softness character.

3.3. Structure Activity/Property Relationships Studies

Molecular structure properties of the molecule are usually the first and the simplest calculated values to produce information that can be used to predict the behavior of the compounds in the body. For this, we have choosing these criteria to characterize the compounds of this series: molecular weight (MW), lipophilicity (log *D* and log *P*),

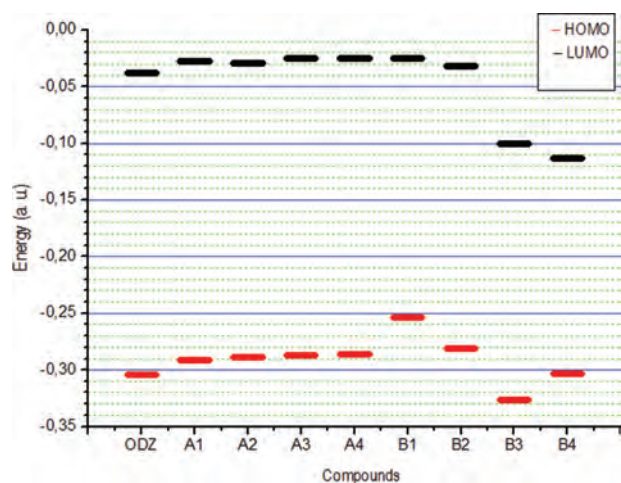


Fig. 3. Changes in the energy levels of HOMO–LUMO orbital of 1,3,4-oxadiazole derivatives.

number of hydrogen-bond donors and acceptors (NHBD and NHBA), polar surface area (PSA), number of rotatable bonds (nrotb) and ionization state (dissociation constant pKa).

3.3.1. Drug-Like Properties of Rule of Thumb

The successful design of new drugs requires optimization of many parameters simultaneously. The absorption is predominantly a function of solubility and permeability. Solubility is perhaps the most basic requirement of an orally available drug. In general, it is desirable for a drug candidate to have high enough water solubility to dissolve in body fluids in adequate concentrations, and at the same time to have high enough lipophilicity to permeate across various biological membranes.

One way to screen out compounds with probable absorption problems is known as Lipinski's "rule of five." According to Lipinski et al.,³³ these four parameters are thought to be associated with solubility, permeability and binding efficiency of drugs which are the basic requirements for any drug to have good pharmacokinetic properties. As most of the drug candidates are designed to be administrated to human body via oral route and thus absorbed from the intestine, the first barrier they meet on their way to systemic circulation is the gut wall. The most usual way of permeation across the gut wall is passive transcellular permeation through the cells, but absorption of many compounds is also affected by ATP-driven efflux pumps (efflux transporters, e.g., P-glycoprotein, BCRP, MRD-family) or active cell uptake (influx) transporters, located on the cell membranes of various in the body.

Generally, passive transport is governed by physico-chemical properties whereas active transport involves specific binding of a molecule to a binding site on a transport protein.⁴⁹

Lipinski used these molecular properties in formulating his rule. The rule states that most molecules with good membrane permeability have log *P* ≤ 5, MW ≤ 500, NHBA ≤ 10, and NHBD ≤ 5. A compound that fulfils at least three out of the four criteria is said to adhere to Lipinski's 'rule of 5.'

Table III. Drug-likeness parameters of anti-tuberculosis compounds.

| Comps | % ABS | MW | Log <i>P</i> | NHBD | NHBA | nrotb | PSA | Acidic pKa | Basic pKa | Δ pKa |
|-------|-------|--------|--------------|------|------|-------|--------|------------|-------------|-------|
| Rules | – | <500 | <5 | <5 | <10 | <10 | <140 | – | – | – |
| 1 | 75.32 | 271.28 | –0.14 | 2 | 7 | 3 | 97.610 | 11.27 | 1.12 | 10.15 |
| 2 | 75.32 | 299.33 | 0.89 | 2 | 7 | 3 | 97.610 | 11.27 | 1.33 | 9.94 |
| 3 | 75.32 | 285.31 | 0.37 | 2 | 7 | 3 | 97.610 | 11.27 | 1.29 | 9.98 |
| 4 | 72.14 | 363.38 | 1.36 | 2 | 8 | 5 | 106.84 | 11.27 | –1.86; 1.10 | 10.17 |
| 5 | 75.32 | 305.72 | 0.46 | 2 | 7 | 3 | 97.610 | 11.27 | –1.88; 0.66 | 10.61 |
| 6 | 84.30 | 288.32 | 0.78 | 0 | 6 | 3 | 71.590 | 6.68 | 0.96 | 5.72 |
| 7 | 84.30 | 316.38 | 1.81 | 0 | 6 | 3 | 71.590 | 6.70 | 1.18 | 5.52 |
| 8 | 84.30 | 302.35 | 1.30 | 0 | 6 | 3 | 71.590 | 6.69 | 1.13 | 5.56 |
| 9 | 81.12 | 380.42 | 2.28 | 0 | 7 | 5 | 80.820 | 6.61 | 0.98 | 5.63 |
| 10 | 84.30 | 322.77 | 1.39 | 0 | 6 | 3 | 71.590 | 6.61 | 0.54 | 6.07 |
| 11 | 80.15 | 347.38 | 2.13 | 1 | 7 | 5 | 83.620 | 7.62 | 1.30 | 6.32 |
| 12 | 80.15 | 375.43 | 3.16 | 1 | 7 | 5 | 83.620 | 7.62 | 1.45 | 6.17 |
| 13 | 80.15 | 361.40 | 2.64 | 1 | 7 | 5 | 83.620 | 7.62 | 1.44 | 6.18 |
| 14 | 76.97 | 439.47 | 3.63 | 1 | 8 | 7 | 92.850 | 7.62 | 1.26 | 6.36 |
| 15 | 80.15 | 381.82 | 2.73 | 1 | 7 | 5 | 83.620 | 7.62 | 0.92 | 6.7 |

Veber³⁴ suggest that compounds which meet only the two criteria of

- (1) 10 or fewer rotatable bonds and
- (2) polar surface area equal to or less than 140 Å² (or 12 or fewer H-bond donors and acceptors) will have a high probability of good oral bioavailability in the rat.

The above mentioned parameters were calculated for all the series of the anti-tubercular agents (Table III). From the data obtained, it was observed that all the derivatives of the series were found to obey the Lipinski rule and Veber's. TPSA and Volume are inversely proportional to %ABS. TPSA was used to calculate the percentage of absorption (%ABS) according to the equation: %ABS = 109 ± 0.345 TPSA.⁵⁰ From all these parameters, it can be observed that all the title compounds exhibited a great %ABS ranging from 72.14% to 84.30%.

Overall permeability, both *in vitro* and *in vivo* can be considered to be the sum of passive (diffusion driven) and active (transporter mediated) processes. The latter can affect both influx and efflux. In particular P-glycoprotein (PGP) mediated efflux is widely known to have a significant effect on absorption and distribution potential. Considering active efflux alone, Petrauskas has proposed the 'rule of four',^{35,51} which states that compounds are likely to be efflux substrates if they have a hydrogen bond acceptor count (sum of N and O atoms) ≥ 8, MW > 400 and an acid with a pKa > 4. Conversely, compounds are likely to be non-substrates if they have an acceptor count ≤ 4, MW < 400 and a base with a pKa < 8. In which, all most our compounds are seems to satisfy the unlikely efflux substrates criteria just for compounds 14 which is likely to be efflux substrate for the P-glycoprotein.

3.3.2. Lipophilicity Profile and the Ionization State

Lipophilicity is a critical information that enable us to better interpret our results since it's a major structural factor

that influences the pharmacokinetic (permeation of physiological membranes (absorption and distribution), plasma protein binding and volume of distribution) and pharmacodynamic (target recognition, target affinity and target specificity) behavior of our anti-tuberculosis compounds. Log *P* (also known as Kow or Pow) and log *D* are the most descriptors of the lipophilicity. There is no constant pH in the body and it is therefore essential that we consider an appropriate pH when predicting the behavior of this anti-tuberculosis compounds. For that we have decided to study the lipophilic character of this new series of anti-tuberculosis. Generally Log *P* is measured in the pH where the compound exist in there neutral form. From (Table IV) we can see that the compounds 1–5 have the values of Log *D* equal to Log *P* in almost the rang of physiologically relevant pH (1–8) for this compounds we can predict their behavior only form examining the Log *P* profile. The predicted Log *P* values are –0.14, 0.89, 0.37, 1.36 and 0.46 for compounds 1–5 respectively. The conclusion we draw from this is that the compounds 2–5 shows a preference to be associated with the lipid phase, and by extension will likely permeate biological membranes spontaneously, unlike the compound 1, which has negative values, it would be more susceptible to higher aqueous solubility and for lower lipophilicity in the body. As a result, we would expect membrane permeability to be poor for the compound 1 and acceptable for the other compounds 2–5. Log *D*_{7.4} is equal to Log *P* for these compounds, we conclude that all this compounds exist in their neutral form and it's often quoted to give an indication of the lipophilicity of a drug at the pH of blood plasma. High values of Log *D*_{7.4}, the compounds will tend to be metabolized by P450 enzymes in the liver and increasing its value above 0 will decrease renal clearance and increase metabolic clearance.

Whereas, for the compounds 6–15 the difference between the basic and the acidic pKa values is too small

Table IV. Log *D* and Log *P* profile of the anti-tuberculosis compounds.

| pH | Compounds | | | | | | | | | | | | | | |
|------|-----------|-------|-------|------|-------|-------|------|-------|------|-------|------|------|------|------|------|
| | 1 | 2 | 3 | 4 | 5 | 6 | 7 | 8 | 9 | 10 | 11 | 12 | 13 | 14 | 15 |
| 0 | -0.99 | -0.20 | -0.65 | 0.47 | -0.09 | -0.22 | 0.60 | 0.13 | 1.25 | 0.75 | 0.79 | 1.67 | 1.17 | 2.34 | 1.77 |
| 0.5 | -0.76 | 0.08 | -0.39 | 0.71 | 0.11 | 0.19 | 1.04 | 0.57 | 1.67 | 1.07 | 1.25 | 2.14 | 1.64 | 2.79 | 2.18 |
| 1 | -0.49 | 0.40 | -0.08 | 0.98 | 0.29 | 0.50 | 1.41 | 0.92 | 1.99 | 1.26 | 1.64 | 2.56 | 2.06 | 3.17 | 2.47 |
| 1.5 | -0.30 | 0.65 | 0.16 | 1.19 | 0.40 | 0.67 | 1.64 | 1.14 | 2.17 | 1.34 | 1.91 | 2.87 | 2.36 | 3.43 | 2.63 |
| 2 | -0.20 | 0.80 | 0.29 | 1.30 | 0.44 | 0.74 | 1.75 | 1.24 | 2.24 | 1.37 | 2.05 | 3.04 | 2.53 | 3.56 | 2.70 |
| 2.5 | -0.16 | 0.86 | 0.35 | 1.34 | 0.46 | 0.77 | 1.79 | 1.28 | 2.27 | 1.38 | 2.10 | 3.12 | 2.60 | 3.60 | 2.72 |
| 3 | -0.15 | 0.88 | 0.36 | 1.35 | 0.46 | 0.78 | 1.80 | 1.29 | 2.28 | 1.39 | 2.12 | 3.14 | 2.63 | 3.62 | 2.73 |
| 3.5 | -0.14 | 0.88 | 0.37 | 1.36 | 0.46 | 0.78 | 1.81 | 1.29 | 2.28 | 1.39 | 2.13 | 3.15 | 2.64 | 3.63 | 2.73 |
| 4 | -0.14 | 0.89 | 0.37 | 1.36 | 0.46 | 0.78 | 1.81 | 1.29 | 2.28 | 1.39 | 2.13 | 3.15 | 2.64 | 3.63 | 2.73 |
| 4.5 | -0.14 | 0.89 | 0.37 | 1.36 | 0.46 | 0.78 | 1.81 | 1.29 | 2.28 | 1.38 | 2.13 | 3.16 | 2.64 | 3.63 | 2.73 |
| 5 | -0.14 | 0.89 | 0.37 | 1.36 | 0.46 | 0.78 | 1.80 | 1.29 | 2.27 | 1.38 | 2.13 | 3.16 | 2.64 | 3.63 | 2.73 |
| 5.5 | -0.14 | 0.89 | 0.37 | 1.36 | 0.46 | 0.76 | 1.79 | 1.28 | 2.26 | 1.36 | 2.13 | 3.15 | 2.64 | 3.63 | 2.73 |
| 6 | -0.14 | 0.89 | 0.37 | 1.36 | 0.46 | 0.72 | 1.75 | 1.23 | 2.21 | 1.31 | 2.12 | 3.15 | 2.64 | 3.62 | 2.73 |
| 6.5 | -0.14 | 0.89 | 0.37 | 1.36 | 0.46 | 0.61 | 1.64 | 1.12 | 2.08 | 1.18 | 2.11 | 3.13 | 2.62 | 3.61 | 2.71 |
| 7 | -0.14 | 0.89 | 0.37 | 1.36 | 0.46 | 0.38 | 1.42 | 0.90 | 1.84 | 0.94 | 2.06 | 3.09 | 2.57 | 3.56 | 2.67 |
| 7.4 | -0.14 | 0.89 | 0.37 | 1.36 | 0.46 | 0.13 | 0.17 | 0.65 | 1.58 | 0.68 | 1.98 | 3.00 | 2.49 | 3.48 | 2.58 |
| 7.5 | -0.14 | 0.89 | 0.37 | 1.36 | 0.46 | 0.06 | 1.10 | 0.58 | 1.51 | 0.61 | 1.94 | 2.97 | 2.46 | 3.44 | 2.55 |
| 8 | -0.14 | 0.89 | 0.37 | 1.36 | 0.46 | -0.26 | 0.78 | 0.27 | 1.20 | 0.31 | 1.71 | 2.74 | 2.22 | 3.21 | 2.31 |
| 8.5 | -0.14 | 0.89 | 0.37 | 1.36 | 0.46 | -0.48 | 0.56 | 0.04 | 1.00 | 0.11 | 1.37 | 2.40 | 1.88 | 2.87 | 1.97 |
| 9 | -0.14 | 0.89 | 0.37 | 1.36 | 0.46 | -0.58 | 0.45 | -0.07 | 0.91 | 0.01 | 1.02 | 2.04 | 1.53 | 2.52 | 1.62 |
| 9.5 | -0.14 | 0.88 | 0.37 | 1.36 | 0.46 | -0.62 | 0.40 | -0.11 | 0.87 | -0.02 | 0.75 | 1.78 | 1.26 | 2.25 | 1.35 |
| 10 | -0.15 | 0.88 | 0.36 | 1.35 | 0.45 | -0.64 | 0.39 | -0.12 | 0.86 | -0.03 | 0.61 | 1.63 | 1.12 | 2.11 | 1.21 |
| 10.5 | -0.17 | 0.85 | 0.34 | 1.33 | 0.43 | -0.64 | 0.39 | -0.13 | 0.86 | -0.04 | 0.55 | 1.57 | 1.06 | 2.05 | 1.15 |
| 11 | -0.24 | 0.79 | 0.27 | 1.26 | 0.36 | -0.64 | 0.38 | -0.13 | 0.86 | -0.04 | 0.53 | 1.55 | 1.04 | 2.03 | 1.13 |
| 11.5 | -0.39 | 0.63 | 0.12 | 1.11 | 0.21 | -0.64 | 0.38 | -0.13 | 0.86 | -0.04 | 0.52 | 1.55 | 1.03 | 2.02 | 1.12 |
| 12 | -0.65 | 0.37 | -0.14 | 0.85 | -0.05 | -0.64 | 0.38 | -0.13 | 0.86 | -0.04 | 0.52 | 1.55 | 1.03 | 2.02 | 1.12 |
| 12.5 | -0.95 | 0.08 | -0.44 | 0.55 | -0.35 | -0.64 | 0.38 | -0.13 | 0.86 | -0.04 | 0.52 | 1.54 | 1.03 | 2.02 | 1.12 |
| 13 | -1.18 | -0.15 | -0.66 | 0.32 | -0.57 | -0.64 | 0.38 | -0.13 | 0.86 | -0.04 | 0.52 | 1.54 | 1.03 | 2.02 | 1.12 |
| 13.5 | -1.29 | -0.27 | -0.78 | 0.21 | -0.69 | -0.64 | 0.38 | -0.13 | 0.86 | -0.04 | 0.52 | 1.54 | 1.03 | 2.02 | 1.12 |
| 14 | -1.34 | -0.31 | -0.83 | 0.16 | -0.74 | -0.64 | 0.38 | -0.13 | 0.86 | -0.04 | 0.52 | 1.54 | 1.03 | 2.02 | 1.12 |

Notes: Green: physiologically relevant pH; Yellow: Log *P* values and Orange: Log *D* at blood pH.

(ΔpK_a value about 6, Table III and Fig. 4) which mean that the neutral form of this anti-tuberculosis compounds is existent at a very small range of the physiological relevant pH, we can see that, in the Table IV of Log *P* and Log *D* values. For that, we are going to examine the Log *D* profile to better predict the behavior of our anti-tuberculosis compounds. Where, the Log *D* value for these compounds is changing within the range of 0.06 and 3.62. Which, lead us to deduce that all the compounds preference to be associated with the lipid phase, and by extension will likely permeate biological membranes spontaneously.

Figure 4 and Table III show the pK_a values of our compounds, we see that they are ampholytes i.e., they have the basic and acidic character and can exist as an un-ionized form, or as an anion depending on the pH value, but because the difference between pK_a acidic and pK_a basic is >3 , there will be no simultaneous ionization of the two groups. In contrast to other ionizable drugs with only an acidic or basic group, an amphoteric drug exhibits unique physicochemical and pharmacokinetic properties. Usually, their volume of distribution is lower than that of a basic drug, which suggests that the amphoteric drug tends to stay in the blood. Unlike

normal ionizable molecules, which at some pH can be predominantly chargeless, many ampholyte can transition between several different charge states, without ever becoming chargeless; thus their lipophilicity tends to be low to moderate. These properties would be better suited for the drug targets located in the plasma, since the distribution into tissues/organs is not favorable for ampholytes.

According to the pH-partition Hypothesis, absorption is favored for the chargeless form of the drug molecule. Transporters expressed in the intestinal surface, such as Pgp and OAT (organic anion transporter), could affect efflux/active uptake of the compound. It is thought that the development of amphoteric compounds into a drug is likely to be more challenging than compounds of other charge types, may be partly due to the lack of understanding of the factors governing their membrane permeability. Given that ampholytes are expected to be poorly absorbed by transmembrane passive diffusion processes, absorption via the paracellular route may be important. In the latter route, small solvated zwitter ions could diffuse through water-filled channels between cells. Such channels are known to be capacity-limited, size-restricted, and

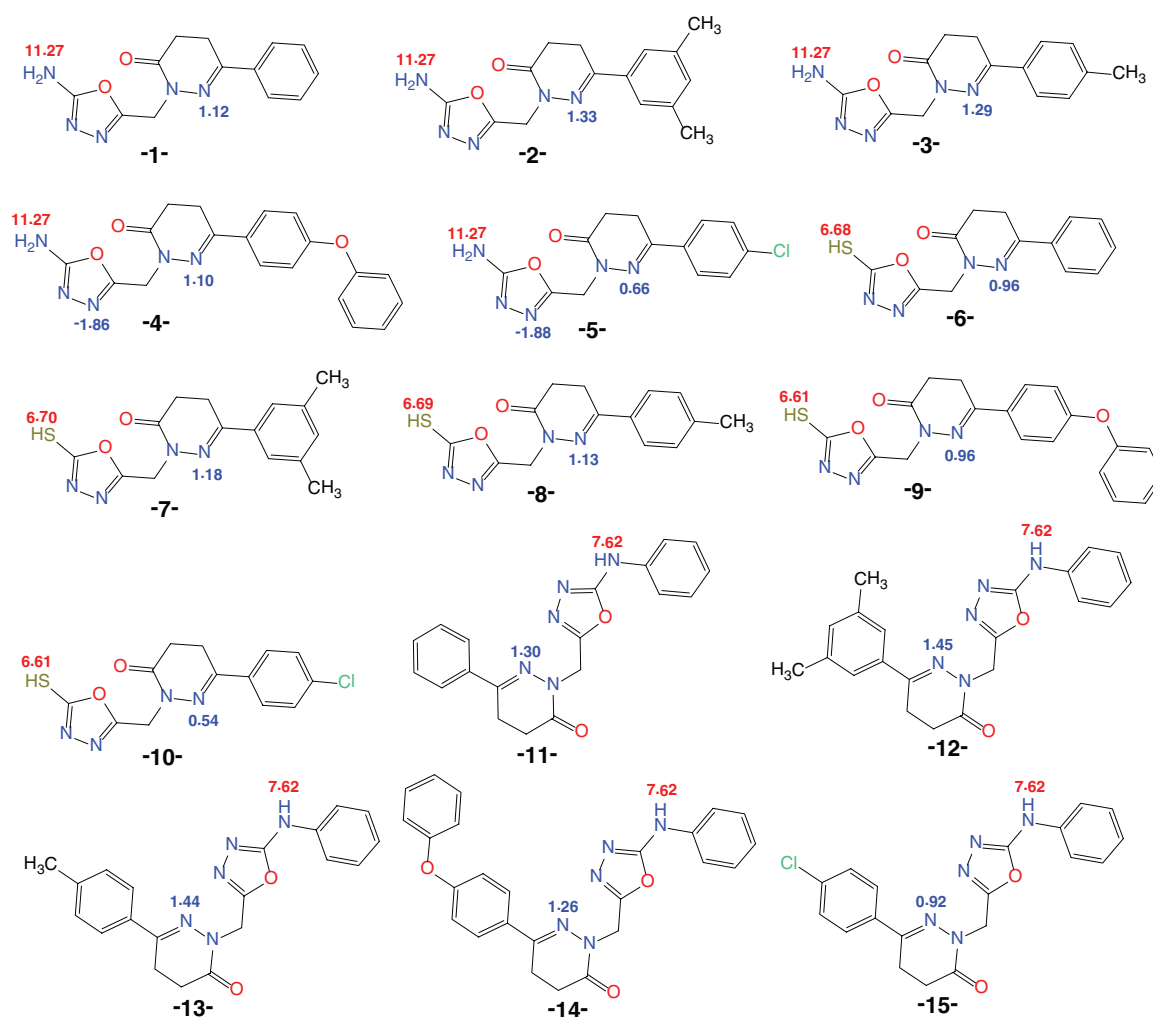


Fig. 4. The multiprotic acid/base sites of anti-tuberculosis compounds.

cation-selective, thus attenuating free diffusion in the water phase.

3.3.3. Structure Activity/Affinity Relationships (PEI and GE Analysis)

Our antitubercular activity was obtained by measurement of percentage inhibition against *M. tuberculosis* H37Rv at a single concentration (6.25 $\mu\text{g/ml}$). A simple efficiency index, PEI, can be introduced to guide the selection of the best compounds that use their atoms most efficiently. The idea of Per cent Efficiency Index is derived from Ligand Efficiency, which is defined as: $LE = \Delta G/N$.

Where: $\Delta G = -RT \ln K$, is the free energy of binding and, N , is the number of non-hydrogen atoms which can be seen as a measure of molecular size. Hence, it is simpler and more straightforward to calculate MW. In addition, MW is superior in dealing with the contribution of different heteroatoms. Abad-Zapatero and Metz³⁷ introduced the Per cent Efficiency Index (PEI) defined as the fractional (0–1 scale) inhibition of a compound divided by the MW in kDa.

As we can see in our results that our compounds divide in two groups where the first one have the biggest values of PEI in the range of 2.32–3.17, all these compounds are the most active with % in between 84–91. Moreover, the second with the low values of PEI in the range of 1.11–1.96 where the % in is between 45–56.

The hall purpose of PEI is instead of considering the efficiency of the whole compound, the average efficiency contribution per atom is taken into account. For the compound 1 with the biggest value of PEI 3.17. Which it is not the most potent compound but it has a combination between a good potency and the small size.

The group efficiency (GE) metric introduced by Verdonk and Rees³⁸ represents the binding efficiency of a functional group that has been added to an existing molecule “A” to form molecule “B”, it is defined as

$$GE = -\frac{\Delta\Delta G}{\Delta\text{HA}}$$

$$\Delta\Delta G = \Delta G(B) - \Delta G(A)$$

$$\Delta\text{HA} = \text{HA}(B) - \text{HA}(A)$$

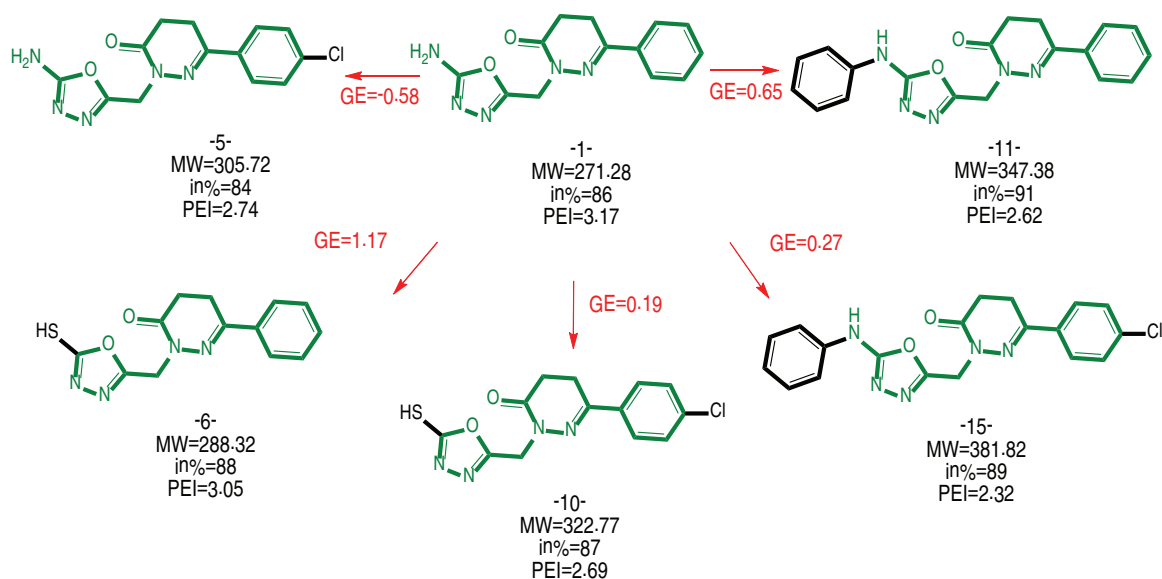


Fig. 5. Group Efficiency analysis of the most efficient compounds of studied series.

Where the affinity gained by molecule “B”, through the introduction of additional non-hydrogen atoms ΔHA to molecule “A”, is expressed as the difference of the free energies of binding ($-\Delta\Delta G$).³⁹

The PEI analysis show that compounds 1, 5, 6, 10, 11 and 15 with the highest values, are favored because this allows atoms to be added to modulate *in vivo* properties while still ending up with a candidate with a molecular weight that fits the Lipinski guidelines.

Figure 5 shows GE analysis of the efficiency of various parts of those anti-tuberculosis compounds where it's clear in compounds 5, 10 and 15 that the additions of 4-chloro substituent decrease the molecular efficiency. The addition of phenyl ring to compound 1 it improves potency by 5% and raise molecular size by about 77.104 Da has a good GE equal to 0.65. The latter has decreased to $GE = 0.27$ by adding Cl group. Moreover, the GE of the NH_2 substitution group with SH group is the most effective addition ($GE = 1.17$) for anti-tubercular activity.

4. CONCLUSION

It is now understood that 1,3,4-oxadiazole characters changes with regard to substitution groups. These behaviors are based on electronic and structural characteristics that constitute the soft and hard classifications of the HSAB theory. In this present study, we analyze the electronic properties of 1,3,4-oxadiazole ring and its derivatives, in order to deepen our understanding of its various therapeutic significance in general. The alkyls, amine and hydroxyl substitution at the 2-position of 1,3,4-oxadiazole ring increases the hardness of the system, while the cyanide and ketone one decreases it.

With regard to the anti-tuberculosis series, the lipophilicity balance and ionization state seem to play an

important role. Where they reveal their ampholytes character, which lead us to explore the Log *D* profile that shows they have good permeability.

And all compounds followed Lipinski's rule as they have a molecular weight under 500 Da, a limited lipophilicity (expressed by $\text{Log } P < 5$), far less than 5 H-bond donors (expressed as the sum of OHs and NHs), and also far less than 10 H-bond acceptors (expressed as the sum of Os and Ns) and Viber's rules also. In addition, they present a high percentage of absorption (%ABS), with all of the compounds being potentially able to cross biological membranes and to have a good oral bioavailability.

The correlation between the size and % inhibition of this anti-tuberculosis series was expressed by Per cent Efficiency Index (PEI). The calculated PEI suggests that compound 1 could be adopted as lead to locate a potential active anti-tuberculosis compound. Moreover, the Group Efficiency (GE) show the quality of SH and phenyl added group to maintain (or increase) the optimization of the anti-tubercular activity.

References and Notes

1. R. R. Somani and P. Y. Shirodkar, *J. Der. Pharma. Chem.* 1, 130 (2009).
2. G. Şahin, E. Palaska, M. Ekizoğlu, and M. Özalp, *J. Il. Farmaco.* 57, 539 (2002).
3. M. Ishii, S. D. Jorge, A. Alfredo de Oliveira, F. Palace-Berl, I. Y. Sonehara, K. F. Pasqualoto, and L. C. Tavares, *J. Bioorg. Med. Chem.* 19, 6292 (2011).
4. C. Soares de Oliveira, B. F. Lira, J. M. Barbosa-Filho, J. G. F. Lorenzo, and P. Filgueiras de Athayde-Filho, *J. Molecules* 17, 10193 (2012).
5. B. Kumar, V. Raj, A. Kumar, and V. Singh, *Inter. J. Cur. Phar. Research* 4, 9 (2012).
6. F. Zhang, X. L. Wang, J. Shi, S. F. Wang, Y. Yin, Y. S. Yang, W. M. Zhang, and H. L. Zhu, *J. Bioorg. Med. Chem.* 22, 468 (2014).

7. R. Gudipati, R. N. R. Anreddy, and S. Manda, *Saudi. Pharm. J.* 19, 153 (2011).
8. X. M. Zhang, M. Qiu, J. Sun, Y. B. Zhang, Y. S. Yang, X. L. Wang, J. F. Tang, and H. L. Zhu, *J. Bioorg. Med. Chem.* 19, 6518 (2011).
9. S. J. Gilani, O. Alam, S. A. Khan, N. Siddiqui, and H. Kumar, *J. Der. Pharmacia. Lettre.* 1, 1 (2009).
10. J. P. Raval, T. N. Akhaja, D. M. Jaspara, K. N. Myangar, and N. H. Patel, *J. Saudi. Chemical. Society* 18, 101 (2014).
11. A. A. Siddiqui, M. Islam, and S. Kumar, *J. Der. Pharmacia. Lettre.* 2, 319 (2010).
12. D. Zampieri, M. G. Mamolo, E. Laurini, M. Fermeglia, P. Posocco, S. Pricl, E. Banfi, G. Scialino, and L. Vio, *J. Bioorg. Med. Chem.* 17, 4693 (2009).
13. F. Macaeve, Z. Ribkovskaia, S. Pogrebnoi, V. Boldescu, G. Rusu, N. Shvets, A. Dimoglo, A. Geronikaki, and R. Reynolds, *J. Bioorg. Med. Chem.* 19, 6792 (2011).
14. M. Cruz-Monteagudo, F. Borges, M. Natalia D. S. Cordeiro, J. L. C. Fajin, C. Morell, R. M. Ruiz, Y. Canizares-Carmenate, and E. R. Dominguez, *J. Comb. Chem.* 10, 897 (2008).
15. N. Melkemi and S. Belaidi, *J. Comput. Theor. Nanosci.* 11, 801 (2014).
16. S. Belaidi, A. Kerassa, T. Lanez, and M. Cinar, *J. Comput. Theor. Nanosci.* 12, 2127 (2015).
17. Z. Almi, S. Belaidi, and L. Segueni, *Reviews in Theor. Sci.* 3, 264 (2015).
18. S. Belaidi, T. Salah, N. Melkemi, L. Sinha, and O. Prasad, *J. Comput. Theor. Nanosci.* 12, 2421 (2015).
19. Z. Almi, S. Belaidi, N. Melkemi, S. Boughdiri, and L. Belkhiri, *J. Quantum Matter* 5, 124 (2016).
20. L. Bouchlaleg, S. Belaidi, T. Salah, and A. M. Alafeefy, *J. Comput. Theor. Nanosci.* 12, 3949 (2015).
21. S. Belaidi, O. Youcef, T. Salah, and T. Lanez, *J. Comput. Theor. Nanosci.* 12, 4855 (2015).
22. S. Belaidi, H. Belaidi, and D. Bouzidi, *J. Comput. Theor. Nanosci.* 12, 1737 (2015).
23. A. Kerassa, S. Belaidi, and T. Lanez, *J. Quantum Matter* 5, 45 (2016).
24. S. Belaidi, H. Belaidi, A. Kerassa, M. Saoula, and D. Bouzidi, *J. Quantum Matter* 6 (2016), In press.
25. D. Harkati, S. Belaidi, A. Kerassaand, and N. Gherraf, *J. Quantum Matter* 5, 36 (2016).
26. M. Mellaoui, S. Belaidi, D. Bouzidi, and N. Gherraf, *J. Quantum Matter* 3, 435 (2014).
27. S. Belaidi, Z. Almi, and D. Bouzidi, *J. Comput. Theor. Nanosci.* 11, 2481 (2014).
28. O. Youcef, S. Belaidiand, and T. Salah, *J. Quantum Matter* 4 (2016), In press.
29. Y. Rouahna, S. Belaidi, D. Harkati, and A. Kerassa, *J. Comput. Theor. Nanosci.* 12, 4233 (2015).
30. T. Salah, S. Belaidi, N. Melkemi, I. Daoud, and S. Boughdiri, *J. Theor. Comput. Chem.* 15, 1650021 (2016).
31. M. D. Segall, *J. Curr. Pharm. Design.* 18, 1292 (2012).
32. M. D. Segall, *J. Expert. Opin. Drug Disc.* 9, 803 (2014).
33. C. A. Lipinski, F. Lombardo, B. W. Dominy, and P. J. Feeney, *Adv. Drug Delivery Reviews* 46, 3 (2001).
34. D. F. Veber, S. R. Johnson, H. Y. Cheng, B. R. Smith, K. W. Ward, and K. D. Kopple, *J. Med. Chem.* 45, 2615 (2002).
35. R. Didziapetris, P. Japertas, A. Avdeef, and A. Petrauskas, *J. Drug Target* 11, 391 (2003).
36. C. Abad-Zapatero, *J. Expert. Opin. Drug Disc.* 2, 469 (2007).
37. C. Abad-Zapatero and J. T. Metz, *J. Drug. Disc. Today* 10, 464 (2005).
38. M. L. Verdonk and D. C. Rees, *J. Chem. Med. Chem.* 3, 1179 (2008).
39. S. Schultes, C. de Graaf, E. E. J. Haaksma, I. J. P. de Esch, R. Leurs, and O. Krämer, *J. Drug. Disc. Today Tech.* 7, 157 (2010).
40. Gaussian 09, Revision B.01, M. J. Frisch, G. W. Trucks, H. B. Schlegel, G. E. Scuseria, M. A. Robb, J. R. Cheeseman, G. Scalmani, V. Barone, B. Mennucci, G. A. Petersson, H. Nakatsuji, M. Caricato, X. Li, H. P. Hratchian, A. F. Izmaylov, J. Bloino, G. Zheng, J. L. Sonnenberg, M. Hada, M. Ehara, K. Toyota, R. Fukuda, J. Hasegawa, M. Ishida, T. Nakajima, Y. Honda, O. Kitao, H. Nakai, T. Vreven, J. A. Montgomery, Jr., J. E. Peralta, F. Ogliaro, M. Bearpark, J. J. Heyd, E. Brothers, K. N. Kudin, V. N. Staroverov, T. Keith, R. Kobayashi, J. Normand, K. Raghavachari, A. Rendell, J. C. Burant, S. S. Iyengar, J. Tomasi, M. Cossi, N. Rega, J. M. Millam, M. Klene, J. E. Knox, J. B. Cross, V. Bakken, C. Adamo, J. Jaramillo, R. Gomperts, R. E. Stratmann, O. Yazyev, A. J. Austin, R. Cammi, C. Pomelli, J. W. Ochterski, R. L. Martin, K. Morokuma, V. G. Zakrzewski, G. A. Voth, P. Salvador, J. J. Dannenberg, S. Dapprich, A. D. Daniels, O. Farkas, J. B. Foresman, J. V. Ortiz, J. Cioslowski, and D. J. Fox, Gaussian, Inc., Wallingford CT (2010).
41. Calculator Plugins were used for structure property prediction and calculation, Marvin 6.3.0, 2014, ChemAxon (<http://www.chemaxon.com>).
42. Marvin was used for drawing, displaying and characterizing chemical structures, substructures and reactions, Marvin 6.3.0, 2014, ChemAxon (<http://www.chemaxon.com>).
43. J. S. Kwiatkowski, J. Leszczyński, and I. Teca, *J. Mol. Structure* 436, 451 (1997).
44. A. Kerassa, S. Belaidi, D. Harkati, T. Lanez, L. Sinha, and O. Prasad, *Reviews. Theor. Sci.* 3, 1 (2015).
45. K. R. S. Chandrakumar and S. Pal, *Inter. J. Mol. Sci.* 3, 324 (2002).
46. R. G. Pearson, *J. Amer. Chem. Soc.* 85, 3533 (1963).
47. G. Klopman, *J. Amer. Chem. Soc.* 90, 223 (1968).
48. T. Salah, S. Belaidi, N. Melkemi, and N. Tchouar, *Reviews. Theor. Sci.* 3, 355 (2015).
49. J. V. Turner and S. Agatonovic-Kustrin, *In Silico Prediction of Oral Bioavailability*, Elsevier Ltd. (2007), Vol. 5, pp. 699–724.
50. Y. H. Zhao, M. H. Abraham, J. Le, A. Hersey, C. N. Luscombe, G. Beck, B. Sherborne, and I. Cooper, *J. Pharm. Res.* 19, 1446 (2002).
51. M. J. Waring, *J. Bioorg. Med. Chem. Letters* 19, 2844 (2009).

ABSTRACT

Tuberculosis (TB) remains the number one killer infectious disease affecting adults in developing countries. Earlier, it was reported that a number of 2, 5-disubstituted-1, 3, 4-oxadiazoles have been designed, synthesized, and screened for their anti-tuberculosis activity against *M. tuberculosis* H37Rv. Our minimalist design format presents opportunities to reveal the soft and hard characters (HSAB theory) of 1, 3, 4-oxadiazole as a function of the various donating and withdrawing substituent groups using the FMOs energies and the density-based descriptors. Where the quantum mechanical geometry optimization were performed using B3LYP functional of density functional theory (DFT). With regard to the 2, 5-disubstituted-1, 3, 4-oxadiazoles anti-tuberculosis series, the lipophilicity balance and ionization state seem to play an important role to reveal their pharmacokinetic and pharmacodynamics behavior. The multi-parameter optimization (MPO) process of these anti-tuberculosis compounds was expressed by various approaches such as Per cent Efficiency Index (PEI), Group Efficiency (GE) analysis, Lipinski, Veber rules, Molecular Docking and QSAR model to guide the exploration of this new anti-tuberculosis agent with a high probability of achieving the required property/activity profile.

Keywords: anti-tuberculosis, descriptor, PEI, GE, Log P, Log D, SAR/SPR, Docking and QSAR.

La tuberculose (TB) demeure la première maladie infectieuse mortelle chez les adultes des pays en développement. Plus tôt, il a été rapporté qu'un certain nombre de 2, 5-disubstitués-1, 3, 4-oxadiazoles ont été conçus, synthétisés et criblés pour leur activité anti-tuberculose contre *M. tuberculosis* H37Rv. Notre conception minimaliste présente des opportunités de révéler les caractères mous et durs (théorie HSAB) de 1, 3, 4-oxadiazole en fonction des différents groupes de substituants (donneur et accepteur) en utilisant les énergies des orbitales frontières et des descripteurs basés sur la densité. Où l'optimisation de la géométrie moléculaire a été réalisée en utilisant la fonctionnelle B3LYP de la théorie de la fonctionnelle de la densité (DFT). En ce qui concerne les séries 2, 5-disubstituée-1, 3, 4-oxadiazoles antituberculeux, l'équilibre de la lipophilie et l'état d'ionisation semblent jouer un rôle important pour révéler leur comportement pharmacocinétique et pharmacodynamique. L'optimisation multi-paramétrique (MPO) de ces composés antituberculeux a été exprimé par diverses approches telles que l'indice d'efficacité en pourcentage (PEI), l'analyse d'efficacité de groupe (GE), les règles de Lipinski, Veber, Docking moléculaire et l'étude QSAR pour guider l'exploration de ce nouvel agent antituberculeux avec une forte probabilité d'atteindre le profil requis de la propriété / activité .

Mots clés : antituberculeux, descripteur, GE, PEI, Log P, Log D, SAR/SPR, Docking et QSAR.

السل (TB) لا يزال رقم واحد للأمراض المعدية القاتلة التي تؤثر على البالغين في البلدان النامية. وقد أفادت عدة دراسات بأن عدد من مشتقات (1، 3، 4-oxadiazoles) ذات نشاط ضد السل. تكشف لنا قائمة من مشتقات (1، 3، 4-oxadiazoles) عن الطابع اللين والصلب (حسب نظرية HSAB) بدلالة مجموعة مستبدلات مختلفة (المانحة والمستقبلة) باستخدام طاقات المدارات الحدودية والصفات المشتقة من الكثافة. حيث تم إجراء تقليل لطاقة البنية الجزيئية باستخدام الوظيفة (B3LYP) لنظرية الكثافة الوظيفية (DFT). وفيما يتعلق بالسلسلة (1، 3، 4-oxadiazoles) المضادة للسل، فإن خاصية المحبة للدهون وحالة التأين تلعبان دورا هاما في كشف حركيتها وديناميكيته الدوائية. وقمنا بتحسين المتعدد العوامل (MPO) لهذه المركبات المضادة للسل باستعمال طرق مختلفة مثل مؤشر الفعالية لنسبة المثوية (PEI)، وتحليل فعالية المجموعة (GE)، قواعد Lipinski، قواعد Veber، Docking ودراسة QSAR لتوجيه استكشاف هذه مضادات السل الجديدة مع وجود احتمال كبير لتحقيق النسبة المطلوبة (خاصية / النشاط البيولوجية).

الكلمات الدالة: مضادات السل، واصفات، GE، PEI، Log P، Log D، SAR/SPR، Docking، وQSAR.

REFERENCES

- ¹ World Health Organization; Global tuberculosis report 2016, ISBN: 9-789241-565394, pp.1, 5 (2016).
- ² Gideon. HP & Flynn. JL. *Immunol. Res.* 50(2-3) pp. 202-12 (2011).
- ³ Barry. CE & Blanchard. JS. *Cur. Opin. Chem. Biol.* 14(4) pp. 456-66 (2010).
- ⁴ Claude Kirimuhuzya. Multi-Drug/Extensively Drug Resistant Tuberculosis (Mdr/Xdr-Tb): Renewed Global Battle Against Tuberculosis?, Understanding Tuberculosis - New Approaches to Fighting Against Drug Resistance, Dr. Pere-Joan Cardona (Ed.), ISBN: 978-953-307-948-6, *InTech*, pp.1, 12 (2012).
- ⁵ Jean Leandro dos Santos, Luiz Antonio Dutra, Thais Regina Ferreira de Melo and Chung Man Chin. New Antitubercular Drugs Designed by Molecular Modification, Understanding Tuberculosis-New Approaches to Fighting Against Drug Resistance, Dr. Pere-Joan Cardona (Ed.), ISBN: 978-953-307-948-6, *InTech*, pp.170 (2012).
- ⁶ John B. Taylor and David J. Triggle. Comprehensive Medicinal Chemistry II Volume 4: Computer-Assisted Drug Design, ISBN: 0-08-044513-6, Elsevier, pp.1, 4, 44, 88, 380, 387 (2006).
- ⁷ Netzeva TI ; Worth AP ; Aldenberg T ; Benigni R ; Cronin MTD ; Gramatica P ; Jaworska JS ; Kahn S ; Klopman G ; Marchant CA et al. *Altern. Lab. Anim.* 33(2) pp. 155-73 (2005).
- ⁸ He L ; Jurs PC. *J. Mol. Graph. Model.* 23(6) pp. 503-23 (2005).
- ⁹ Health and medicine infectious diseases. What is tuberculosis? (2015). Retrieved from <https://www.khanacademy.org/science/health-and-medicine/infectious-diseases/tuberculosis/a/what-is-tuberculosis>
- ¹⁰ World Health Organization. What is multi-drug resistant tuberculosis and how do we control it? Online Q&A (reviewed March 2015). (2015). Retrieved from <http://www.who.int/features/qa/79/en/>
- ¹¹ World Health Organization. Tuberculosis. Fact sheet No. 104. (2015). Retrieved from <http://www.who.int/mediacentre/factsheets/fs104/en/>
- ¹² World Health Organization. HIV/AIDS; Tuberculosis and HIV. (2015). Retrieved from http://www.who.int/hiv/topics/tb/about_tb/en/
- ¹³ Ma Z ; Lienhardt C ; McIlleron H ; Nunn AJ ; Wang X. *Lancet.* 375(9731) pp. 2100-9 (2010).
- ¹⁴ Lalloo UG ; Ambaram A. *Curr. HIV/AIDS Rep.* 7(3) pp. 143-51(2010).
- ¹⁵ Karakousis PC ; Bishai WR ; Dorman SE. *Cell Microbiol.* 6(2) pp. 105-16 (2004).
- ¹⁶ Kochi A ; Vareldzis B. Styblo K. *Res. Microbiol.* 144(2) pp. 104-10 (1993).
- ¹⁷ Karakousis, P. C.. Mechanisms of Action and Resistance of Antimycobacterial Agents. In: Antimicrobial Drug Resistance. D. L. Mayers, *Springer* pp. 271-91 (2009).
- ¹⁸ Canetti G. *Am. Rev. Respir. Dis.* 92(5) pp. 687-703 (1965).
- ¹⁹ Jignesh PR ; Tarunkumar NA ; Dhaval MJ ; Kruti NM ; Nilesh HP. *J. Saudi Chem. Soc.* 18(2) pp. 101-6 (2014).
- ²⁰ Ahsan MJ ; Samy JG ; Khalilullah H ; Nomani Md. S ; Saraswat P ; Gaur R ; Singh A. *Bioorg. Med. Chem. Letters.* 21(41) pp. 7246-50 (2011).
- ²¹ Anees AS ; Mojahid I ; Sateesh K. *Der. Pharmacia. Lettre.* 2(2) pp. 319-27 (2010).

- ²² Daniele Z ; Maria GM ; Erik L ; Maurizio F ; Paola P ; Sabrina P ; Elena B ; Giuditta S ; Luciano V. *Bioorg. Med. Chem.* 17 pp. 4693-707 (2009).
- ²³ Rakesh DS ; Robin BL ; Rajendra PT ; Richard EL. *Euro. J. Med. Chem.* 44(22) pp. 460-72 (2009).
- ²⁴ Fliur M ; Zinaida R ; Serghei P ; Veaceslav B ; Ghenadie R ; Nathaly S ; Anatholy D ; Athina G ; Robert R. *Bioorg. Med. Chem.* 19 pp. 6792-807 (2011).
- ²⁵ Garrett CM ; Mayland C ; Adriel VE ; Scott GF ; Ute M ; Marvin JM. *Euro. J. Med. Chem.* 45 pp. 1703-16 (2010).
- ²⁶ Galina IL ; Michael RW. *Biochim. Biophys. Acta.* 1770(3) pp. 467-77 (2007).
- ²⁷ Hansch C ; Muir R ; Fujita T ; Maloney P ; Geiger E ; Streich MJ. *Am. Chem. Soc.* 85 pp. 2817-24 (1963).
- ²⁸ Hammett LP. *Chem. Rev.* 17 pp. 125-36 (1935).
- ²⁹ Hansch C ; Leo A. Exploring QSAR. In *Fundamentals and Applications in Chemistry and Biology*; Hellen, S., Ed.; *American Chemical Society*: Washington, DC, Vol. 1, pp. 580 (1995).
- ³⁰ Boyd DB. In *Reviews in Computational Chemistry*; Lipkowitz KB ; Boyd DB., Eds.; *VCH*: New York, pp. 355-71 (1991).
- ³¹ Norinder U ; Hogberg T. *Acta Pharm. Nord.* 4 pp. 73-8 (1992).
- ³² Van de Waterbeemd WH ; el Tayar N ; Testa B ; Wikstrom H ; Largent B. *J. Med. Chem.* 30 pp. 2175-81 (1987).
- ³³ Kovatcheva A ; Golbraikh A ; Oloff S ; Xiao YD ; Zheng W ; Wolschann P ; Buchbauer G ; Tropsha A. *J. Chem. Inf. Comput. Sci.* 44 pp. 582-95 (2004).
- ³⁴ Topliss JG ; Edwards RPI. *Med. Chem.* 22 pp. 1238-44 (1979).
- ³⁵ Kier LB ; Hall LH ; Murray WJ ; Randic MJ. *Pharm. Sci.* 64 pp. 1971-4 (1975).
- ³⁶ Kier LB ; Murray WJ ; Randic M ; Hall LH. *J. Pharm. Sci.* 65 pp. 1226-30 (1976).
- ³⁷ Debnath AK ; Lopez de Compadre RL ; Debnath G ; Shusterman AJ ; Hansch C. *J. Med. Chem.* 34 pp. 786-97 (1991).
- ³⁸ Jain AN ; Koile K ; Chapman D. *J. Med. Chem.* 37 pp. 2315-27 (1994).
- ³⁹ Cramer RDIII ; Patterson DE ; Bunce JD. *J. Am. Chem. Soc.* 110 pp. 5959-67 (1988).
- ⁴⁰ Burden FR ; Winkler DA. *J. Med. Chem.* 42 pp. 3183-7 (1999).
- ⁴¹ Carhart RE ; Smith DH ; Venkataraghavan R. *J. Chem. Inf. Comput. Sci.* 25 pp. 64-73 (1985).
- ⁴² Sheridan RP ; SanFeliciano SG ; Kearsley SK. *J. Mol. Graph. Model.* 18 pp. 320-34, 525 (2000).
- ⁴³ Bodor N ; Gabanyi Z ; Wong C. *J. Am. Chem. Soc.* 111 pp. 3783 (1989).
- ⁴⁴ Gavezotti A. *J. Am. Chem. Soc.* 10 pp. 5220 (1983).
- ⁴⁵ Hall LH ; Mohny B ; Kier LB. *Quant. Struct.-Act. Relat.* 10 pp. 43-51 (1991).
- ⁴⁶ Van der Waterbeemd H ; Testa B. *Adv. Drug. Res.* 16 pp. 85-225 (1987).
- ⁴⁷ Hansch C ; Grieco C ; Silipo C ; Vittoria A. *J. Med. Chem.* 20 pp. 1420-35 (1977).

- ⁴⁸ Selassie CD ; Klein TE. In Comparative QSAR; Devillers J , Ed.; *Taylor and Francis*: New York, pp. 235-84 (1998).
- ⁴⁹ Hansch C ; Blaney JM. In Drug Design: Fact or Fantasy?; Jolles G ; Wooldridge KRH., Eds.; *Academic Press*: London, pp. 185-208 (1984).
- ⁵⁰ Testa B ; Carrupt P-A ; Gaillard P ; Billois F ; Weber P. *Pharm. Res.* 13 pp. 335-43 (1996).
- ⁵¹ Carrupt P-A ; Testa B ; Gaillard P. Computational Approaches to Lipophilicity Methods and Applications. In Reviews in Computational Chemistry; Lipkowitz KB ; Boyd DB., Eds.; *John Wiley*: New York, Vol. 11, pp. 241-315 (1997).
- ⁵² El Tayar N ; Testa B ; Carrupt PA. *J. Phys. Chem.* 96 pp. 1455-9 (1992).
- ⁵³ Moriguchi I ; Kanada Y ; Komatsu K. *Chem. Pharm. Bull.* 24 pp. 1799-806 (1976).
- ⁵⁴ Testa B ; Seiler P. *Arzneim.-Forsch./Drug Res.* 31 pp. 1053-8 (1981).
- ⁵⁵ Young RC ; Mitchell RC ; Brown TH ; Ganelling CR ; Griffiths R ; Jones M ; Rana KK ; Saunders D ; Smith IR ; Sore NE ; Wilks TJ. *J. Med. Chem.* 31 pp. 656-71 (1988).
- ⁵⁶ Burton PS ; Conradi RA ; Ho NFH ; Hilgers AR ; Borchardt RT. *J. Pharm. Sci.* 85 pp. 1336-40 (1996).
- ⁵⁷ Van de Waterbeemd H ; Carter RE ; Grassy G ; Kubinyi H ; Martin YC ; Tute M ; Willett P. *Pure Appl. Chem.* 69 pp. 1137-52 (1997).
- ⁵⁸ Ghose AK ; Pritchett A ; Crippen GM. *J. Comput. Chem.* 9 pp. 80 (1988).
- ⁵⁹ Todeschini R ; Consonni V. Handbook of Molecular Descriptors; Mannhold R ; Kubinyi H ; Timmerman H., Eds.; *Wiley-VCH*: New York, (2000).
- ⁶⁰ Leo A ; Hansch C ; Church C. *J. Med. Chem.* 12 pp. 766-71 (1969).
- ⁶¹ Clarke FH ; Cahoon NM. *J. Pharm. Sci.* 76 pp. 611-20 (1987).
- ⁶² Avdeef A. Assessment of Distribution-pH Profiles. In Lipophilicity in Drug Action and Toxicology; Pliska V , Testa B , Van de Waterbeemd H., Eds.; *VCH*: Weinheim, Germany, pp. 109-39 (1996).
- ⁶³ Fallingborg J ; Christensen LA ; Ingelman-Nielsen M ; Jacobsen BA ; Abildgaard K ; Rasmussen HH. *Aliment. Pharmacol. Ther.* 3 pp. 605-13 (1989).
- ⁶⁴ Dressman JB ; Berardi RR ; Dermentzoglou LC ; Russel TL ; Schmaltz SP ; Barnett JL ; Jarvenpaa KM. *Pharm. Res.* 7 pp. 756-61 (1990).
- ⁶⁵ Winiwarter S ; Bonham NM ; Ax F ; Hallberg A ; Lennernäs H ; Karlén A. *J. Med. Chem.* 41 pp. 4939-49 (1998).
- ⁶⁶ Van de Waterbeemd H ; Kansy M. *Chimia.* 46 pp. 299-303 (1992).
- ⁶⁷ Stein WD. The Molecular Basis of Diffusion Across Cell Membranes. In The Movement of Molecules across Cell Membranes; *Academic Press*: New York; pp. 65-125 (1967).
- ⁶⁸ Conradi RA ; Hilgers AR ; Ho NFH ; Burton PS. *Pharm. Res.* 8 pp. 1453-60 (1991).
- ⁶⁹ Palm K ; Luthman K ; Ungell A-L ; Strandlund G ; Artursson P. *J. Pharm. Sci.* 85 pp. 32-9 (1996).
- ⁷⁰ Feher M ; Sourial E ; Schmidt JM. *Int. J. Pharm.* 201 pp. 239-47 (2000).
- ⁷¹ Lee B ; Richards FM. *J. Mol. Biol.* 55 pp. 379-400 (1971).

- ⁷² Richards FM. *Annu. Rev. Biophys. Bioeng.* 6 pp. 151-76 (1977).
- ⁷³ Connolly ML. *J. Appl. Crystallogr.* 16 pp. 548-58 (1983).
- ⁷⁴ Ertl P ; Rohde B ; Selzer P. *J. Med. Chem.* 43 pp. 3714-7 (2000).
- ⁷⁵ Lipinski CA ; Lombardo F ; Dominy BW ; Feeney P. *J. Adv. Drug Deliv. Rev.* 23 pp. 3-25 (1997).
- ⁷⁶ Ren S ; Das A ; Lien EJ. *J. Drug Target.* 4 pp. 103-7 (1996).
- ⁷⁷ Karelson M ; Lobanov VS. *Chem. Rev.* 96 pp. 1027-43 (1996).
- ⁷⁸ Cramer RD ; Patterson DE ; Bunce JD. *J. Am. Chem. Soc.* 110 pp. 5959-67 (1988).
- ⁷⁹ Kubinyi H ; Folkers G ; Martin YC. Eds. 3D QSAR in Drug Design. In Recent Advances, *Kluwer Academic Publishers: Dordrecht, The Netherlands*, Vol. 3 pp. 368 (1998).
- ⁸⁰ Chatterjee S ; Hadi AS ; Price B. Regression analysis by example. *Wiley-Interscience: New York*, (2000).
- ⁸¹ Golbraikh A ; Tropsha A. *J. Mol. Graph. Model.* 20 pp. 269-76 (2002).
- ⁸² Kubinyi H ; Hamprecht FA ; Mietzner T. *J. Med. Chem.* 41 pp. 2553-64 (1998).
- ⁸³ Worth AP ; Hartung T ; Leeuwen CJ. *SAR QSAR Environ. Res.* 15 pp. 345-58 (2004).
- ⁸⁴ Leach AR. Molecular modeling: Principles and applications. *Pearson Education Ltd.: Harlow, England*, (2001).
- ⁸⁵ Shao J. *J. Am. Stat. Assoc.* 88 pp. 486-94 (1993).
- ⁸⁶ Besal E. *J. Math. Chem.* 29 pp. 191-5 (2001).
- ⁸⁷ Wold S ; Ericksson L. Partial least squares projections to latent structures (PLS) in chemistry. In Encyclopedia of computational chemistry, Ragu & Schleyer, P. (ed.), *John Wiley & Sons: Chichester*, Vol. 3 pp. 2006-21 (1998).
- ⁸⁸ Yasri A ; Hartsough D. *J. Chem. Inf. Comput. Sci.* 41 pp. 1218-27 (2001).
- ⁸⁹ Schneider G ; Wrede P. *Prog. Biophys. Mol. Biol.* 70 pp. 175-222 (1998).
- ⁹⁰ Kubinyi H ; Hamprecht FA ; Mietzner T. *J. Med. Chem.* 41 pp. 2553-64 (1998).
- ⁹¹ Guha R ; Jurs PC. *J. Chem. Inf. Model.* 45 pp. 65-73 (2005).
- ⁹² Novellino E ; Fattorusso C ; Greco G. *Pharm. Acta Helv.* 70 pp. 149-54 (1995).
- ⁹³ Norinder U. *J. Chemom.* 10 pp. 95-105 (1996).
- ⁹⁴ Zefirov NS ; Palyulin VA. *J. Chem. Inf. Comput. Sci.* 41 pp. 1022-7 (2001).
- ⁹⁵ Roy PP ; Roy K. *QSAR Comb. Sci.* 27 pp. 302-13 (2008).
- ⁹⁶ Golbraikh A ; Tropsha A. *J. Mol. Graphics Mod.* 20 pp. 269-76 (2002).
- ⁹⁷ Burkert U ; Allinger NL. Molecular Mechanics; ACS Monograph 177; *American Chemical Society: Washington, DC*, (1982).
- ⁹⁸ Niketic SR ; Rasmussen K. The Consistent Force Field: A Documentation; *Springer-Verlag: Berlin, Germany*, (1977).

- ⁹⁹ Benbrahim I. Study of QSAR properties of a 1, 3, 4-oxadiazole bioactive series; *Master thesis*: Univ. of Biskra; (2013).
- ¹⁰⁰ Yamaguchi Y ; Osamura Y ; Goddard JD ; Schaefer HF , III. A New Dimension to Quantum Chemistry: Analytic Derivative Methods in Ab Initio Molecular Electronic Structure Theory; *Oxford University Press*: New York, (1994).
- ¹⁰¹ Loew GH ; Villar HO ; Alkorta I. *Pharmaceut. Res.* 10 pp. 475-86 (1993).
- ¹⁰² Topol IA ; Burt SK ; Derety E ; Tang TH ; Perczel A ; Rashin A ; Csizmadia IG. *J. Am. Chem. Soc.* 123 pp. 6054-60 (2001).
- ¹⁰³ Barden JC ; Schaefer HF, III. In *Computational Medicinal Chemistry for Drug Discovery*; Bultnik P., Ed.; *Marcel Dekker*: New York, pp. 133-49 (2004).
- ¹⁰⁴ Geerlings P ; De Proft F ; Langenaeker W. *Chem. Rev.* 103 pp. 1793-73 (2003).
- ¹⁰⁵ Hohenberg P ; Kohn W. *Phys. Rev. B* 136 pp. 864 (1964).
- ¹⁰⁶ Lee C ; Yang W ; Parr RG. *Phys. Rev. B* 37 pp. 785-9 (1988).
- ¹⁰⁷ Becke AD. *J. Chem. Phys.* 98 pp. 5648-52 (1993).
- ¹⁰⁸ Becke AD. *Phys. Rev. A* 38 pp. 3098-100 (1988).
- ¹⁰⁹ Perdew JP. *Phys. Rev. B* 33 pp. 8822-4 (1986).
- ¹¹⁰ Ziegler T ; Autschbach J. *Chem. Rev.* 105 pp. 2695-722 (2005).
- ¹¹¹ Dewar MJS ; Zoebisch EG ; Healy EF ; Stewart JJP. *J. Am. Chem. Soc.* 107 pp. 3902-9 (1985).
- ¹¹² Stewart JJP. *J. Comput. Chem.* 10 pp. 209-20, 221-64 (1989).
- ¹¹³ Shaffer AA ; Wierschke SG. *J. Comput. Chem.* 14 pp. 75-88 (1993).
- ¹¹⁴ Allinger NL ; Chen KS ; Lii JH. *J. Comput. Chem.* 17 pp. 642-68 (1996).
- ¹¹⁵ Cornell WD ; Cieplak P ; Bayly CI ; Gould IR ; Merz KM ; Ferguson DM ; Spellmeyer DC ; Fox T ; Caldwell JW ; Kollman PA. *J. Am. Chem. Soc.* 117 pp. 5179-97 (1995).
- ¹¹⁶ Sybyl 6.4, Tripos Associates, St. Louis, MO, USA.
- ¹¹⁷ Halgren T. *J. Comput. Chem.* 17 pp. 490-519 (1996).
- ¹¹⁸ Todebush PM ; Bowen JP. In *Free Energy Calculations in Rational Drug Design*; Reddy MR ; Erion MD., Eds.; *Plenum Publishers*: New York, pp. 37-59 (2001).
- ¹¹⁹ Ooms F. *Curr. Med. Chem.* 7 pp. 141-58 (2000).
- ¹²⁰ Bleicher KH ; Böhm H-J ; Müller K ; Alanine AI. *Nat. Rev. Drug Dis.* 2 pp. 369-78 (2003).
- ¹²¹ Klebe G. *Drug Disc. Today: Technol.* 1 pp. 225-30 (2004).
- ¹²² Goodnow RA , Jr.; Gillespie P ; Bleicher K. In *Chemoinformatics in Drug Discovery*; Oprea T., Ed.; *Wiley-VCH*: Weinheim, Germany, pp. 381-435 (2005).
- ¹²³ Clark T. In *Rational Approaches to Drug Design*; Höltje H-D , Sippl W., Eds.; *Prous Science*: Barcelona, Spain, pp. 29-40 (2001).

- ¹²⁴ Hansch C. *Drug Devel. Res.* 1 pp. 267-309 (1981).
- ¹²⁵ Hansch C. *Acc. Chem. Res.* 26 pp. 147-53 (1993).
- ¹²⁶ Leach AR ; Shoichet BK ; Peishoff CE. *J. Med. Chem.* 49 pp. 5851-5 (2006).
- ¹²⁷ Coupez B ; Lewis RA. *Curr. Med. Chem.* 13 pp. 2995-3003 (2006).
- ¹²⁸ Sousa SF ; Fernandes PA ; Ramos MJ. *Proteins.* 65 pp. 15-26 (2006).
- ¹²⁹ Mohan V ; Gibbs AC ; Cummings MD ; Jaeger EP ; DesJarlais RL. *Curr. Pharm. Des.* 11 pp. 323-33 (2005).
- ¹³⁰ Kitchen DB ; Decornez H ; Furr JR ; Bajorath J. *Nature Rev. Drug Discov.* 3 pp. 935-49 (2004).
- ¹³¹ Brooijmans N ; Kuntz ID. *Annu. Rev. Biophys. Biomol. Struct.* 32 pp. 335-73 (2003).
- ¹³² Taylor RD ; Jewsbury PJ ; Essex JW. *J. Comp. Aided Mol. Design.* 16 pp. 151-66 (2002).
- ¹³³ Halperin I ; Ma B ; Wolfson H ; Nussinov R. *Proteins: Struct. Funct. Genet.* 47 pp. 409-43 (2002).
- ¹³⁴ Kolb P ; Ferreira RS ; Irwin JJ ; Shoichet BK. *Curr Opin Biotechnol.* 20 pp. 429-36 (2009).
- ¹³⁵ Kolb P ; Irwin JJ. *Curr Top Med Chem.* 9 pp. 755-70 (2009).
- ¹³⁶ Koppen H. *Curr Opin Drug Discov Devel.* 12 pp. 397-407 (2009).
- ¹³⁷ Rester U. *Curr Opin Drug Discov Devel.* 11 pp. 559-68 (2008).
- ¹³⁸ McInnes C. *Curr Opin Chem Biol.* 11 pp. 494-502 (2007).
- ¹³⁹ Seifert MH ; Kraus J , Kramer B. *Curr Opin Drug Discov Devel.* 10 pp. 298-307 (2007).
- ¹⁴⁰ Shoichet BK. *Nature.* 432 pp. 862-5 (2004).
- ¹⁴¹ Huey R ; Morris GM ; Olson AJ ; Goodsell DS. *J. Comput. Chem.* 28 pp. 1145-52 (2006).
- ¹⁴² Somani RR ; Shirodkar PY. *J. Der. Pharma. Chem.* 1 pp. 130 (2009).
- ¹⁴³ Şahin G ; Palaska E ; Ekizoğlu M ; Özalp M. *J. Il.Farmaco.* 57 pp. 539 (2002).
- ¹⁴⁴ Ishii M ; Jorge SD ; Alfredo de Oliveira A ; Palace-Berl F ; Sonehara IY ; Pasqualoto KF ; Tavares LC ; *J. Bioorg. Med. Chem.* 19 pp. 6292 (2011).
- ¹⁴⁵ Soares de Oliveira C ; Lira BF ; Barbosa-Filho JM ; Lorenzo JGF ; Filgueiras de Athayde-Filho P ; *J. Molecules* 17 pp. 10193 (2012).
- ¹⁴⁶ Kumar B ; Raj V ; Kumar A ; Singh V ; *Inter. J. Cur. Phar. Research.* 4 pp. 9 (2012).
- ¹⁴⁷ Zhang F ; Wang XL ; Shi J ; Wang SF ; Yin Y ; Yang YS ; Zhang WM ; Zhu HL ; *J. Bioorg. Med. Chem.* 22 pp. 468 (2014).

- ¹⁴⁸ Gudipati R ; Anreddy RNR ; Manda S ; *Saudi. Pharm. J.* 19 pp. 153(2011).
- ¹⁴⁹ Zhang XM ; Qiu M ; Sun J ; Zhang YB ; Yang YS ; Wang XL ; Tang JF ; Zhu HL ; *J. Bioorg. Med. Chem.* 19 pp. 6518 (2011).
- ¹⁵⁰ Gilani SJ ; Alam O ; Khan SA ; Siddiqui N ; Kumar H ; *J. Der. Pharmacia.Lettre.* 1 pp. 1 (2009).
- ¹⁵¹ Melkemi N ; Belaidi S. *J.Comput.Theor.Nanosci.* 11 pp. 801 (2014) .
- ¹⁵² Belaidi S ; Kerassa A ; Lanez T ; Cinar M. *J.Comput.Theor.Nanosci.* 12 pp. 2127 (2015).
- ¹⁵³ Almi Z ; Belaidi S ; Segueni L. *Reviews in Theor. Sci.* 3 pp. 264 (2015).
- ¹⁵⁴ Belaidi S ; Salah T ; Melkemi N ; Sinha L ; Prasad O. *J. Comput. Theor. Nanosci.* 12 pp. 2421(2015).
- ¹⁵⁵ Almi Z ; Belaidi S ; Melkemi N ; Boughdiri S ; Belkhiri L. *J. Quantum.Matter.* 5 pp. 124 (2016).
- ¹⁵⁶ Bouchlaleg L ; Belaidi S ; Salah T ; Alafeefy AM. *J.Comput.Theor. Nanosci.* 12 pp. 3949 (2015).
- ¹⁵⁷ Belaidi S ; Youcef O ; Salah T ; Lanez T. *J.Comput.Theor.Nanosci.* 12 pp. 4855 (2015).
- ¹⁵⁸ Belaidi S ; Belaidi H ; Bouzidi D. *J. Comput.Theor. Nanosci.* 12 pp. 1737 (2015).
- ¹⁵⁹ Kerassa A ; Belaidi S ; Lanez T. *J. Quantum.Matter.* 5 pp. 45 (2016).
- ¹⁶⁰ Belaidi S ; Belaidi H ; Kerassa A ; Saoula M ; Bouzidi D. *J. Quantum.Matter.* 6 (2016).
- ¹⁶¹ Harkati D ; Belaidi S ; Kerassa A ; Gherraf N. *J. Quantum.Matter.* 5 pp. 36 (2016).
- ¹⁶² Mellaoui M ; Belaidi S ; Bouzidi D ; Gherraf N. *J. Quantum.Matter.* 3 pp. 435 (2014).
- ¹⁶³ Belaidi S ; Almi Z ; Bouzidi D. *J. Comput. Theor. Nanosci.* 11 pp. 2481 (2014).
- ¹⁶⁴ Youcef O ; Belaidi S ; Salah T. *J. Quantum.Matter.* 4 pp. (2016).
- ¹⁶⁵ Rouahna Y ; Belaidi S ; Harkati D ; Kerassa A. *J.Comput.Theor.Nanosci.* 12 pp. 4233 (2015).
- ¹⁶⁶ Salah T ; Belaidi S ; Melkemi N ; Daoud I ; Boughdiri S. *J.Theor.Comput. Chem.* 15 pp. 1650021(2016).
- ¹⁶⁷ Segall MD. *J. Curr. Pharm. Design.* 18 pp. 1292 (2012).
- ¹⁶⁸ Segall MD. *J. Expert.Opin.Drug. Disc.* 9 pp. 803 (2014).
- ¹⁶⁹ Lipinski CA ; Lombardo F ; Dominy BW ; Feeney PJ. *Adv. Drug.Delivery.Reviews.* 46 pp. 3 (2001).
- ¹⁷⁰ Veber DF ; Johnson SR ; Cheng HY ; Smith BR ; Ward KW ; Kopple KD. *J. Med. Chem.* 45 pp. 2615 (2002).
- ¹⁷¹ Didziapetris R ; Japertas P ; Avdeefand A ; Petrauskas A. *J. Drug. Target.* 11 pp. 391(2003).
- ¹⁷² Abad-Zapatero C. *J. Expert.Opin.Drug. Disc.* 2 pp. 469 (2007).
- ¹⁷³ Abad-Zapatero C ; Metz JT. *J. Drug. Disc.Today.* 10 pp. 464 (2005).
- ¹⁷⁴ Verdonk ML ; Rees DC. *J. ChemMedChem.* 3 pp. 1179 (2008).
- ¹⁷⁵ Schultes S ; de Graaf C ; Haaksma EEJ ; de Esch IJP ; Leurs R ; Krämer O. *J. Drug. Disc.Today. Tech.* 7 pp. 157 (2010).

- ¹⁷⁶ Gaussian 09, Revision B.01, M. J. Frisch, G. W. Trucks, H. B. Schlegel, G. E. Scuseria, M. A. Robb, J. R. Cheeseman, G. Scalmani, V. Barone, B. Mennucci, G. A. Petersson, H. Nakatsuji, M. Caricato, X. Li, H. P. Hratchian, A. F. Izmaylov, J. Bloino, G. Zheng, J. L. Sonnenberg, M. Hada, M. Ehara, K. Toyota, R. Fukuda, J. Hasegawa, M. Ishida, T. Nakajima, Y. Honda, O. Kitao, H. Nakai, T. Vreven, J. A. Montgomery, Jr., J. E. Peralta, F. Ogliaro, M. Bearpark, J. J. Heyd, E. Brothers, K. N. Kudin, V. N. Staroverov, T. Keith, R. Kobayashi, J. Normand, K. Raghavachari, A. Rendell, J. C. Burant, S. S. Iyengar, J. Tomasi, M. Cossi, N. Rega, J. M. Millam, M. Klene, J. E. Knox, J. B. Cross, V. Bakken, C. Adamo, J. Jaramillo, R. Gomperts, R. E. Stratmann, O. Yazyev, A. J. Austin, R. Cammi, C. Pomelli, J. W. Ochterski, R. L. Martin, K. Morokuma, V. G. Zakrzewski, G. A. Voth, P. Salvador, J. J. Dannenberg, S. Dapprich, A. D. Daniels, O. Farkas, J. B. Foresman, J. V. Ortiz, J. Cioslowski, and D. J. Fox, Gaussian, Inc., Wallingford CT (2010).
- ¹⁷⁷ J. S. Kwiatkowski, J. Leszczynski, and I. Teca, *J. Mol. Structure* 436, 451 (1997).
- ¹⁷⁸ Kerassa A ; Belaidi S ; Harkati D ; Lanez T ; Sinha L ; Prasad O. *Reviews.Theor. Sci.* 3 pp. 1 (2015).
- ¹⁷⁹ Chandrakumar KRS ; Pal S. *Inter. J. Mol. Sci.* 3 pp. 324 (2002).
- ¹⁸⁰ Pearson RG. *J. Amer. Chem. Soc.* 85 pp. 3533 (1963).
- ¹⁸¹ Klopman G. *J. Amer. Chem. Soc.* 90 pp. 223 (1968).
- ¹⁸² Salah T ; Belaidi S ; Melkemi N ; Tchouar N. *Reviews.Theor. Sci.* 3 pp. 355 (2015).
- ¹⁸³ Turner JV ; Agatonovic-Kustrin S. In *Silico Prediction of Oral Bioavailability, Elsevier Ltd, Vol.5*, pp.699-724 (2007).
- ¹⁸⁴ Zhao YH ; Abraham MH ; Le J ; Hersey A ; Luscombe CN ; Beck G ; Sherborne B ; Cooper I. *J. Pharm. Res.* 19 pp. 1446 (2002).
- ¹⁸⁵ Waring MJ. *J. Bioorg. Med. Chem. Letters.* 19 pp. 2844 (2009).
- ¹⁸⁶ HyperChem (Molecular Modeling System) Hypercube, Inc., 1115 NW, Gainesville, FL 32601, USA (2008).
- ¹⁸⁷ Bodor N ; Gabanyi Z ; Wong C. *J. Am. Chem. Soc.* 111 pp. 3783 (1989).
- ¹⁸⁸ Gavezotti A. *J. Am. Chem. Soc.* 10 pp. 5220 (1983).
- ¹⁸⁹ Ghose ; Crippen. *J. Chem. Inf. Comput. Sci.* 27 pp. 21 (1987).
- ¹⁹⁰ Miller KJ. *J. Am. Chem. Soc.* 112 pp. 8533 (1990).
- ¹⁹¹ Calculator Plugins were used for structure property prediction and calculation, Marvin 6.3.0, 2014, ChemAxon (<http://www.chemaxon.com>).
- ¹⁹² Marvin was used for drawing, displaying and characterizing chemical structures, substructures and reactions, Marvin 6.3.0, 2014, ChemAxon (<http://www.chemaxon.com>).
- ¹⁹³ Klopman G ; Li J-Y ; Wang S ; Dimayuga M. *J. Chem. Inf. Comput. Sci.* 34 pp. 752 ; doi PHYSPROP© database (1994).
- ¹⁹⁴ Spss 19 For Windows, SPSS software packages, SPSS Inc., 444 North Michigan Avenue, Suite 3000, Chicago, Illinois, 60611, USA
- ¹⁹⁵ Ekins S ; et al. *Drug Metab Dispos.* 35 pp. 493-500 (2007).
- ¹⁹⁶ Sandhya K ; Matthew DK ; Sean E. *Trends Pharmacol Sci.* 30(3) pp. 138-47 (2009).
- ¹⁹⁷ Jacob RB ; Andersen T ; McDougal OM. *PLoS Comput Biol.* 8(5) (2012).

- ¹⁹⁸ Sargis D ; Arthur JO. *Chem. Bio.* 1263 pp. 243-50 (2014).
- ¹⁹⁹ LigPlot⁺ Version v.1.4.5, Roman L. European Molecular Biology Laboratory- European Bioinformatics Institute (EMBL-EBI); (2009).
- ²⁰⁰ Protein Data Bank (Downloaded from <http://www.rcsb.org/pdb/explore/explore.do?structureId=2W0B>)
- ²⁰¹ Scior T ; et al. *J Chem Inf Model.* 52 pp. 867-81(2012).
- ²⁰² Perryman AL ; et al. *J Mol Biol.* 397 pp. 600-15 (2010).
- ²⁰³ Kumalo HM ; Soliman ME. *Cell. Mol. Bioeng.* 9(1) pp.175-89 (2015).

Tuberculosis (TB) remains the number one killer infectious disease affecting adults in developing countries. Earlier, it was reported that a number of 2, 5-disubstituted-1, 3, 4-oxadiazoles have been designed, synthesized, and screened for their anti-tuberculosis activity against *M. tuberculosis* H37Rv. Our minimalist design format presents opportunities to reveal the soft and hard characters (HSAB theory) of 1, 3, 4-oxadiazole as a function of the various donating and withdrawing substituent groups using the FMOs energies and the density-based descriptors. Where the quantum mechanical geometry optimization were performed using B3LYP functional of density functional theory (DFT). With regard to the 2, 5-disubstituted-1, 3, 4-oxadiazoles anti-tuberculosis series, the lipophilicity balance and ionization state seem to play an important role to reveal their pharmacokinetic and pharmacodynamics behavior. The multi-parameter optimization (MPO) process of these anti-tuberculosis compounds was expressed by various approaches such as Percent Efficiency Index (PEI), Group Efficiency (GE) analysis, Lipinski, Veber rules, Molecular Docking and QSAR model to guide the exploration of this new anti-tuberculosis agent with a high probability of achieving the required property/activity profile.

Keywords: anti-tuberculosis, descriptor, PEI, GE, Log P, Log D, SAR/SPR, Docking and QSAR.

La tuberculose (TB) demeure la première maladie infectieuse mortelle chez les adultes des pays en développement. Plus tôt, il a été rapporté qu'un certain nombre de 2, 5-disubstitués-1, 3, 4-oxadiazoles ont été conçus, synthétisés et criblés pour leur activité anti-tuberculose contre *M. tuberculosis* H37Rv. Notre conception minimaliste présente des opportunités de révéler les caractères mous et durs (théorie HSAB) de 1, 3, 4-oxadiazole en fonction des différents groupes de substituants (donneur et accepteur) en utilisant les énergies des orbitales frontières et des descripteurs basés sur la densité. Où l'optimisation de la géométrie moléculaire a été réalisée en utilisant la fonctionnelle B3LYP de la théorie de la fonctionnelle de la densité (DFT). En ce qui concerne les séries 2, 5-disubstituée-1, 3, 4-oxadiazoles antituberculeux, l'équilibre de la lipophilie et l'état d'ionisation semblent jouer un rôle important pour révéler leur comportement pharmacocinétique et pharmacodynamique. L'optimisation multi-paramétrique (MPO) de ces composés antituberculeux a été exprimé par diverses approches telles que l'indice d'efficacité en pourcentage (PEI), l'analyse d'efficacité de groupe (GE), les règles de Lipinski, Veber, Docking moléculaire et l'étude QSAR pour guider l'exploration de ce nouvel agent antituberculeux avec une forte probabilité d'atteindre le profil requis de la propriété / activité .

Mots clés : antituberculeux, descripteur, GE, PEI, Log P, Log D, SAR/SPR, Docking et QSAR.

السل (TB) لا يزال رقم واحد للأمراض المعدية القاتلة التي تؤثر على البالغين في البلدان النامية. وقد أفادت عدة دراسات بأن عدد من مشتقات (1، 3، 4-oxadiazoles) ذات نشاط ضد السل. تكشف لنا قائمة من مشتقات (1، 3، 4-oxadiazoles) عن الطابع اللين والصلب (حسب نظرية HSAB) بدلالة مجموعة مستبدلات مختلفة (المانحة والمستقبلة) باستخدام طاقات المدارات الحدودية والصفات المشتقة من الكثافة. حيث تم إجراء تقليل لطاقة البنية الجزيئية باستخدام الوظيفة (B3LYP) لنظرية الكثافة الوظيفية (DFT). وفيما يتعلق بالسلسلة (1، 3، 4-oxadiazoles) المضادة للسل، فإن خاصية المحبة للدهون وحالة التأين تلعبان دوراً هاماً في كشف حركيتها وديناميكيته الدوائية. وقمنا بتحسين المتعدد العوامل (MPO) لهذه المركبات المضادة للسل باستعمال طرق مختلفة مثل مؤشر الفعالية لنسبة المثوية (PEI)، وتحليل فعالية المجموعة (GE)، قواعد Lipinski، قواعد Docking، Veber ودراسة QSAR لتوجيه استكشاف هذه مضادات السل الجديدة مع وجود احتمال كبير لتحقيق النسبة المطلوبة (خاصية / النشاط البيولوجية).

الكلمات الدالة: مضادات السل، واصفات، GE، PEI، Log P، Log D، SAR/SPR، Docking و QSAR.